

Prostate Cancer
**and the DNA Damage Response:
Models and Mechanisms**

Wenhao Zhang
張文浩

**Prostate Cancer and the DNA Damage Response:
Models and Mechanisms**

Wenhao Zhang

張文浩

The research described in this thesis was performed at the Department of Molecular Genetics and Department of Experimental Urology, Erasmus Medical Center, Rotterdam, the Netherlands.

The research in this thesis was financially supported by China Scholarship Council (CSC), the Dutch Cancer Society and the Daniel den Hoed Foundation.

© Wenhao Zhang, 2019.

ISBN: 978-94-6332-604-9

Layout: the author of this book and GVO drukkers & vormgevers B.V., Ede

Cover design: the author of this book

Printed by: GVO drukkers & vormgevers B.V., Ede

The author appreciates the kind financial support for printing this thesis from: Erasmus University Rotterdam

Prostate Cancer and the DNA Damage Response:
Models and Mechanisms

Prostaatkanker en de DNA schade respons:
modellen en mechanismen

Proefschrift

ter verkrijging van de graad van doctor aan de
Erasmus Universiteit Rotterdam
op gezag van rector magnificus

Prof. Dr. R.C.M.E. Engels

en volgens besluit van het College voor Promoties

De openbare verdediging zal plaatsvinden op

Dinsdag 18 februari 2020 om 13:30

Door

Wenhao Zhang

geboren te Qinghai, China

Promotiecommissie

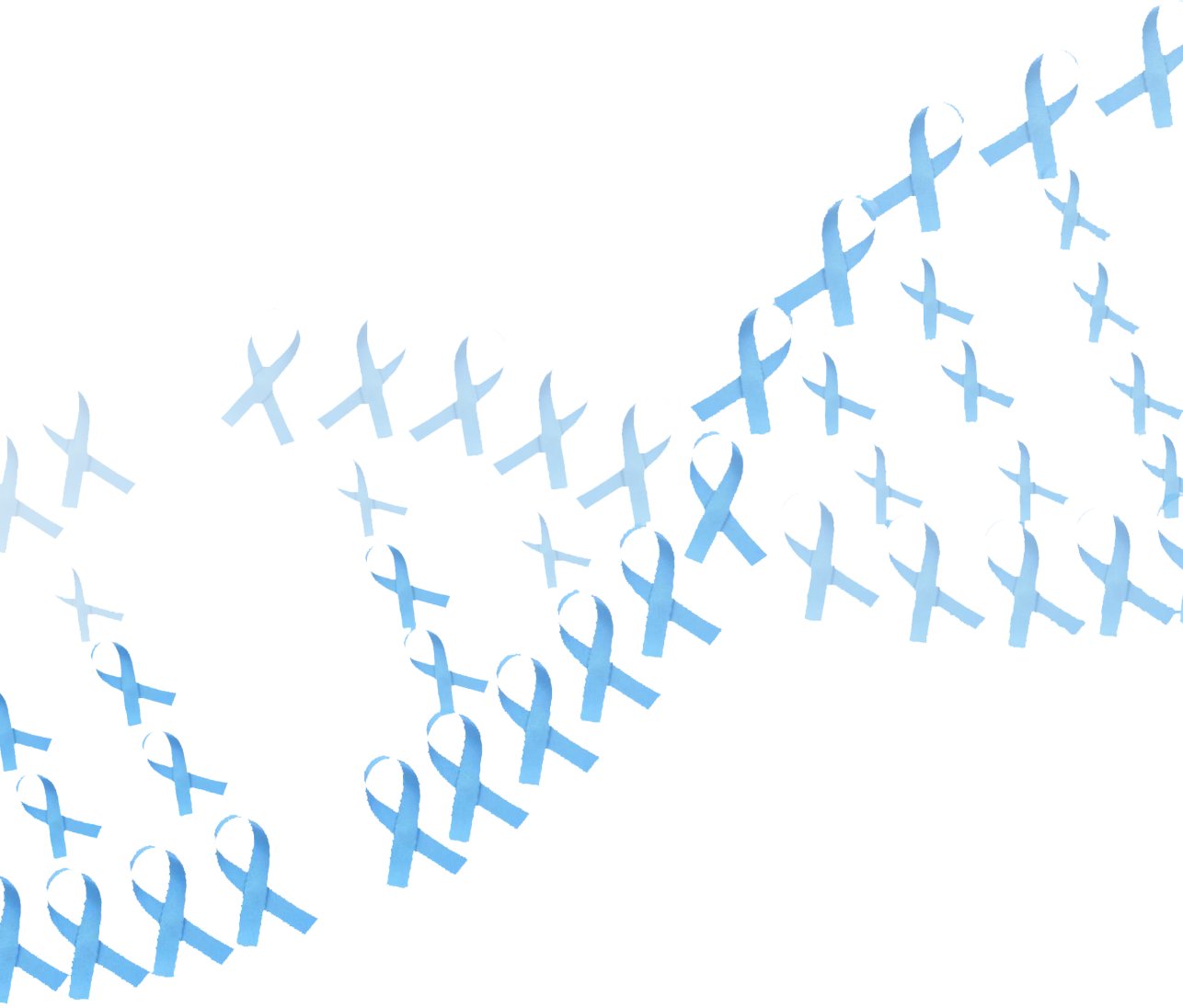
Promotor: Prof. Dr. R. Kanaar

Overige leden Prof. Dr. Ir. G.W. Jenster
Dr. J. Essers
Dr. G. van der Pluijm

Copromotoren: Dr. J. Nonnekens
Dr. D.C. van Gent
Dr. Ir. W.M. van Weerden

Contents

Chapter 1	General introduction	7
Chapter 2	Role of the DNA damage response in prostat cancer formation, progression and treatment	17
Chapter 3	<i>Ex vivo</i> treatment of prostate tumor tissue recapitulates <i>in vivo</i> therapy response	43
Chapter 4	Extracellular vesicle profiling for monitoring <i>ex vivo</i> prostate cancer therapy response	67
Chapter 5	Radiosensitivity of prostate cancer: assesment in patient-derived xenograft tissue slices and organoids	81
Chapter 6	Apalutamide sensitizes prostate cancer to ionizing radiation via inhibition of non-homologous end-joining DNA repair	97
Chapter 7	Summary, considerations and conclusions	121
Appendix		129



Chapter 1

A general introduction

1. Prostate cancer

Prostate cancer (PCa) is the most commonly diagnosed cancer and fifth leading cause of cancer-related death among men in western countries (1). The prostate is a gland located below the urinary bladder and in front of the rectum and contains a peripheral zone and transition zone. PCa usually arises in the peripheral glands. PCa shows heterogeneity in disease progression, with a considerable fraction of patients who have no symptoms and will not die from PCa, while a minority of patients has an aggressive disease course. In general, PCa is detected on the basis of elevated serum prostate-specific antigen (PSA) level in the blood. Biopsies from the prostate gland confirm the diagnosis. The pathologist then assigns a grade, named Gleason score, to each tumor. Based on the PSA level, Gleason score and radiological information, the risk of disease for progression will be classified (Table 1).

Table 1 Risk classification of prostate cancer.

	Low-risk	Intermediate-risk	High-risk		
PSA	<10 ng/mL	10-20 ng/mL	>20 ng/mL	any	any
Gleason	< 7	7	> 7	any	any
TNM	cT1 (Clinically inapparent tumor) to cT2a (Tumor involves one half of one lobe or less)	cT2b (Tumor involves more than half of one lobe, but not both lobes)	cT2c (Tumor involves both lobes)	cT3-4 (Tumor extends through the prostatic capsule or invades adjacent structures) or cN+ (Regional lymph node metastasis)	cM+ (Distant metastasis)
	Localized		Locally advanced	Metastatic	

PSA = prostate-specific antigen; GS = Gleason score; TNM = Clinical Tumor Node Metastasis (TNM) classification of PCa.

This classification guides clinicians to choose the proper treatment for PCa. When PCa is still organ confined, treatments may not be needed with only active surveillance, or patients can be offered with surgery (radical prostatectomy), radiation therapy with or without hormonal therapy. Although localized PCa can be well managed, a significant part (10-15%) of patients will eventually develop into the advanced stage of PCa or present *de novo* with this stage (5%) (2). At this stage, patients have the option of systemic treatment which usually includes androgen receptor (AR)-targeted treatment. Because the growth and survival of PCa cells is highly dependent on AR-signaling, patients initially respond well to either surgical and medical castration. However,

eventually all patients will progress and develop into the final stage of PCa: metastatic castration-resistant prostate cancer (mCRPC), which is defined by either PSA or radiological progression, despite low level of testosterone (<50 ng/dl) (3). New therapeutic strategies for mCRPC are being offered to progressive patients, such as new combinations and/or new treatment sequences of second-generation anti-androgen therapy (enzalutamide, abiraterone, apalutamide), second line chemotherapy (cabazitaxel) and bone-targeting radionuclide therapy (radium-223) which have shown notable benefit for patient survival (4) (Figure 1). Despite this progress in the development of new drugs, mCRPC continues to be incurable, and patients will eventually die of the disease.

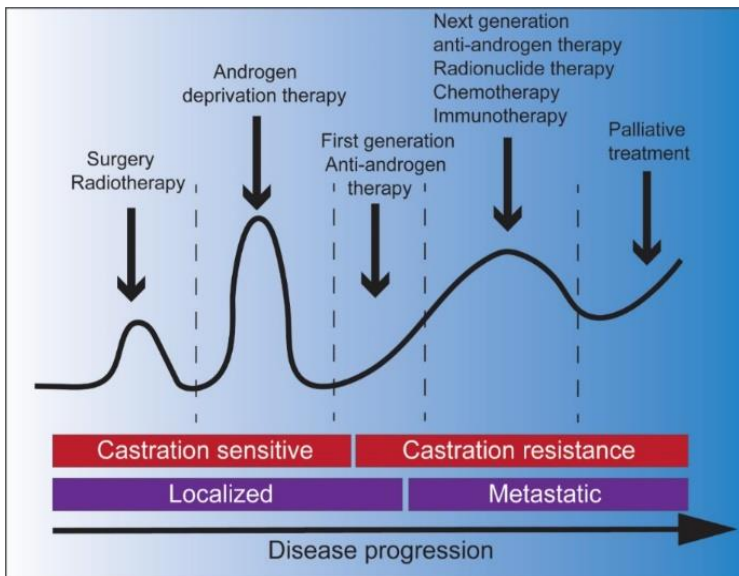


Figure 1. Treatment landscape of prostate cancer

2. Prostate cancer biomarkers

As mentioned above, PSA remains the most used test to detect PCa to date despite its limited specificity and an elevated rate of overdiagnosis. New biomarkers which are able to improve (i) early detection of PCa, (ii) risk stratification, (iii) prognosis, and (iv) treatment monitoring as well as capture tumor heterogeneity and periodically reassess the molecular phenotype of PCa are needed. Accumulating studies show that liquid biopsies may achieve the clinical expectation which examine tumor cells or tumor genomic content in circulating fluids, such as circulating tumor cells (CTCs), circulating tumor DNA (ctDNA) and extracellular vesicles (EVs) (5-7). These can be isolated from body fluids and analyzed for determining tumor-specific mutations, gene rearrangements and gene expression. EVs are small membrane vesicles secreted by

various types of cells into the extracellular environment (8). They were initially considered cell debris, however, in recent years, several studies suggest that EVs have a role in physiological and pathogenic processes (8, 9). They are enclosed by a phospholipid bilayer and contain DNA, RNA and proteins (10, 11). Different types of vesicles have been identified based on their biogenesis and size, such as exosomes, microvesicles and apoptotic bodies (12). EVs may reflect the tumor cell origin in terms of content (protein, RNA, DNA). Well-known PCa associated transcripts such as the kallikrein related peptidase 3 (*PSA*) gene and the transmembrane serine protease 2-ETS transcription factor ERG (*TMPRSS2-ERG*) fusion are detected inside urinary EVs in men with PCa (13, 14), thus measuring transcripts in PCa simple-derived EVs is expected to be a powerful method for the diagnosis, prognosis, and monitoring of PCa. However, this field is technically challenging, as majority of patient-derived EVs contain only low quantities of small RNA and it is uncertain whether the EVs are tumor-specific.

3. *In vitro* prostate cancer models

Most preclinical studies of PCa depend heavily on two-dimensional (2D) cancer cell lines. These PCa cell lines are valuable in both fundamental and translational research. Their homogeneity and ease of handling makes them an ideal model system for large high-throughput experiments. However, 2D cell lines do not recapitulate the complex architecture of tumors nor the important interaction between tumor cells and their microenvironment. These limitations could lead to misinterpretation of involved molecular mechanisms or a failure when transitioning a new drug from the bench to the clinic. Animal models such as patient-derived xenografts (PDXs) allow for *in vivo* screening but these experiments are slow and resource-intensive. Furthermore, the success rate for developing PDX models for PCa is quite low. The recent advances in *in vitro* three-dimensional (3D) culture technologies, such as cell-line based spheroid culture, tumor organoid culture and precision-cut tumor slice culture have opened new avenues for the development of more reliable *in vitro* PCa models. The limited cell-cell interactions in 2D monolayer cultures could induce major changes in cellular physiology. 3D spheroid culture of the same cells may represent the original tumor more faithfully. Although they capture some features of tumor cell biology better than 2D culture, they fail to mimic tumor heterogeneity. Another 3D model is organoid culture. Tissue-derived adult stem cells can be embedded in a 3D matrix and grown into self-organizing organotypic structures, termed organoids (15). Similar technology allows 3D culture of tumor cells in spheroid structures - referred to as tumor organoids. Organoid cultures can represent (part of) the heterogeneity of the original tumor. Some drawbacks are also clear: 1. lack of stromal cells in the majority of cases, 2. the requirement of a collagen gel for 3D culturing complicates potential drug screening and makes culturing more labor intensive, 3. it is not completely clear how well these tumor organoids recapitulate structural and functional aspects of their *in vivo* counterpart tumors. More recently, organoids have been co-cultured with additional cellular or microbial elements in order to increase the comparability to *in vivo* tumors (16). Finally,

as an alternative 3D model, *ex vivo* culturing of tumor slices represent a solid model system for drug sensitivity testing due to its relatively short generation time and reflection of the natural tumor microenvironment. Starting from the 1970s, various studies have described *ex vivo* culture systems for PCa tumors. This has resulted in the development of different tumor culture methods, ranging from direct culturing of 1-2 mm³ human tissue samples in cell culture medium to more recently developed techniques to culture precision-cut tissue slices on various scaffolds and supporting filters, such as gelatin, collagen sponges, titanium mesh inserts or cell strainers (17-20). *Ex vivo* culture of prostate tumors faces many challenges, such as the lack of long-term tumor cell viability, low cancer cells proliferation and overgrowth with normal basal cells, but it has the potential as a short-term personalized culture system. Taken together, each model has its own pro and cons, therefore, models should be chosen based on the specific situation and research question (Table 2).

Table 2 Comparison of *in vitro* PCa tumor models.

	Cell	Spheroid	Organoid	Tissue slice
Establishment difficulty	high	low	high	med
Maintenance difficulty	low	low	med	high
Morphology preservation	-/+	+	++	+++
Viability maintenance	+++	+++	++	+
Microenvironment preservation	-	-	++	+++
Success rate of initiation	+++	+++	+	++
Drug screening	+++	+++	++	+
Amenable to genetic modification	+++	+++	++	-
Matched normal controls	-	-	+	++
Costs	low	low	high	low

Respective features were judged as best (+++), suitable (++), possible (+) or unsuitable (-).

4. Radiation therapy

Radiation therapy is the first-line treatment for localized PCa, which can be administered as either external beam radiation therapy (EBRT) or brachytherapy, in which a radioactive source is implanted in or close to tumor. Conventionally, fractionated EBRT up to 78 Gy in 39 fractions of 2 Gy was introduced for patients with localized PCa (4). Irradiation (IR) induces cell death by the production of reactive oxygen species (ROS) as well as by direct ionization of the DNA which leads to single-strand breaks (SSBs) and double-strand breaks (DSBs). Depending on the risk group of PCa patients, single or combination treatment with androgen deprivation therapy (ADT) will be provided for patients. For high-risk PCa, adjuvant ADT is recommended as

combination treatment, which significantly improves overall cancer-related survival (21, 22). Based on its beneficial effects, this combination is currently the standard of care for locally advanced PCa. Even though combination strategy has been shown to improve the overall therapeutic outcome compared to IR alone, the effect is rather modest. Clinicians still face the difficulty that biomarkers for selection of patients that will benefit from this combination are still lacking.

5. DNA damage response

Since outcome of radiotherapy relies on the induction of DNA damage and its subsequent repair, it is evident that the status of the DNA damage response (DDR) is one of the important factors that can predict treatment outcome. Besides IR, the DNA is constantly damaged by exogenous sources as well as by endogenous DNA-damaging agents (23, 24) as DNA is an intrinsically instable molecule and vulnerable to chemical modifications (23). Incorrect or failed repair of damaged DNA can lead to genetic alterations, instability and give rise to cancer. DNA damage comes in various forms, including base oxidation, deamination, alkylation, interstrand crosslinks, adduct formation, SSBs, and DSBs. To prevent genomic instability and deal with enormous load of DNA damage, multiple distinct repair pathways have been identified to cope with the divergent types of damages mentioned above such as base excision repair (BER), nucleotide excision repair (NER), mismatch repair (MMR), and DSBs repair (25). DSBs are the most relevant in the context of cancer treatment, as many traditional anti-cancer treatments induce DSBs which is the most toxic and lethal form of DNA damage. DSB repair consists of two main pathways: homologous recombination (HR) and non-homologous end-joining (NHEJ). NHEJ is the major contributor to DSBs repair that simply joins the two ends of broken DNA and can be performed in all cell cycle phases. HR uses the sister chromatids as a template to repair DSBs, thus it only happens in the S and G2 phases of the cell cycle and is highly accurate (Figure 2) (25). Clinical and preclinical studies have revealed that alterations in DDR pathways play a role in PCa etiology and progression, especially in advanced stage (26-29). The efficacy of DNA-damaging anti-cancer treatments can be affected depending on the exact repair pathway deficiency, opening a window of opportunity to individualize cancer treatment based on tumor characteristics. For example, patients harboring DNA repair defects may have increased radiosensitivity or can be targeted by specific treatments, such as poly(ADP-ribose) polymerase (PARP) inhibitors (30). Future studies are needed to broaden our understanding of DDR in PCa, as well as to determine how this knowledge can be used to improve therapeutic approaches.

6. Scope of the thesis

This thesis describes several *in vitro* 3D PCa models and explores the mechanism of DNA repair and its regulation by AR signaling in PCa. Chapter 2 provides an overview of the importance of preclinical and clinical research for DDR in PCa and discusses how these recent and ongoing studies will help to improve diagnostic, prognostic and therapeutic approaches for PCa management. Chapter 3 describes an *ex vivo* culture

system for PCa PDX tumor-derived tissue slices. We characterized and validated the system by testing drugs on tumor slices with different genotypes. In chapter 4, we evaluated the use of EVs in monitoring PCa treatment response by investigating EVs from tissue slice culture medium. The quantity and quality of RNA from EVs were characterized and gene expression alteration upon anti-androgen treatment was compared to its cell of origin. In chapter 5, we report on the generation of PCa PDX-derived organoid cultures. By establishing the PCa organoids culture, we evaluated radiosensitivity on these novel models and compared to tissue slices models. Finally, in chapter 6, we investigate how radiosensitivity can be enhanced by anti-androgen treatments. This combination is used in a clinical setting, but its mechanisms remains unclear and controversial. We provide evidence that NHEJ is directly regulated by AR signaling.

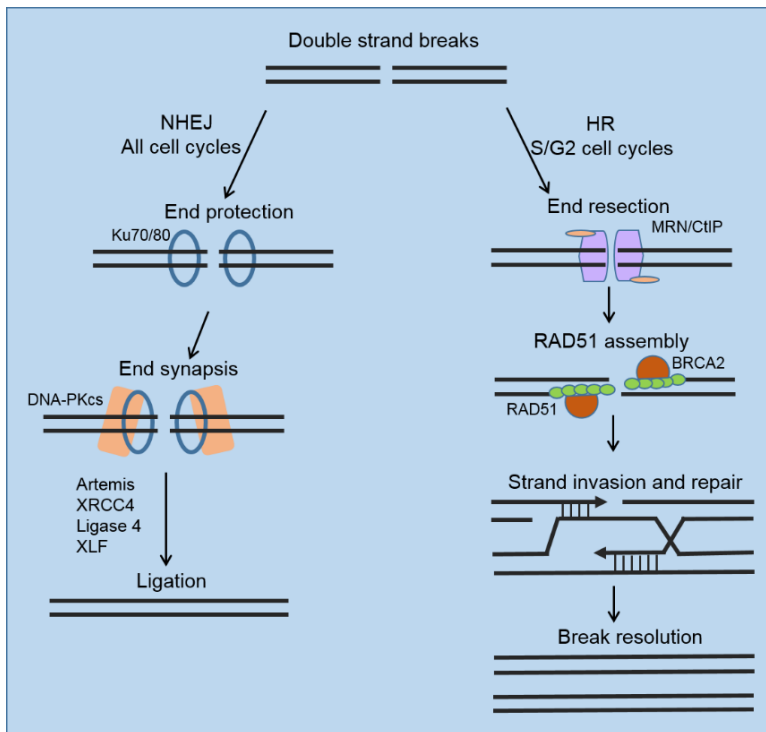


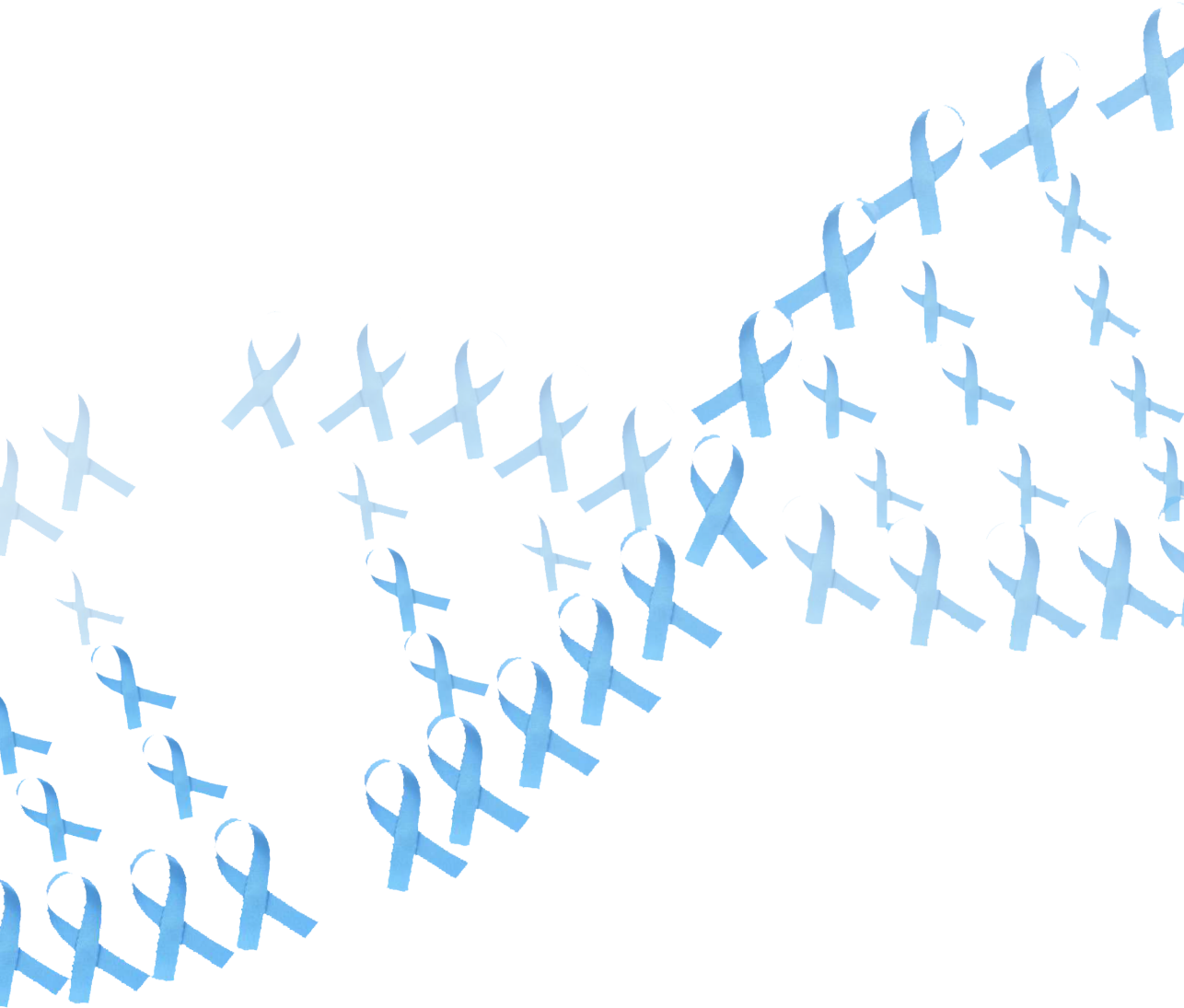
Figure 2 Double-strand break repair.

Double-strand break repair consists two major pathways: non-homologous end-joining (NHEJ) and homologous recombination (HR). NHEJ occurs during all cell cycle phases and simply rejoins broken DNA ends. HR is restricted to the S and G2 phases of the cell cycle as it makes use of the sister chromatid to accurately repair broken DNA.

Reference

1. Ferlay J, Soerjomataram I, Dikshit R, Eser S, Mathers C, Rebelo M, et al. Cancer incidence and mortality worldwide: sources, methods and major patterns in GLOBOCAN 2012. *Int J Cancer*. 2015;136(5):E359-86.
2. Thomas TS, Pachynski RK. Treatment of Advanced Prostate Cancer. *Mo Med*. 2018;115(2):156-61.
3. Cornford P, Bellmunt J, Bolla M, Briers E, De Santis M, Gross T, et al. EAU-ESTRO-SIOG Guidelines on Prostate Cancer. Part II: Treatment of Relapsing, Metastatic, and Castration-Resistant Prostate Cancer. *Eur Urol*. 2017;71(4):630-42.
4. Nuhn P, De Bono JS, Fizazi K, Freedland SJ, Grilli M, Kantoff PW, et al. Update on Systemic Prostate Cancer Therapies: Management of Metastatic Castration-resistant Prostate Cancer in the Era of Precision Oncology. *Eur Urol*. 2019;75(1):88-99.
5. Zainfeld D, Goldkorn A. Liquid Biopsy in Prostate Cancer: Circulating Tumor Cells and Beyond. *Cancer Treat Res*. 2018;175:87-104.
6. Stone L. Biomarkers from liquid biopsy. *Nature Reviews Urology*. 2016;13:434.
7. Minciaccchi VR, Zijlstra A, Rubin MA, Di Vizio D. Extracellular vesicles for liquid biopsy in prostate cancer: where are we and where are we headed? *Prostate Cancer Prostatic Dis*. 2017;20(3):251-8.
8. Colombo M, Raposo G, Thery C. Biogenesis, secretion, and intercellular interactions of exosomes and other extracellular vesicles. *Annu Rev Cell Dev Biol*. 2014;30:255-89.
9. Yoon YJ, Kim OY, Gho YS. Extracellular vesicles as emerging intercellular comunicasomes. *BMB Rep*. 2014;47(10):531-9.
10. Février B, Raposo G. Exosomes: endosomal-derived vesicles shipping extracellular messages. *Current Opinion in Cell Biology*. 2004;16(4):415-21.
11. Raposo G, Stoorvogel W. Extracellular vesicles: exosomes, microvesicles, and friends. *J Cell Biol*. 2013;200(4):373-83.
12. van der Pol E, Böing AN, Harrison P, Sturk A, Nieuwland R. Classification, Functions, and Clinical Relevance of Extracellular Vesicles. *Pharmacological Reviews*. 2012;64(3):676-705.
13. Dijkstra S, Birker IL, Smit FP, Leyten GHJM, de Reijke TM, van Oort IM, et al. Prostate Cancer Biomarker Profiles in Urinary Sediments and Exosomes. *The Journal of Urology*. 2014;191(4):1132-8.
14. Donovan MJ, Noerholm M, Bentink S, Belzer S, Skog J, O'Neill V, et al. A molecular signature of PCA3 and ERG exosomal RNA from non-DRE urine is predictive of initial prostate biopsy result. *Prostate Cancer And Prostatic Diseases*. 2015;18:370.
15. Tuveson D, Clevers H. Cancer modeling meets human organoid technology. *Science*. 2019;364(6444):952-5.
16. Yin X, Mead BE, Safaee H, Langer R, Karp JM, Levy O. Engineering Stem Cell Organoids. *Cell Stem Cell*. 2016;18(1):25-38.
17. Maund SL, Nolley R, Peehl DM. Optimization and comprehensive characterization of a faithful tissue culture model of the benign and malignant human prostate. *Lab Invest*. 2014;94(2):208-21.

18. Papini S, Rosellini A, De Matteis A, Campani D, Selli C, Caporali A, et al. Establishment of an organotypic *in vitro* culture system and its relevance to the characterization of human prostate epithelial cancer cells and their stromal interactions. *Pathol Res Pract.* 2007;203(4):209-16.
19. Centenera MM, Gillis JL, Hanson AR, Jindal S, Taylor RA, Risbridger GP, et al. Evidence for efficacy of new Hsp90 inhibitors revealed by *ex vivo* culture of human prostate tumors. *Clin Cancer Res.* 2012;18(13):3562-70.
20. Zhang W, van Weerden WM, de Ridder CMA, Erkens-Schulze S, Schonfeld E, Meijer TG, et al. *Ex vivo* treatment of prostate tumor tissue recapitulates *in vivo* therapy response. *Prostate.* 2019;79(4):390-402.
21. Bolla M, Collette L, Blank L, Warde P, Dubois JB, Mirimanoff RO, et al. Long-term results with immediate androgen suppression and external irradiation in patients with locally advanced prostate cancer (an EORTC study): a phase III randomised trial. *Lancet.* 2002;360(9327):103-6.
22. Bolla M, Gonzalez D, Warde P, Dubois JB, Mirimanoff RO, Storme G, et al. Improved survival in patients with locally advanced prostate cancer treated with radiotherapy and goserelin. *N Engl J Med.* 1997;337(5):295-300.
23. Hoeijmakers JH. DNA damage, aging, and cancer. *N Engl J Med.* 2009;361(15):1475-85.
24. Tubbs A, Nussenzweig A. Endogenous DNA Damage as a Source of Genomic Instability in Cancer. *Cell.* 2017;168(4):644-56.
25. Jackson SP, Bartek J. The DNA-damage response in human biology and disease. *Nature.* 2009;461(7267):1071-8.
26. Castro E, Goh C, Olmos D, Saunders E, Leongamornlert D, Tymrakiewicz M, et al. Germline BRCA mutations are associated with higher risk of nodal involvement, distant metastasis, and poor survival outcomes in prostate cancer. *J Clin Oncol.* 2013;31(14):1748-57.
27. Grindedal EM, Moller P, Eeles R, Stormorken AT, Bowitz-Lothe IM, Landro SM, et al. Germ-line mutations in mismatch repair genes associated with prostate cancer. *Cancer Epidemiol Biomarkers Prev.* 2009;18(9):2460-7.
28. Kote-Jarai Z, Jugurnauth S, Mulholland S, Leongamornlert DA, Guy M, Edwards S, et al. A recurrent truncating germline mutation in the BRIP1/FANCD1 gene and susceptibility to prostate cancer. *Br J Cancer.* 2009;100(2):426-30.
29. Leongamornlert D, Mahmud N, Tymrakiewicz M, Saunders E, Dadaev T, Castro E, et al. Germline BRCA1 mutations increase prostate cancer risk. *Br J Cancer.* 2012;106(10):1697-701.
30. Zhang W, van Gent DC, Incrocci L, van Weerden WM, Nonnekens J. Role of the DNA damage response in prostate cancer formation, progression and treatment. *Prostate Cancer Prostatic Dis.* 2019.



Chapter 2

Role of the DNA damage response in prostate cancer formation,
progression and treatment

Wenhao Zhang¹, Dik C. van Gent^{1,2}, Luca Incrocci³, Wytke M. van Weerden⁴, Julie Nonnekens^{1,5*}

1. Department of Molecular Genetics, Erasmus MC, Rotterdam, The Netherlands; 2. Oncode Institute, Erasmus MC, Rotterdam, The Netherlands; 3. Department of Radiation Oncology, Erasmus MC Cancer Institute, Rotterdam, The Netherlands; 4. Department of Experimental Urology, Erasmus MC, Rotterdam, The Netherlands; 5. Department of Radiology and Nuclear Medicine, Erasmus MC, Rotterdam, The Netherlands

Published in Prostate Cancer and Prostatic Disease, 2019, in press

Abstract

Clinical and preclinical studies have revealed that alterations in DNA damage response (DDR) pathways may play an important role in prostate cancer (PCa) etiology and progression. These alterations can influence PCa responses to radiotherapy and anti-androgen treatment. The identification of DNA repair gene aberrations in PCa has driven the interest for further evaluation whether these genetic changes may serve as biomarkers for patient stratification. In this review, we summarize the current knowledge on DDR alterations in PCa, their potential impact on clinical interventions and prospects for improved management of PCa. We particularly focus on the influence of DDR gene mutations on PCa initiation and progression and describe the underlying mechanisms. A better understanding of these mechanisms, will contribute to better disease management as treatment strategies can be chosen based on the specific disease properties, since a growing number of treatments are targeting DDR pathway alterations (such as Poly(ADP-ribose) polymerase inhibitors). Furthermore, the recently discovered crosstalk between the DDR and androgen receptor signaling opens a new array of possible strategies to optimize treatment combinations. We discuss how these recent and ongoing studies will help to improve diagnostic, prognostic and therapeutic approaches for PCa management.

1. Introduction

Prostate cancer (PCa) is the second most common cancer in men and the fourth most common tumor type worldwide (1). Although organ-confined disease can be well managed, curative therapeutic options for disseminated disease are limited. First-line therapy for disseminated PCa is androgen deprivation therapy (ADT) that prevents androgen receptor (AR) pathway signaling as most PCas are dependent on activated AR signaling for cell survival (2, 3). In time, patients under ADT may progress to castration-resistant PCa (CRPC), requiring first line chemotherapy (commonly docetaxel) (4). New therapeutic strategies for CRPC are being offered to patients, such as new combinations and sequences of second-generation anti-androgen therapy (enzalutamide, abiraterone, apalutamide) or second line chemotherapy (cabazitaxel), which have shown notable benefit for patient survival (4). In addition, promising new treatment modalities, such as Radium-223 and prostate-specific membrane antigen (PSMA)-directed radioligand therapy, are being exploited for patients with (bone) metastatic disease. Despite this progress in the development of new drugs, CRPC continues to be incurable, and drug resistance remains an issue.

Clinical and preclinical studies have revealed that alterations in DNA damage response (DDR) pathways play a role in PCa etiology and progression, especially in CRPC patients (5-10). These DNA repair defects may be targeted by specific treatments, such as Poly(ADP-ribose) polymerase (PARP) inhibitors (11). Moreover, several studies provided evidence that AR signaling links to the DDR in PCa cells, which may have relevance for the first line disease management using ADT and AR-targeted agents (12, 13). In this review, we summarize the current knowledge of DDR alterations in PCa, the AR-DDR crosstalk and the potential exploitation of DDR targeting drugs to improve clinical interventions.

2. DNA damage response pathways

DNA damage has emerged as a major culprit in cancer initiation and progression. The DNA is constantly damaged by exogenous sources such as genotoxic chemicals, ultraviolet (UV) and ionizing radiation (IR), as well as by endogenous DNA damaging agents, such as reactive oxygen and nitrogen species (14, 15). These sources will induce various damages to the DNA, including base oxidation, deamination, alkylation, interstrand crosslinks, adduct formation, single-strand breaks (SSBs) and double-strand breaks (DSBs). Additionally, spontaneous DNA damage is induced during replication. Collisions of the replication fork with DNA-binding proteins or the transcription machinery are the most common causes leading to replication fork stalling or collapse, which in turn induces DNA damage (16, 17). Incorrect or failed repair of damaged DNA can lead to genetic alterations. Important consequences of genetic alterations are loss of tumor suppressor genes and activation of oncogenes, which may trigger the development of malignant cells or increase aggressiveness of tumor cells. Normal cells maintain genomic integrity using various DDR mechanisms to repair damaged DNA or induce cell death. The concept of DDR has been introduced to describe a series of biological reactions including DNA lesion site detection, repair protein recruitment,

damage repair, cell cycle checkpoint control and cell death pathways.

The highly diverse spectrum of DNA lesions can be repaired by a number of different DNA repair pathways, which have been reviewed extensively elsewhere (18-20). In short, base excision repair (BER) involves multiple enzymes to excise and replace a single damaged nucleotide base, such as an oxidized base, but also an SSB (21). Mismatch repair (MMR) is mainly involved in repair of base mismatches and insertions/deletions that can occur during replication and recombination (22). The Fanconi anemia (FA) pathway repairs DNA interstrand crosslinks in the genome (23). DSBs are resolved either by high-fidelity homologous recombination (HR) or error-prone non-homologous end joining (NHEJ). The HR pathway is only active when the cell is in the S/G2 cell cycle stage since it requires the presence of the sister chromatid as a repair template (24). DSBs can be generated during replication when the replication fork encounters a DNA lesion and these breaks are exclusively repaired by HR. NHEJ is active during all cell cycle stages and functions by directly ligating broken DNA ends. Since no template is used during NHEJ, repair via this pathway is error prone (Figure 1) (24). After DNA damage induction, depending on the severity of the lesion and repair capacity, cells will continue to proliferate if damages are repaired, or cells stop proliferation, become senescent, or undergo programmed cell death (apoptosis) to remove damaged DNA from the cellular population (25). Alterations in any of these pathways can result in genomic instability and consequently predispose to cancer, affect disease progression and/or influence therapy efficacy. Nonetheless, impaired DNA repair can also be a possible Achilles heel of the cancer that can be exploited for treatment (26).

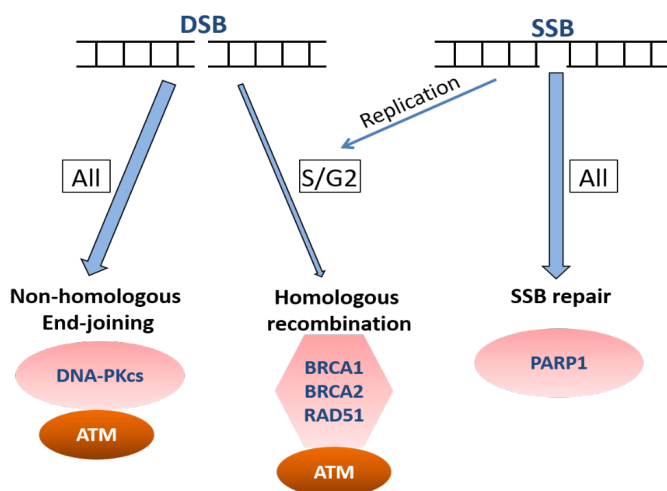


Figure 1 DNA double strand (DSB) and single strand break (SSB) repair pathways.

The majority of the DSBs are repaired by the error-prone Non-Homologous End-Joining pathway (NHEJ, available during all cell cycle stages) and a smaller fraction of the DSBs are repaired via

Homologous Recombination (HR, only during S/G2 cell cycle stages). SSBs are repaired by the Single Strand Break Repair pathway (available during all cell cycle stages). During DNA replication can an unrepaired SSB be converted into a DSB which can then only be repaired by HR.

3. Molecular mechanisms underlying PCa risk

Multiple studies have indicated that germline mutations in DNA repair genes are associated with a higher risk of developing PCa. The individuals at risk have one inherited dysfunctional allele of the DNA repair gene and a second event (mutation or epigenetic silencing) can cause inactivation of the functional allele. The most common germline mutated DDR genes in primary PCa or CRPC are found in the Breast Cancer 1 and 2 (*BRCA1* and *BRCA2*) genes. Similar to the role of mutations in *BRCA1/2* in the development of breast cancer and ovarian cancer (14), various studies have shown that inactivating *BRCA1/2* mutations, predominantly *BRCA2*, increase predisposition to PCa (Table 1) (7-9, 27-29). *BRCA1/2* are tumor suppressor genes and both encode large proteins which act in multiple cellular pathways. *BRCA1* and *BRCA2* are both involved in the HR pathway (30, 31), while *BRCA1* has also been found to have other functions (32). Loss-of-function mutations in *BRCA1/2* lead to a deficiency in error-free HR repair. Therefore, DSBs will be repaired alternatively by other non- conservative and potentially mutagenic mechanisms, such as the NHEJ pathway. The resulting genomic instability (chromosomal translocations and deletions) and mutations may be the underlying mechanism of *BRCA1/2* associated cancers (33, 34). This could increase the risk of acquiring fusion genes, such as the *TMPRSS2/ERG* fusion that is found in 40-50% of PCa cases (35), although no solid evidence has been acquired to link *BRCA1/2* mutation status to this fusion. Furthermore, the reason why *BRCA1/2* mutations are particularly associated with specific cancer types, such as breast, ovarian and PCa remains unknown.

Francis et al. showed that *BRCA2* can act as a tumor suppressor in the prostate (36). Using a genetically engineered mouse model, it was found that deletion of *Brca2* in prostate epithelia resulted in focal hyperplasia and low-grade prostate intraepithelial neoplasia (PIN) in animals over 12 months old. Epithelial cells in these lesions showed an increase in DNA damage. The evidence that other inherited gene mutations in DSB repair genes, such as BRCA1 Interacting Protein C-Terminal Helicase 1 (*BRIP1*) and Nibrin (*NBS1*), are also associated with PCa has been documented less extensively (6, 8). Besides DSB gene alterations, mutations in the MMR genes MutS homolog 2 and 6 (*MSH2* and *MSH6*) are also associated with increased PCa risk (7, 27). MMR mutations would mainly cause point mutations or small insertions and deletions of short repetitive sequences of DNA which may result in microsatellite instability (37). Therefore, underlying mechanisms of PCa can be linked to Lynch syndrome, a hereditary 'non-polyposis'-colorectal carcinoma that is caused by MMR pathway mutations. The increased risk of PCa in MMR mutation carriers and in families with Lynch syndrome provide the rationale to include PCa in the Lynch syndrome tumor spectrum, which is relevant for risk estimates and surveillance recommendations in MMR mutation

carriers (38).

Table 1 Germline DDR mutations increase PCa risk

Gene	Pathway	Relevance
<i>BRCA1</i> (9)	HR	Deleterious <i>BRCA1</i> mutations confer a relative PCa risk of 3.75, and a 8.6% cumulative risk by age 65.
<i>BRCA1</i> and <i>BRCA2</i> (28, 49, 61)	HR	<i>BRCA2</i> mutation carriers have an increased risk of PCa and a higher histological grade. <i>BRCA1</i> and <i>BRCA2</i> mutation carriers had a higher risk of recurrence and PCa-specific death.
<i>MSH2</i> , <i>MLH1</i> and <i>MSH6</i> (27)	MMR	Increased PCa risk. Evidence to link PCa to Lynch syndrome.
<i>MLH1</i> , <i>MSH2</i> , <i>MSH6</i> , and <i>PMS2</i> (7)	MMR	MMR genes may confer a high risk of PCa when mutated.
<i>MSH2</i> , <i>MLH1</i> and <i>MSH6</i> (29)	MMR	MMR gene mutation carriers have at least a twofold or greater increased risk of developing MMR-deficient PCa where the risk is highest for <i>MSH2</i> mutation carriers.
<i>BRIP1</i> (8)	FA	Truncating mutations in <i>BRIP1</i> might confer an increased risk of PCa

BRCA1/2: Breast Cancer 1 and 2; *MSH2/6*: MutS protein homolog 2 and 6; *MLH1*: MutL homolog 1; *PMS2*: PMS1 homolog 2; *BRIP1*: BRCA1 interacting protein C-terminal helicase1; HR: homologous recombination; MMR: mismatch repair; FA: fanconi anemia pathway.

4. DDR defects in PCa

4.1 DDR defects in primary PCa

The clinical behavior of localized PCa is highly variable: while some men have aggressive cancer leading to metastasis and death, many others have indolent cancers and these men can be cured by local therapy or may be safely observed without treatment (39). Several studies have identified primary PCa tumors harboring a diversity of DDR gene alterations (summarized in table 2) (40-45). These studies identified a heterogeneous panel of repair defects caused by homozygous mutations or copy number alterations in primary prostate tumors compared to paired normal tissue in Ataxia–telangiectasia mutated (*ATM*), *BRCA2*, *RAD51*, mediator of DNA damage checkpoint 1 (*MDC1*), *PARP1* and FA complementation group D2 (*FANCD2*), although the level of incidence varied between the studies. This considerable heterogeneity of repair defect prevalence among different studies could at least in part be attributed to the diversity of the study populations, as the genetic background can differ significantly between indolent, non-symptomatic and progressive PCa (46-48). Loss-of-function DDR gene mutations can contribute to a more aggressive PCa phenotype with a higher probability of nodal involvement and distant metastasis (5, 49-

51). This aggressive phenotype was also reported in patients harboring *BRCA1/2* and *ATM* combined mutations (52) and *NBS1* mutations alone (6). Recent clinical data have shown a strong prognostic value of a DDR mutation signature which may be used for risk stratification for high-risk PCa patients. Treatment outcome for *BRCA1/2* mutation carriers showed worse outcomes for these patients than non-carriers when conventionally treated with surgery or radiation therapy (53)

The studies discussed above found DDR mutations in primary PCa, with a heterogeneous and overall low mutation rate. However, a direct (mechanistic) link between these mutations and PCa predisposition and treatment has not yet been established. As primary PCa is typically well managed and not lethal, it will therefore be of more interest to focus on the landscape of DDR defects in advanced PCa.

Table 2 Prevalence of selected DDR gene alteration in primary PCa

Study	Pathway	Barbieri et al (29)	Baca et al (30)	Cancer Genome Atlas (31)	Fraser et al (95)	Ren et al (32)	Total
Patients (n)		112	57	333	449	65	1017
<i>ATM</i>	General	2.8% (3)	12.5%(7)	7.2%(24)	1.8%(8)	3.1%(2)	4.3%(44)
<i>ATR</i>			1.8%(1)	2.4%(8)		5%(3)	1.2%(12)
<i>BRCA1</i>		1.8%(2)		1.2%(4)		1.5%(1)	0.69%(7)
<i>BRCA2</i>	HR		7.1%(4)	3.3%(11)		1.5%(1)	1.58%(16)
<i>RAD51</i>			3.6%(2)	2.1%(7)			0.88%(9)
<i>PARP1</i>	BER		3.6%(2)	3.0%(10)		3.1%(2)	1.38%(14)
<i>MLH1</i>	MMR			0.3%(1)			0.09%(1)
<i>MSH2</i>				1.5%(5)			0.49%(5)
<i>FANCD2</i>	FA		1.8%(1)	0.9%(3)		1.5%(1)	0.49%(5)
All genes		4.6%	30.4%	21.9%	1.8%	15.7%	11.1%

Data was acquired from The Memorial Sloan Kettering cBioportal database (<http://cbiportal.org>) for certain DDR genes from different study. *ATM*: Ataxia–telangiectasia mutated serine/threonine kinase; *ATR*: ATM and RAD3-related serine/threonine kinase; *BRCA1/2*: Breast Cancer 1 and 2; *RAD51*: RAD51 recombinase; *PARP1*: poly(ADP-ribose) polymerase 1; *MLH1*: MutL homolog 1; *MSH2*: MutS protein homolog 2; *FANCD2*: FA complementation group D2. HR: homologous recombination; BER: base excision repair; MMR: mismatch repair; FA: fanconi anemia pathway.

4.2 DDR defects in mCRPC

An enrichment of DDR gene alterations can be found during PCa progression, especially when the disease develops into metastatic CRPC (mCRPC) (summarized in Table 3) (54-56). Heavily pre-treated mCRPC contained more genetic alterations in DDR genes (46%) than treatment-naive high grade localized tumors (27%) (54). A multi-institutional clinical sequencing study revealed that the majority of affected individuals with CRPC harbor clinically actionable homozygous molecular alterations,

with 23% of mCRPC harboring DDR aberrations and 8% harboring DDR germline mutations (55). Aberrations in *BRC1*, *BRC2* and *ATM* were observed at substantially higher frequencies (19.3% overall) in mCRPC compared to those in primary PCa. Among these DDR alterations, *BRC2* was the most frequently altered (12.7%), and ~90% of these *BRC2* defective tumors exhibited biallelic loss. As aberrations in these genes are expected to confer sensitivity to PARP inhibitors (56), nearly 20% of mCRPC patients may potentially benefit from this therapy. Additionally, three out of four mCRPC tumors in this cohort which presented hypermutations are harboring defects in the MMR pathway genes *MLH1* or *MSH2* (55). Whether this abundance of DDR alterations is specifically targeted to these genes or a general consequence of high mutational burden for advanced disease is still unclear.

Table 3 Prevalence of selected DDR genes alteration in mCRPC

	DDR pathway involved	Grasso et al (54)	Robinson et al (55)	Total
Patients (n)		59	150	209
<i>ATM</i>	General	11.8% (7)	5.3% (8)	7.2% (15)
<i>ATR</i>		5% (3)	8.6% (13)	7.7% (16)
<i>BRC1</i>			0.7% (1)	0.5% (1)
<i>BRC2</i>	HR	11.8% (7)	9.3% (14)	10.0% (21)
<i>RAD51</i>		1.7% (1)	2.0% (3)	1.9% (4)
<i>PARP1</i>	BER	3% (2)	2.7% (4)	5.5% (6)
<i>MLH1</i>	MMR	1.7% (1)	1.3% (2)	1.4% (3)
<i>MSH2</i>		3.3% (2)	2.7% (4)	2.9% (6)
<i>FANCD2</i>	FA	3.3% (2)	2.7% (4)	2.9% (6)
All genes		41.6%	35.3%	40%

Data was acquired from The Memorial Sloan Kettering cBioportal database (<http://cbioportal.org>). *ATM*: Ataxia–telangiectasia mutated serine/threonine kinase; *ATR*: ATM and RAD3-related serine/threonine kinase; *BRC1/2*: Breast Cancer 1 and 2; *RAD51*: RAD51 recombinase; *PARP1*: poly(ADP-ribose) polymerase 1; *MLH1*: MutL homolog 1; *MSH2*: MutS protein homolog 2; *FANCD2*: FA complementation group D2. HR: homologous recombination; BER: base excision repair; MMR: mismatch repair; FA: fanconi anemia pathway

4.3 DDR defects and response to PCa treatment

Various retrospective and prospective studies have been performed in which treatment outcome to conventional PCa treatment was compared in DDR mutation carriers and wild type individuals. The prognostic and predictive impact related to standard therapies for DDR mutated mCRPC has yet to be determined, since these trials (summarized in Table 4) report inconsistent and conflicting outcomes: one study found no difference between the patient groups (57), while other studies reported DDR mutation carriers to have either inferior (58) or improved responses (59, 60) to the

therapy. This inconsistency could be explained in several ways. First, the number of mCRPC patients harboring DDR mutations is very limited in each cohort. Second, the results can be biased due to different sampling, as metastatic biopsies are only feasible for patients with low-to-moderate tumor burden. This might exclude highly aggressive tumors and blood-based sequencing may underestimate the mutation rate as the somatic status is unknown for certain patients. Third, the disease showed extensive heterogeneity and patients had received various pre-treatments in the different cohorts. A recent prospective study showed that *BRC A2* mutation carriers have a worse outcome in mCRPC disease and this may be affected by the first line treatment used (61). However, future prospective studies are needed to shed further light on this issue and will hopefully resolve the above-mentioned controversy.

Table 4 Clinical outcome of mCRPC patients with wild type vs DDR gene mutations after standard AR targeting therapy

Author and year	Study design	Sampling	Treatment	DDR defect patients	PSA-PFS	OS
Annala et al 2017 (58)	Retrospective	Blood	Enzalutamide	24/319 (7.5%)	3.3 mo DDR (-)	29.7 mo DDR (-)
	Four cohorts	Germline	Abiraterone		vs 6.2 mo WT	vs 34.1 mo WT
Mateo et al 2018 (57)	Retrospective	Blood	Enzalutamide/	60/390 (15.4%)	8.3 mo DDR	36 mo DDR (-) vs
	Two cohorts	Germline	Abiraterone		(-), vs 8.3 mo WT	38.4 mo WT
Antonarakis et al 2018 (59)	Retrospective	Blood	Enzalutamide/	22/172 (12%)	10.2 mo DDR	41.1 mo DDR (-)
	/ prospective	Germline	Abiraterone		(-) vs 7.6 mo WT	vs 28.3 mo WT
Hussain et al 2018 (60)	Randomized phase II multicenter trial	Biopsy	Abiraterone	20/80 (25%)	16.6 mo DDR	N/A
		Mixed	plus Prednisone		(-) vs 8.2 mo WT	
Castro et al 2019 (61)	Prospective multicenter cohort	Blood	Abiraterone	16/302 (5.3%)	8.1 mo DDR (-)	N/A
		Germline	Enzalutamide	8/126 (6.3%)	Vs 9.2 mo WT (combined)	

PSA: prostate specific antigen; PFS: progression-free survival; OS: overall survival; DDR: DNA damage response; WT: wild-type.

5. AR and DDR pathway crosstalk

Clinical trials have shown that the combination of ADT or anti-androgens with radiotherapy significantly increases patient survival and reduces distant metastases compared to radiotherapy alone (64-69). It is widely perceived that suppression of the AR axis enhances the cytotoxic effects of radiotherapy and based on the beneficial effects, this combination is currently the standard of care for locally advanced PCa.

The molecular mechanism of radiosensitization induced by ADT was investigated in preclinical studies. Goodwin et al. reported that ADT potentiates the tumor-killing effect of ionizing radiation (IR) in AR proficient cells both *in vitro* and *in vivo*: ADT treated C4-2 (androgen independent) cells had a diminished capacity to repair IR induced DSBs. This study showed that the AR pathway directly regulates the NHEJ factor DNA-dependent protein kinase catalytic subunit (DNA-PKcs), resulting in a slight increase in NHEJ activity upon androgen addition in a plasmid-based functional assay (12). The involvement of NHEJ was confirmed by Polkinghorn et al. who identified a set of 32 DDR genes as direct AR target genes (70). Other studies using patient samples have demonstrated that castration primarily reduces Ku70 protein expression, which is essential for NHEJ (71, 72). These studies suggest that ADT enhances IR effects by impairing NHEJ activity. Reciprocally, IR treatment caused marked induction of the androgen target genes *TMPRSS2* and *FKBP5* (12), suggesting that DNA damage induces AR activity (Figure 2).

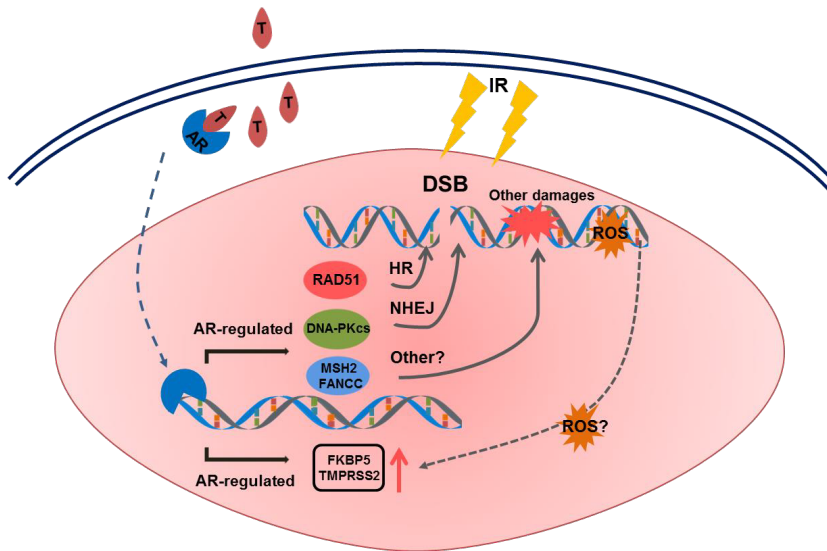


Figure 2. Interplay between androgen receptor (AR) and DNA damage repair in prostate cancer.

Activation of AR by dihydrotestosterone (T) leads to transcriptional upregulation of DNA repair genes in various repair pathways. Reciprocally, irradiation result in upregulation of keys genes in the AR pathway via ROS. HR, homologous recombination; NHEJ, non-homologous end-joining; ROS, reactive oxygen species; IR: irradiation.

In addition to direct regulation of the NHEJ pathway, other studies show that AR signaling plays a role in regulating genes involved in the HR, MMR and FA pathways

(12, 70, 73). Enzalutamide treatment suppressed the expression of the HR genes *BRCA1*, *RAD54L* and RecQ Mediated Genome Instability 2 (*RMI2*) (73). A combination strategy in which enzalutamide pretreatment was followed by the PARP inhibitor olaparib resulted in significantly increased PCa cell apoptosis and inhibited colony formation *in vitro*. Further *in vivo* evaluation showed clear synergistic suppressive effects on PCa xenografts in hormone-sensitive models, but not in CRPC models (73). However, from these studies, it is not yet clear whether enzalutamide directly induces HR deficiency, also called the BRCAness phenotype. A reduction of the S/G2 cell cycle fraction might also have caused reduction of HR gene expression, which resulted in reduced HR in the total cell population. Whatever the mechanistic explanation may be, this study warrants further clinical investigation into AR and PARP inhibitor combination therapies.

Based on these results, it is clear that both preclinical and clinical studies have found that AR signaling regulates the expression and/or function of DDR genes. Elucidation of the precise regulatory mechanisms and pathway interactions requires additional studies, which should focus on direct measurement of NHEJ and HR capacity in the presence and absence of AR signaling.

6. Exploiting DDR alterations for PCa treatment

As discussed above, 10-25% of PCa patients are harboring DDR mutations, especially among mCRPC patients. This section summarizes clinical and preclinical evidence how DDR alterations could be exploited therapeutically.

6.1 Immune checkpoint inhibitors

The successful development of immune checkpoint inhibitors such as programmed cell death protein 1 (PD-1) and programmed death-ligand 1 (PD-L1) inhibitors revolutionized the field of cancer immunotherapy (74). The interaction of PD-L1 on tumor cells with PD-1 on T-cells reduces T-cell functionality, preventing the immune system from attacking the tumor cells. Inhibitors that block this interaction can unleash a patient's own T cells to kill tumors (75). Immunotherapy responses appear to correlate with the mutational burden, presumably by the increase in neo-antigens (76). PCa patients harboring MMR mutations, such as in *MLH1* or *MSH2*, could be selected for PD-1 blockade immunotherapy, as a favorable response to PD-1 blockade therapy was observed previously in MMR deficient tumors, as a result of the high level of neo-antigens in various solid tumors (77). Interestingly, ductal adenocarcinoma, an aggressive histopathology of PCa, is associated with MMR defects, suggesting that these patients are possible candidates for this type of immunotherapy (78). Interestingly, an increase in neo-antigens was also observed in patients who harbor a HR deficiency (79). Altogether, these subgroups represent nearly 20% of mCRPC patients, making the use of PD-1/PD-L1 inhibitors a potentially attractive strategy for clinical trials in these patients.

6.2 PARP inhibitor treatments

Monotherapy

Tumors with compromised HR are highly sensitive to reduction of SSB repair by PARP1 inhibition, a phenomenon called synthetic lethality (80-82). The mechanism of action of PARP inhibitors was originally described as inhibition of SSB repair via blocking the catalytic activity of PARP1. Unrepaired SSBs will be converted into the more genotoxic DSBs during DNA replication. These DSBs are repaired via HR in normal cells, but cannot be repaired in HR-deficient cancer cells, leading to tumor-specific cell death. Recently, this model has been updated as studies have shown that various PARP inhibitors are able to trap PARP1 at the DNA damage site (83-85). Trapped PARP results in DSBs when the replication fork encounters this lesion, which require HR for resolution (Figure 3). Considering the different PARP trapping abilities of the different PARP inhibitors, various therapeutic responses can be expected, with talazoparib having the most profound PARP trapping and cytotoxic effects (86).

Following previous *in vitro* (80, 81) and *in vivo* studies in Brca2 knockout breast and ovarian tumor mouse models (87, 88), a number of trials evaluated PARP inhibitors as a single agent in CRPC patients with HR defects. The TOPARP study evaluated olaparib in a population of 50 mCRPC patients. Interestingly, 14 out of 16 DDR mutation carriers responded to olaparib treatment, compared to 2 of 33 patients in the non-DDR mutated group (56). The promising results from this study led to the initiation of a large number of clinical trials targeting PARP by different inhibitors with or without HR gene mutation preselection in order to validate the effect, evaluate its safety profile and define the optimal timing of prescribing PARP inhibitors in mCRPC (89-92). Interestingly, a recently published multicenter retrospective study including 23 mCRPC patients harboring DDR mutations (2 *BRC1A1*, 15 *BRC2A2* and 6 *ATM*) showed that men with *ATM* mutations responded inferior to PARP inhibitor treatment compared to *BRC1A1/2* mutation carriers (93). These data suggest that *ATM* mutated patients may not benefit from PARP inhibitor treatment as previously thought, and preselection of patients is importance to avoid unnecessary toxicity.

It is to be expected that due to increased use of next generation sequencing approaches, it is likely that more PCa patients with HR defects will be detected. However, the implementation and standardization of genomic testing still remains a major challenge. Besides blood based germline mutation and biopsy based somatic mutation testing, new studies are looking into circulating tumor cells (CTC) or cell-free DNA based detection of a panel of clinically actionable genes to select eligible patients (90, 94, 95). Moreover, the efforts made for identifying tumors with HR deficiency by using mutational signatures (HRDetect) or functional HRD tests will guide us to a more personalized cancer management approach (96-100).

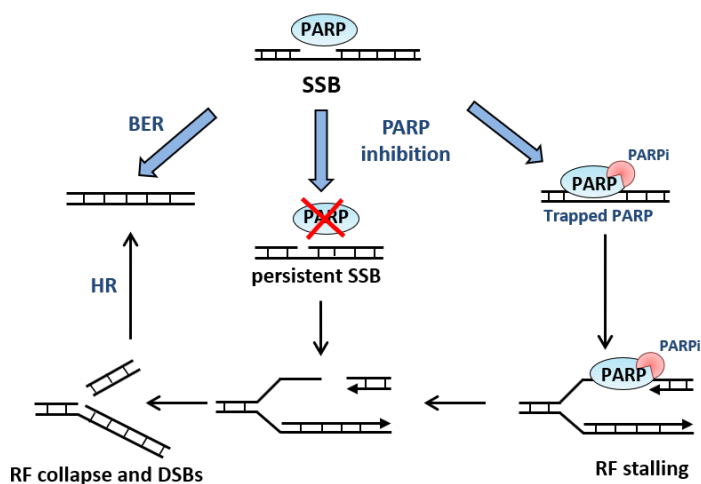


Figure 3. Mechanism of action of Poly(ADP-ribose) polymerase (PARP) inhibitor.

PARP enhances repair of single-strand breaks (SSBs) via base excision repair (BER). If SSBs remain unrepaired due to inhibition of PARP catalytic activity with PARP inhibitors (PARPi), double-strand breaks (DSBs) can be formed during replication. Alternatively, PARPi can trap the PARP protein on the DNA, which causes replication fork (RF) stalling and collapse. Homologous recombination (HR) is essential for repairing these DSBs.

Combination therapies

Besides PARP inhibition as monotherapy, trials have been initiated to evaluate combination of PARP inhibitors with other treatments in mCRPC patients. In view of the working mechanism of PARP inhibitors, an obvious strategy is to combine them with DNA-damaging agents, such as chemotherapy, radiotherapy and radioligand therapy (ongoing clinical trials are summarized in Table 5). Synergy with PARP inhibitors was identified in various clinical trials in other tumor types (101). However overlapping hematological toxicities may represent a major hurdle when combining DNA-damaging agents and PARP inhibitors (102).

Previous preclinical work offered the rationale for the potential synergy of combining AR-targeting agents with PARP inhibitors. First, blockage of AR signaling and PARP inhibition cause downregulation of the DNA repair capacity of the cells via different complementary pathways (DSB repair and SSB repair) (73, 103). According to preclinical studies, anti-androgen treatments may induce a BRCAness phenotype, which can be targeted by PARP inhibition. Second, PARP1 has been reported to promote AR-dependent transcription and PARP inhibitors will therefore reduce AR-functioning (104). Unfortunately, a randomized multicenter trial failed to show a significant difference in prostate-specific antigen (PSA) response rate and median progression-free survival (PFS) between patients treated with abiraterone/prednisone plus the PARP inhibitor veliparib compared to abiraterone/prednisone alone (105).

Lack of effectivity can be explained by inefficient PARP trapping by veliparib. Interestingly, another recent randomized double-blind phase 2 trial showed significantly longer PFS for mCRPC patients receiving olaparib plus abiraterone treatment than single abiraterone therapy. Although the combination strategy showed more adverse events than monotherapy, the health-related quality of life did not decline (106). These clinical data support the preclinical results in which synergy between olaparib and AR signaling inhibitor was found, regardless of the HR status (73, 103).

Other trials are combining PARP inhibitors with vascular endothelial growth factor (VEGF) inhibitors, which function by inhibiting tumor angiogenesis. Preclinical studies showed that restriction of angiogenesis induces hypoxia, which may create a BRCAness phenotype by reducing the expression of BRCA1 and RAD51 (107). The VEGF inhibitors bevacizumab and cediranib were reported to induce severe hypoxia, causing a reduction of HR capacity and increased sensitivity to PARP inhibitors (108). Based on these data, a clinical study targeting both processes in mCRPC patients is ongoing (Table 5).

Another approach that has been explored is the use of PARP inhibitors as radiosensitizer for patients with high-risk localized PCa (radiotherapy) or with metastatic lesions (radioligand therapy). Irradiation induces cell death by the production of reactive oxygen species (ROS) as well as by direct ionization of the DNA which leads to SSBs and DSBs. PARP inhibition is predicted to enhance this effect by preventing the repair of radiation-induced SSBs. *In vitro* models support the idea that PARP inhibitors can enhance radiation-induced cytotoxicity (109, 110). Similar results were also found in targeted radioligand therapy for PCa (111), suggesting targeted radiotherapy can be further optimized in combination with PARP inhibitors. As described above, the MMR pathway has been implicated in the immunotherapy response and alterations in other DDR genes may also increase efficacy of immunotherapy (79, 112). Therefore, several studies were started in which PARP inhibitors were combined with immunotherapy. The PARP1 inhibitor talazoparib has been found to exhibit immunoregulatory effects in a *Brcal* deficient ovarian cancer mouse model as the number of peritoneal CD8 (+) T cells and NK cells increased significantly after talazoparib treatment (113). Furthermore, Higuchi et al. have shown that cytotoxic T-lymphocyte antigen-4 (CTLA-4) antibody synergized with PARP inhibitors therapeutically in the *Brcal* deficient ovarian cancer mouse model and support the clinical testing of this combination regimen (114). The first clinical trial with a small cohort of patients showed that the PD-L1 inhibitor durvalumab plus olaparib in mCRPC patients has acceptable toxicity and efficacy, and the therapeutic response is superior in men with DDR abnormalities (115). This triggered other studies to investigate whether mCRPC patients with DDR defects would benefit from this particular combination therapy. Clinical trials are ongoing to evaluate its safety, optimal dosing and efficacy (Table 5).

Table 5 Ongoing clinical trials with combination PAPR inhibition therapy

Strategy	Trial	Treatment	Subjects	Period	Design	Primary end point
PARP inhibitor plus AR-targeting agent	NCT02924766	Niraparib + Apalutamide or Abiraterone	mCRPC	October 2016 – June 2018	A phase 1 and single group, open label study	Safety and pharmacokinetics of Niraparib
	NCT02324998	Olaparib ± Degarelix	Radical prostatectomy in men with early, localized intermediate-/high-risk Pca	December 2016 - July 2018	Randomized	Determination of PARP inhibition
	NCT03395197	Talazoparib + Enzalutamide versus Enzalutamide	mCRPC with DDR defect	December 2017 - May 2022	Part 1: an open-label, non-randomized, safety and PK run-in study Part 2: a randomized, double-blind, placebo-controlled, multinational study	part 1: Confirm the dose of Talazoparib part 2: Radiographic PFS
	NCT01576172	Abiraterone ± Veliparib	mCRPC	March 2012 - December 2018	A Randomized Gene (ETS) Fusion Stratified Phase 2 Trial	PSA response rate
	NCT03012321	Olaparib, Abiraterone, or Abiraterone + Olaparib	mCRPC with DDR defects	January 2017 - January 2022	Phase II study randomized, open-label, multicenter	PFS
	NCT03076203	Niraparib + Ra ²³ dichloride	mCRPC	March 2017 - May 2018	Phase IB Trial Single Group Open Label	MTD
PARP inhibitor plus radioligand Therapy	NCT03317392	Ra ²²³ dichloride + Olaparib versus Ra ²²³ dichloride	mCRPC	October 2018 - April 2020	A Phase 1/2 Study	MTD Radiographic PFS
	NCT02893917	Olaparib versus Olaparib + Cediranib	mCRPC	December 2016 - December 2019	Phase II trial randomized	Radiographic PFS
PARP inhibitor plus immuno-therapy	NCT03431350	Niraparib + PD-1 monoclonal antibody, JNJ-63723283	mCRPC	February 2018 - June 2018	A Phase 1b/2 study, Non-Randomized, Open Label,	Part 1: Incidence of Specified Toxicities Part 2: Objective RR and AEs
	NCT03330405	Talazoparib Plus Avelumab	Advanced or metastatic solid tumors (including Pca)	October 2017 - March 2020	A Phase 1b/2 non-randomized sequential assignment study	DLT OR

mCRPC: metastatic castration resistant prostate cancer; RR: response rate; PSA: prostate specific antigen; PFS: progression-free survival; MTD: maximum tolerated dose; AEs: adverse events; DLT: dose limiting toxicity; OR: overall response.

6.3 Platinum-based chemotherapy

Platinum-based agents cause crosslinking of DNA, most notably interstrand crosslinks that covalently couple both DNA strands (116). These crosslinks interfere with DNA replication and translation and induce apoptosis. Although platinum compounds have long been studied in advanced PCa patients in a large number of clinical trials, the various treatment regimens have not demonstrated a significant overall survival benefit in the overall patient population, and no treatment has received approval. Tumors with mutations in *BRCA1/2* are specifically susceptible to platinum-based chemotherapy since the interstrand crosslinks can only be adequately repaired by HR-based DNA repair. Recent clinical trials provided evidence that breast and ovarian cancer patients with *BRCA1/2* mutations are highly sensitive to platinum-based chemotherapy (99, 117, 118). Pomerantz et al. retrospectively analyzed a single-institution cohort of mCRPC patients who received carboplatin-based chemotherapy and showed that *BRCA2* mutation carriers had a higher response rate to carboplatin-based chemotherapy than non-*BRCA2* associated patients (119). Furthermore, a few case reports also highlighted exceptional responses to platinum-treatment in mCRPC patients with HR defects (120, 121). With such promising results, more trials of carboplatin alone and in combination with docetaxel have been designed in advanced PCa harboring DDR aberrations (ongoing clinical trials are summarized in Table 6).

Table 6 Ongoing clinical trials with platinum based chemotherapy

Trial	Treatment	Subjects	Period	Design	Primary end point
NCT02311764C	Carboplatin	mCRPC with <i>PTEN</i> loss and/or DDR defect	February 2015 - April 2019	A Single Arm Open Label Phase II Pilot Study	PSA Response
NCT02598895	Docetaxel + Carboplatin	mCRPC with <i>BRCA1/2</i> inactivation	January 2016 – June 2018	Pilot and single group assignment study	PSA Response
NCT02985021	Docetaxel + Carboplatin	mCRPC with <i>BRCA1/2</i> , <i>ATM</i> inactivation	November 2016 - November 2019	A phase 2 study Single Group Assignment, Open label	PSA response

mCRPC: metastatic castration resistant prostate cancer; PSA: prostate specific antigen; *PTEN*: phosphatase and tensin homolog; *ATM*: Ataxia–telangiectasia mutated serine/threonine kinase; *BRCA1/2*: Breast Cancer 1 and 2

6.4 DNA-PKcs targeting treatment

Besides the discovery of the AR-DDR crosstalk via the key mediator DNA-PKcs, a following study has identified a new function of DNA-PKcs as a potent driver of PCa progression. Goodwin et al. found that DNA-PKcs functions as a selective modulator of transcriptional networks that induce cell migration, invasion and metastasis and suppression of DNA-PKcs inhibits tumor metastases. Moreover, DNA-PKcs levels are significantly increased in advanced disease and can be independently predictive for biochemical recurrence, poor overall survival (122). Based on these findings, a phase I

clinical trial is ongoing (NCT02833883) in which the combination of enzalutamide and DNA-PKcs inhibitor CC-115 is evaluated for treatment of mCRPC.

7. Conclusion

The identification of DDR defects in mCRPC has driven the interest for further evaluation of these gene deficiencies in patient stratification. PARP inhibitors may become part of the standard care of mCRPC patients who harbor HR deficiency; however, the most optimal use of PARP inhibitors alone or in combination with other treatment modalities remains to be elucidated. Given the clearly aggressive course of DDR-deficient PCa, there is an urgent need to identify these patients at an early stage where the right treatment strategy could greatly improve prognosis. The discovery that the AR may regulate DDR factors opens a new array of possible strategies to optimize treatment combinations. Future studies are needed to broaden our understanding of DDR defects and interactions between DNA repair pathways and other processes in PCa, as well as to determine how this knowledge can be used to improve diagnostic, prognostic and therapeutic approaches.

Funding source

This work was supported by the Chinese Scholarship Council (WZ, grant number 201506270172), the Dutch Cancer Foundation (DvG, WvW, JN, grant number 10317), the Daniel den Hoed Foundation (JN), the Erasmus University Rotterdam (JN).

Conflict of interest

We have no competing financial interests in relation to the described work.

References

1. Bray F, Ferlay J, Soerjomataram I, Siegel RL, Torre LA, Jemal A. Global cancer statistics 2018: GLOBOCAN estimates of incidence and mortality worldwide for 36 cancers in 185 countries. *CA Cancer J Clin*. 2018 Nov;68(6):394-424.
2. Cornford P, Bellmunt J, Bolla M, Briers E, De Santis M, Gross T, et al. EAU-ESTRO-SIOG guidelines on prostate cancer. Part II: treatment of relapsing, metastatic, and castration-resistant prostate cancer. *European urology*. 2017;71(4):630-42.
3. Mottet N, Bellmunt J, Bolla M, Briers E, Cumberbatch MG, De Santis M, et al. EAU-ESTRO-SIOG guidelines on prostate cancer. Part 1: screening, diagnosis, and local treatment with curative intent. *European urology*. 2017;71(4):618-29.
4. Nuhn P, De Bono JS, Fizazi K, Freedland SJ, Grilli M, Kantoff PW, et al. Update on Systemic Prostate Cancer Therapies: Management of Metastatic Castration-resistant Prostate Cancer in the Era of Precision Oncology. *Eur Urol*. 2019 Jan;75(1):88-99.
5. Castro E, Goh C, Olmos D, Saunders E, Leongamornlert D, Tymrakiewicz M, et al. Germline BRCA mutations are associated with higher risk of nodal involvement, distant metastasis, and poor survival outcomes in prostate cancer. *J Clin Oncol*. 2013 May 10;31(14):1748-57.
6. Cybulski C, Wokolorczyk D, Kluzniak W, Jakubowska A, Gorski B, Gronwald J, et al. An inherited NBN mutation is associated with poor prognosis prostate cancer. *Br J Cancer*. 2013 Feb 5;108(2):461-8.
7. Grindedal EM, Moller P, Eeles R, Stormorken AT, Bowitz-Lothe IM, Landro SM, et al. Germ-line mutations in mismatch repair genes associated with prostate cancer. *Cancer Epidemiol Biomarkers Prev*. 2009 Sep;18(9):2460-7.
8. Kote-Jarai Z, Jugurnauth S, Mulholland S, Leongamornlert DA, Guy M, Edwards S, et al. A recurrent truncating germline mutation in the BRIP1/FANCD1 gene and susceptibility to prostate cancer. *Br J Cancer*. 2009 Jan 27;100(2):426-30.
9. Leongamornlert D, Mahmud N, Tymrakiewicz M, Saunders E, Dadaev T, Castro E, et al. Germline BRCA1 mutations increase prostate cancer risk. *British journal of cancer*. 2012;106(10):1697.
10. Mateo J, Boysen G, Barbieri CE, Bryant HE, Castro E, Nelson PS, et al. DNA Repair in Prostate Cancer: Biology and Clinical Implications. *European Urology*. 2017 2017/03/01;71(3):417-25.
11. Tangutoori S, Baldwin P, Sridhar S. PARP inhibitors: A new era of targeted therapy. *Maturitas*. 2015;81(1):5-9.
12. Goodwin JF, Schiewer MJ, Dean JL, Schrecengost RS, de Leeuw R, Han S, et al. A hormone-DNA repair circuit governs the response to genotoxic insult. *Cancer Discov*. 2013 Nov;3(11):1254-71.
13. Thompson TC, Li L, Broom BM. Combining enzalutamide with PARP inhibitors: Pharmaceutically induced BRCAness. *Oncotarget*. 2017;8(55):93315.
14. Lord CJ, Ashworth A. BRCAness revisited. *Nat Rev Cancer*. 2016 Feb;16(2):110-20.
15. Tubbs A, Nussenzweig A. Endogenous DNA damage as a source of genomic instability in cancer. *Cell*. 2017;168(4):644-56.
16. Aguilera A, Gaillard H. Transcription and recombination: when RNA meets DNA. *Cold Spring Harb Perspect Biol*. 2014 Aug 1;6(8).
17. Syeda AH, Hawkins M, McGlynn P. Recombination and replication. *Cold Spring Harb Perspect Biol*. 2014 Oct 23;6(11):a016550.
18. Ciccia A, Elledge SJ. The DNA damage response: making it safe to play with knives. *Mol Cell*. 2010 Oct 22;40(2):179-204.
19. Hoeijmakers JHJ. DNA damage, aging, and cancer. *New England Journal of Medicine*. 2009;361(15):1475-85.
20. Jackson SP, Bartek J. The DNA-damage response in human biology and disease. *Nature*. 2009 Oct 22;461(7267):1071-8.

21. Wallace SS. Base excision repair: a critical player in many games. *DNA Repair (Amst)*. 2014 Jul;19:14-26.
22. Li Z, Pearlman AH, Hsieh P. DNA mismatch repair and the DNA damage response. *DNA Repair (Amst)*. 2016 Feb;38:94-101.
23. Moldovan GL, D'Andrea AD. How the fanconi anemia pathway guards the genome. *Annu Rev Genet*. 2009;43:223-49.
24. Ceccaldi R, Rondinelli B, D'Andrea AD. Repair Pathway Choices and Consequences at the Double-Strand Break. *Trends Cell Biol*. 2016 Jan;26(1):52-64.
25. d'Adda di Fagagna F. Living on a break: cellular senescence as a DNA-damage response. *Nat Rev Cancer*. 2008 Jul;8(7):512-22.
26. Dhawan M, Ryan CJ, Ashworth A. DNA Repair Deficiency Is Common in Advanced Prostate Cancer: New Therapeutic Opportunities. *Oncologist*. 2016 Aug;21(8):940-5.
27. Dominguez-Valentin M, Joost P, Therkildsen C, Jonsson M, Rambech E, Nilbert M. Frequent mismatch-repair defects link prostate cancer to Lynch syndrome. *BMC Urol*. 2016 Mar 24;16:15.
28. Gallagher DJ, Gaudet MM, Pal P, Kirchoff T, Balistreri L, Vora K, et al. Germline BRCA mutations denote a clinicopathologic subset of prostate cancer. *Clin Cancer Res*. 2010 Apr 1;16(7):2115-21.
29. Rosty C, Walsh MD, Lindor NM, Thibodeau SN, Mundt E, Gallinger S, et al. High prevalence of mismatch repair deficiency in prostate cancers diagnosed in mismatch repair gene mutation carriers from the colon cancer family registry. *Fam Cancer*. 2014 Dec;13(4):573-82.
30. Venkitaraman AR. Functions of BRCA1 and BRCA2 in the biological response to DNA damage. *J Cell Sci*. 2001 Oct;114(Pt 20):3591-8.
31. Venkitaraman AR. Cancer Susceptibility and the Functions of BRCA1 and BRCA2. *Cell*. 2002 2002/01/25;108(2):171-82.
32. Gudmundsdottir K, Ashworth A. The roles of BRCA1 and BRCA2 and associated proteins in the maintenance of genomic stability. *Oncogene*. [Review]. 2006;25:5864.
33. Jeggo PA, Pearl LH, Carr AM. DNA repair, genome stability and cancer: a historical perspective. *Nat Rev Cancer*. 2016 Jan;16(1):35-42.
34. Roy R, Chun J, Powell SN. BRCA1 and BRCA2: different roles in a common pathway of genome protection. *Nat Rev Cancer*. 2011 Dec 23;12(1):68-78.
35. Wang M, Li Q, Gu C, Zhu Y, Yang Y, Wang J, et al. Polymorphisms in nucleotide excision repair genes and risk of primary prostate cancer in Chinese Han populations. *Oncotarget*. 2017;8(15):24362.
36. Francis JC, McCarthy A, Thomsen MK, Ashworth A, Swain A. Brca2 and Trp53 deficiency cooperate in the progression of mouse prostate tumourigenesis. *PLoS Genet*. 2010 Jun 24;6(6):e1000995.
37. Jiricny J. Postreplicative mismatch repair. *Cold Spring Harb Perspect Biol*. 2013 Apr 1;5(4):a012633.
38. Latham A, Srinivasan P, Kemel Y, Shia J, Bandlamudi C, Mandelker D, et al. Microsatellite Instability Is Associated With the Presence of Lynch Syndrome Pan-Cancer. *J Clin Oncol*. 2019 Feb 1;37(4):286-95.
39. Attard G, Parker C, Eeles RA, Schröder F, Tomlins SA, Tannock I, et al. Prostate cancer. *The Lancet*. [doi: 10.1016/S0140-6736(14)61947-4]. 2016;387(10013):70-82.
40. Baca SC, Prandi D, Lawrence MS, Mosquera JM, Romanell A, Drier Y, et al. Punctuated evolution of prostate cancer genomes. *Cell*. 2013 Apr 25;153(3):666-77.
41. Barbieri CE, Baca SC, Lawrence MS, Demichelis F, Blattner M, Theurillat JP, et al. Exome sequencing identifies recurrent SPOP, FOXA1 and MED12 mutations in prostate cancer. *Nat Genet*. 2012 May 20;44(6):685-9.
42. Cancer Genome Atlas Research N. The Molecular Taxonomy of Primary Prostate Cancer. *Cell*. 2015 Nov 5;163(4):1011-25.

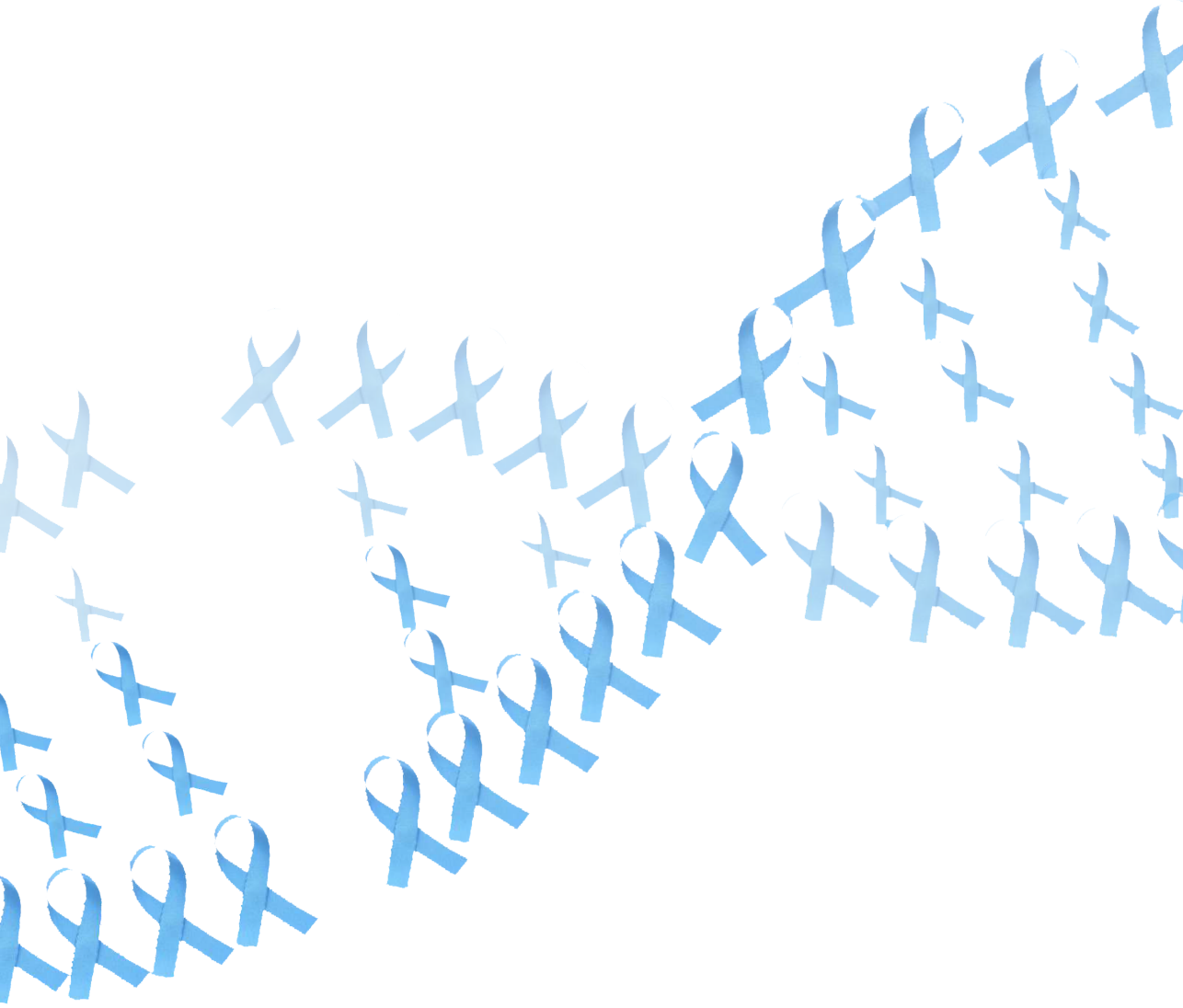
43. Cerami E, Gao J, Dogrusoz U, Gross BE, Sumer SO, Aksoy BA, et al. The cBio cancer genomics portal: an open platform for exploring multidimensional cancer genomics data. *Cancer Discov*. 2012 May;2(5):401-4.
44. Ren S, Wei GH, Liu D, Wang L, Hou Y, Zhu S, et al. Whole-genome and Transcriptome Sequencing of Prostate Cancer Identify New Genetic Alterations Driving Disease Progression. *Eur Urol*. 2017 Sep 18.
45. Fraser M, Sabelnykova VY, Yamaguchi TN, Heisler LE, Livingstone J, Huang V, et al. Genomic hallmarks of localized, non-indolent prostate cancer. *Nature*. 2017 Jan 19;541(7637):359-64.
46. Bangma CH, Roobol MJ. Defining and predicting indolent and low risk prostate cancer. *Crit Rev Oncol Hematol*. 2012 Aug;83(2):235-41.
47. Irshad S, Bansal M, Castillo-Martin M, Zheng T, Aytes A, Wenske S, et al. A molecular signature predictive of indolent prostate cancer. *Sci Transl Med*. 2013 Sep 11;5(202):202ra122.
48. Kamoun A, Cancel-Tassin G, Fromont G, Elarouci N, Armenoult L, Ayadi M, et al. Comprehensive molecular classification of localized prostate adenocarcinoma reveals a tumour subtype predictive of non-aggressive disease. *Annals of Oncology*. [doi: 10.1093/annonc/mdy224]. 2018;29(8):1814-21.
49. Bancroft EK, Page EC, Castro E, Lilja H, Vickers A, Sjoberg D, et al. Targeted prostate cancer screening in BRCA1 and BRCA2 mutation carriers: results from the initial screening round of the IMPACT study. *Eur Urol*. 2014 Sep;66(3):489-99.
50. Carter BS, Beaty TH, Steinberg GD, Childs B, Walsh PC. Mendelian inheritance of familial prostate cancer. *Proceedings of the National Academy of Sciences of the United States of America*. 1992;89(8):3367-71.
51. Petrovics G, Price DK, Lou H, Chen Y, Garland L, Bass S, et al. Increased frequency of germline BRCA2 mutations associates with prostate cancer metastasis in a racially diverse patient population. *Prostate Cancer Prostatic Dis*. 2018 Dec 12.
52. Na R, Zheng SL, Han M, Yu H, Jiang D, Shah S, et al. Germline Mutations in ATM and BRCA1/2 Distinguish Risk for Lethal and Indolent Prostate Cancer and are Associated with Early Age at Death. *Eur Urol*. 2017 May;71(5):740-7.
53. Evans JR, Zhao SG, Chang SL, Tomlins SA, Erho N, Sboner A, et al. Patient-Level DNA Damage and Repair Pathway Profiles and Prognosis After Prostatectomy for High-Risk Prostate Cancer. *JAMA Oncol*. 2016 Apr;2(4):471-80.
54. Grasso CS, Wu YM, Robinson DR, Cao X, Dhanasekaran SM, Khan AP, et al. The mutational landscape of lethal castration-resistant prostate cancer. *Nature*. 2012 Jul 12;487(7406):239-43.
55. Robinson D, Van Allen Eliezer M, Wu Y-M, Schultz N, Lonigro Robert J, Mosquera J-M, et al. Integrative Clinical Genomics of Advanced Prostate Cancer. *Cell*. 2015 2015/05/21;161(5):1215-28.
56. Mateo J, Carreira S, Sandhu S, Miranda S, Mossop H, Perez-Lopez R, et al. DNA-Repair Defects and Olaparib in Metastatic Prostate Cancer. *N Engl J Med*. 2015 Oct 29;373(18):1697-708.
57. Mateo J, Cheng HH, Beltran H, Dolling D, Xu W, Pritchard CC, et al. Clinical Outcome of Prostate Cancer Patients with Germline DNA Repair Mutations: Retrospective Analysis from an International Study. *Eur Urol*. 2018 May;73(5):687-93.
58. Annala M, Struss WJ, Warner EW, Beja K, Vandekerkhove G, Wong A, et al. Treatment Outcomes and Tumor Loss of Heterozygosity in Germline DNA Repair-deficient Prostate Cancer. *Eur Urol*. 2017 Jul;72(1):34-42.
59. Antonarakis ES, Lu C, Luber B, Liang C, Wang H, Chen Y, et al. Germline DNA-repair Gene Mutations and Outcomes in Men with Metastatic Castration-resistant Prostate Cancer Receiving First-line Abiraterone and Enzalutamide. *Eur Urol*. 2018 Aug;74(2):218-25.

60. Hussain M, Daignault-Newton S, Twardowski PW, Albany C, Stein MN, Kunju LP, et al. Targeting Androgen Receptor and DNA Repair in Metastatic Castration-Resistant Prostate Cancer: Results From NCI 9012. *J Clin Oncol*. 2018 Apr 1;36(10):991-9.
61. Castro E, Romero-Laorden N, Del Pozo A, Lozano R, Medina A, Puente J, et al. PROREPAIR-B: A Prospective Cohort Study of the Impact of Germline DNA Repair Mutations on the Outcomes of Patients With Metastatic Castration-Resistant Prostate Cancer. *J Clin Oncol*. 2019 Jan 9;JCO1800358.
62. Poeppel TD, Handkiewicz-Junak D, Andreeff M, Becherer A, Bockisch A, Fricke E, et al. EANM guideline for radionuclide therapy with radium-223 of metastatic castration-resistant prostate cancer. *Eur J Nucl Med Mol Imaging*. 2018 May;45(5):824-45.
63. Isaacsson Velho P, Qazi F, Hassan S, Carducci MA, Denmeade SR, Markowski MC, et al. Efficacy of Radium-223 in Bone-metastatic Castration-resistant Prostate Cancer with and Without Homologous Repair Gene Defects. *Eur Urol*. 2018 Oct 4.
64. Bolla M, Collette L, Blank L, Warde P, Dubois JB, Mirimanoff RO, et al. Long-term results with immediate androgen suppression and external irradiation in patients with locally advanced prostate cancer (an EORTC study): a phase III randomised trial. *Lancet*. 2002 Jul 13;360(9327):103-6.
65. Bolla M, de Reijke TM, Van Tienhoven G, Van den Bergh AC, Oddens J, Poortmans PM, et al. Duration of androgen suppression in the treatment of prostate cancer. *N Engl J Med*. 2009 Jun 11;360(24):2516-27.
66. Bolla M, Gonzalez D, Warde P, Dubois JB, Mirimanoff RO, Storme G, et al. Improved survival in patients with locally advanced prostate cancer treated with radiotherapy and goserelin. *N Engl J Med*. 1997 Jul 31;337(5):295-300.
67. Shipley WU, Seiferheld W, Lukka HR, Major PP, Heney NM, Grignon DJ, et al. Radiation with or without Antiandrogen Therapy in Recurrent Prostate Cancer. *N Engl J Med*. 2017 Feb 2;376(5):417-28.
68. Warde P, Mason M, Ding K, Kirkbride P, Brundage M, Cowan R, et al. Combined androgen deprivation therapy and radiation therapy for locally advanced prostate cancer: a randomised, phase 3 trial. *Lancet*. 2011 Dec 17;378(9809):2104-11.
69. Widmark A, Klepp O, Solberg A, Damber JE, Angelsen A, Fransson P, et al. Endocrine treatment, with or without radiotherapy, in locally advanced prostate cancer (SPCG-7/SFUO-3): an open randomised phase III trial. *Lancet*. 2009 Jan 24;373(9660):301-8.
70. Polkinghorn WR, Parker JS, Lee MX, Kass EM, Spratt DE, laquinta PJ, et al. Androgen receptor signaling regulates DNA repair in prostate cancers. *Cancer Discov*. 2013 Nov;3(11):1245-53.
71. Al-Ubaidi FL, Schultz N, Loseva O, Egevad L, Granfors T, Helleday T. Castration therapy results in decreased Ku70 levels in prostate cancer. *Clin Cancer Res*. 2013 Mar 15;19(6):1547-56.
72. Tarish FL, Schultz N, Tanoglidis A, Hamberg H, Letocha H, Karaszi K, et al. Castration radiosensitizes prostate cancer tissue by impairing DNA double-strand break repair. *Sci Transl Med*. 2015 Nov 4;7(312):312re11.
73. Li L, Karanika S, Yang G, Wang J, Park S, Broom BM, et al. Androgen receptor inhibitor-induced "BRCAness" and PARP inhibition are synthetically lethal for castration-resistant prostate cancer. *Sci Signal*. 2017 May 23;10(480).
74. Pardoll DM. The blockade of immune checkpoints in cancer immunotherapy. *Nature Reviews Cancer*. [Review Article]. 2012;12:252.
75. Weber J. Immune checkpoint proteins: a new therapeutic paradigm for cancer--preclinical background: CTLA-4 and PD-1 blockade. *Semin Oncol*. 2010 Oct;37(5):430-9.
76. Rizvi NA, Hellmann MD, Snyder A, Kvistborg P, Makarov V, Havel JJ, et al. Mutational landscape determines sensitivity to PD-1 blockade in non-small cell lung cancer. *Science*. 2015;348(6230):124-8.

77. Le DT, Durham JN, Smith KN, Wang H, Bartlett BR, Aulakh LK, et al. Mismatch repair deficiency predicts response of solid tumors to PD-1 blockade. *Science*. 2017 Jul 28;357(6349):409-13.
78. Schweizer MT, Cheng HH, Tretiakova MS, Vakar-Lopez F, Klemfuss N, Konnick EQ, et al. Mismatch repair deficiency may be common in ductal adenocarcinoma of the prostate. *Oncotarget*. 2016 Dec 13;7(50):82504-10.
79. Strickland KC, Howitt BE, Shukla SA, Rodig S, Ritterhouse LL, Liu JF, et al. Association and prognostic significance of BRCA1/2-mutation status with neoantigen load, number of tumor-infiltrating lymphocytes and expression of PD-1/PD-L1 in high grade serous ovarian cancer. *Oncotarget*. 2016 Mar 22;7(12):13587-98.
80. Bryant HE, Schultz N, Thomas HD, Parker KM, Flower D, Lopez E, et al. Specific killing of BRCA2-deficient tumours with inhibitors of poly (ADP-ribose) polymerase. *Nature*. 2005;434(7035):913.
81. Farmer H, McCabe N, Lord CJ, Tutt AN, Johnson DA, Richardson TB, et al. Targeting the DNA repair defect in BRCA mutant cells as a therapeutic strategy. *Nature*. 2005 Apr 14;434(7035):917-21.
82. O'Neil NJ, Bailey ML, Hieter P. Synthetic lethality and cancer. *Nature Reviews Genetics*. [Review Article]. 2017;18:613.
83. Lord CJ, Ashworth A. PARP inhibitors: Synthetic lethality in the clinic. *Science*. 2017 Mar 17;355(6330):1152-8.
84. Murai J, Huang SY, Das BB, Renaud A, Zhang Y, Doroshow JH, et al. Trapping of PARP1 and PARP2 by Clinical PARP Inhibitors. *Cancer Res*. 2012 Nov 1;72(21):5588-99.
85. Murai J, Huang SY, Renaud A, Zhang Y, Ji J, Takeda S, et al. Stereospecific PARP trapping by BMN 673 and comparison with olaparib and rucaparib. *Mol Cancer Ther*. 2014 Feb;13(2):433-43.
86. Shen Y, Rehman FL, Feng Y, Boshuizen J, Bajrami I, Elliott R, et al. BMN 673, a novel and highly potent PARP1/2 inhibitor for the treatment of human cancers with DNA repair deficiency. *Clin Cancer Res*. 2013 Sep 15;19(18):5003-15.
87. Hay T, Matthews JR, Pietzka L, Lau A, Cranston A, Nygren AO, et al. Poly(ADP-ribose) polymerase-1 inhibitor treatment regresses autochthonous Brca2/p53-mutant mammary tumors in vivo and delays tumor relapse in combination with carboplatin. *Cancer Res*. 2009 May 1;69(9):3850-5.
88. Kortmann U, McAlpine JN, Xue H, Guan J, Ha G, Tully S, et al. Tumor growth inhibition by olaparib in BRCA2 germline-mutated patient-derived ovarian cancer tissue xenografts. *Clin Cancer Res*. 2011 Feb 15;17(4):783-91.
89. Christenson ES, Antonarakis ES. PARP inhibitors for homologous recombination-deficient prostate cancer. *Expert Opinion on Emerging Drugs*. [doi: 10.1080/14728214.2018.1459563]. 2018 2018/04/03;23(2):123-33.
90. Dhawan M, Ryan CJ. BRCAness and prostate cancer: diagnostic and therapeutic considerations. *Prostate Cancer Prostatic Dis*. 2018 Nov;21(4):488-98.
91. Palmbos PL, Hussain MH. Targeting PARP in Prostate Cancer: Novelty, Pitfalls, and Promise. *Oncology (Williston Park)*. 2016 May;30(5):377-85.
92. Ramakrishnan Geethakumari P, Schiewer MJ, Knudsen KE, Kelly WK. PARP Inhibitors in Prostate Cancer. *Curr Treat Options Oncol*. 2017 Jun;18(6):37.
93. Marshall CH, Sokolova AO, McNatty AL, Cheng HH, Eisenberger MA, Bryce AH, et al. Differential Response to Olaparib Treatment Among Men with Metastatic Castration-resistant Prostate Cancer Harboring BRCA1 or BRCA2 Versus ATM Mutations. *Eur Urol*. 2019 Feb 20.
94. Gordon V, Angel ED, Jerry L, Stephanie G, Laura L, Yipeng W, et al. A single cell genomic signature to detect homologous recombination deficiency (HRD) and PARP inhibitors sensitivity using patient's circulating tumor cells (CTCs). *Journal of Clinical Oncology*. 2016;34(15_suppl):e23015-e.

95. Lanman RB, Mortimer SA, Zill OA, Sebisano D, Lopez R, Blau S, et al. Analytical and Clinical Validation of a Digital Sequencing Panel for Quantitative, Highly Accurate Evaluation of Cell-Free Circulating Tumor DNA. *PLoS One*. 2015;10(10):e0140712.
96. Davies H, Glodzik D, Morganello S, Yates LR, Staaf J, Zou X, et al. HRDetect is a predictor of BRCA1 and BRCA2 deficiency based on mutational signatures. *Nat Med*. 2017 Apr;23(4):517-25.
97. Meijer TG, Verkaik NS, Sieuwerts AM, van Riet J, Naipal KAT, van Deurzen CHM, et al. Functional Ex vivo Assay Reveals Homologous Recombination Deficiency in Breast Cancer Beyond BRCA Gene Defects. *Clin Cancer Res*. 2018 Aug 23.
98. Naipal KA, Verkaik NS, Ameziane N, van Deurzen CH, Ter Brugge P, Meijers M, et al. Functional ex vivo assay to select homologous recombination-deficient breast tumors for PARP inhibitor treatment. *Clin Cancer Res*. 2014 Sep 15;20(18):4816-26.
99. Telli ML, Timms KM, Reid J, Hennessy B, Mills GB, Jensen KC, et al. Homologous recombination deficiency (HRD) score predicts response to platinum-containing neoadjuvant chemotherapy in patients with triple-negative breast cancer. *Clinical cancer research*. 2016;22(15):3764-73.
100. Zhang W, van Weerden WM, de Ridder CMA, Erkens-Schulze S, Schonfeld E, Meijer TG, et al. Ex vivo treatment of prostate tumor tissue recapitulates in vivo therapy response. *Prostate*. 2018 Dec 5.
101. Dréan A, Lord CJ, Ashworth A. PARP inhibitor combination therapy. *Critical Reviews in Oncology/Hematology*. 2016 2016/12/01;108:73-85.
102. Hussain M, Carducci MA, Slovin S, Cetnar J, Qian J, McKeegan EM, et al. Targeting DNA repair with combination veliparib (ABT-888) and temozolomide in patients with metastatic castration-resistant prostate cancer. *Investigational New Drugs*. [journal article]. 2014 October 01;32(5):904-12.
103. Asim M, Tarish F, Zecchini HI, Sanjiv K, Gelali E, Massie CE, et al. Synthetic lethality between androgen receptor signalling and the PARP pathway in prostate cancer. *Nat Commun*. 2017 Aug 29;8(1):374.
104. Schiewer MJ, Goodwin JF, Han S, Brenner JC, Augello MA, Dean JL, et al. Dual roles of PARP-1 promote cancer growth and progression. *Cancer Discov*. 2012 Dec;2(12):1134-49.
105. Maha H, Stephanie D-N, Przemyslaw WT, Costantine A, Mark NS, Lakshmi PK, et al. Targeting Androgen Receptor and DNA Repair in Metastatic Castration-Resistant Prostate Cancer: Results From NCI 9012. *Journal of Clinical Oncology*. 2018;36(10):991-9.
106. Clarke N, Wiechno P, Alekseev B, Sala N, Jones R, Kocak I, et al. Olaparib combined with abiraterone in patients with metastatic castration-resistant prostate cancer: a randomised, double-blind, placebo-controlled, phase 2 trial. *Lancet Oncol*. 2018 Jul;19(7):975-86.
107. Bindra RS, Gibson SL, Meng A, Westermarck U, Jasin M, Pierce AJ, et al. Hypoxia-Induced Down-regulation of BRCA1 Expression by E2Fs. *Cancer Research*. 2005;65(24):11597-604.
108. Chan N, Bristow RG. "Contextual" Synthetic Lethality and/or Loss of Heterozygosity: Tumor Hypoxia and Modification of DNA Repair. *Clinical Cancer Research*. 2010;16(18):4553-60.
109. Barreto-Andrade JC, Efimova EV, Mauceri HJ, Beckett MA, Sutton HG, Darga TE, et al. Response of human prostate cancer cells and tumors to combining PARP inhibition with ionizing radiation. *Mol Cancer Ther*. 2011 Jul;10(7):1185-93.
110. Rae C, Mairs RJ. Evaluation of the radiosensitizing potency of chemotherapeutic agents in prostate cancer cells. *Int J Radiat Biol*. 2017 Feb;93(2):194-203.
111. Tesson M, Rae C, Nixon C, Babich JW, Mairs RJ. Preliminary evaluation of prostate-targeted radiotherapy using (131) I-MIP-1095 in combination with radiosensitising chemotherapeutic drugs. *J Pharm Pharmacol*. 2016 Jul;68(7):912-21.

112. Teo MY, Seier K, Ostrovnaya I, Regazzi AM, Kania BE, Moran MM, et al. Alterations in DNA Damage Response and Repair Genes as Potential Marker of Clinical Benefit From PD-1/PD-L1 Blockade in Advanced Urothelial Cancers. *J Clin Oncol*. 2018 Jun 10;36(17):1685-94.
113. Huang J, Wang L, Cong Z, Amoozgar Z, Kiner E, Xing D, et al. The PARP1 inhibitor BMN 673 exhibits immunoregulatory effects in a Brca1(-/-) murine model of ovarian cancer. *Biochem Biophys Res Commun*. 2015 Aug 7;463(4):551-6.
114. Higuchi T, Flies DB, Marjon NA, Mantia-Smaldone G, Ronner L, Gimotty PA, et al. CTLA-4 Blockade Synergizes Therapeutically with PARP Inhibition in BRCA1-Deficient Ovarian Cancer. *Cancer Immunol Res*. 2015 Nov;3(11):1257-68.
115. Karzai F, VanderWeele D, Madan RA, Owens H, Cordes LM, Hankin A, et al. Activity of durvalumab plus olaparib in metastatic castration-resistant prostate cancer in men with and without DNA damage repair mutations. *J Immunother Cancer*. 2018 Dec 4;6(1):141.
116. Dasari S, Tchounwou PB. Cisplatin in cancer therapy: molecular mechanisms of action. *Eur J Pharmacol*. 2014 Oct 5;740:364-78.
117. Byrski T, Dent R, Blecharz P, Foszczynska-Kloda M, Gronwald J, Huzarski T, et al. Results of a phase II open-label, non-randomized trial of cisplatin chemotherapy in patients with BRCA1-positive metastatic breast cancer. *Breast cancer research*. 2012;14(4):R110.
118. Lesnock JL, Darcy KM, Tian C, Deloia JA, Thrall MM, Zahn C, et al. BRCA1 expression and improved survival in ovarian cancer patients treated with intraperitoneal cisplatin and paclitaxel: a Gynecologic Oncology Group Study. *Br J Cancer*. 2013 Apr 2;108(6):1231-7.
119. Pomerantz MM, Spisak S, Jia L, Cronin AM, Csabai I, Ledet E, et al. The association between germline BRCA2 variants and sensitivity to platinum-based chemotherapy among men with metastatic prostate cancer. *Cancer*. 2017 Sep 15;123(18):3532-9.
120. Cheng HH, Pritchard CC, Boyd T, Nelson PS, Montgomery B. Biallelic Inactivation of BRCA2 in Platinum-sensitive Metastatic Castration-resistant Prostate Cancer. *Eur Urol*. 2016 Jun;69(6):992-5.
121. Zafeiriou Z, Bianchini D, Chandler R, Rescigno P, Yuan W, Carreira S, et al. Genomic Analysis of Three Metastatic Prostate Cancer Patients with Exceptional Responses to Carboplatin Indicating Different Types of DNA Repair Deficiency. *Eur Urol*. 2019 Jan;75(1):184-92.
122. Goodwin JF, Kothari V, Drake JM, Zhao S, Dylgjeri E, Dean JL, et al. DNA-PKcs-Mediated Transcriptional Regulation Drives Prostate Cancer Progression and Metastasis. *Cancer Cell*. 2015 Jul 13;28(1):97-113.



Chapter 3

Ex vivo treatment of prostate tumor tissue recapitulates *in vivo* therapy response

Wenhao Zhang¹, Wytske M. van Weerden², Corrina M.A. de Ridder², Sigrun Erkens-Schulze², Edgar Schönfeld¹, Titia G. Meijer^{1,3}, Roland Kanaar^{1,3}, Dik C. van Gent^{1,3}, Julie Nonnekens^{1,4*}

1. Department of Molecular Genetics, Erasmus MC, Rotterdam, The Netherlands; 2. Department of Experimental Urology, Erasmus MC, Rotterdam, The Netherlands; 3. Oncode Institute, Erasmus MC, Rotterdam, The Netherlands; 4. Department of Radiology and Nuclear Medicine, Erasmus MC, Rotterdam, The Netherlands

Published in *Prostate*. 2019;79(4):390-402.

Abstract

Background

In vitro models of prostate cancer (PCa) are not always reliable to evaluate anticancer treatment efficacy. This limitation may be overcome by using viable organotypic tumor slice material. Here we report on the establishment of an *ex vivo* method to culture tissue slices from patient-derived xenografts (PDX) of PCa, to assess responses to PCa treatments.

Methods

Three PDX models were used that are characterized by different androgen receptor (AR) expression and different homology directed DNA repair capacities, due to a breast cancer associated 2 (*BRCA2*) wild type or mutated status. Tumors were removed from mice, sliced using a vibratome and cultured for a maximum of 6 days. To test the sensitivity to androgen antagonist, tumor slices from the AR-expressing and AR-negative PDX tumors were treated with the anti-androgen enzalutamide. For sensitivity to DNA repair intervention, tumor slices from *BRCA2* wild type and mutated PDXs were treated with the poly (ADP-ribose) polymerase-1 inhibitor olaparib. Treatment response in these tumor slices was determined by measuring slice morphology, cell proliferation, apoptosis, AR expression level and secretion of prostate specific antigen (PSA).

Results

We compared various culture conditions (support materials, growth media and use of a 3D smooth rocking platform) to find the optimal condition to maintain tissue viability and proliferative capacity for at least 6 days. Under optimized conditions, enzalutamide treatment significantly decreased proliferation, increased apoptosis, and reduced AR-expression and PSA secretion of AR-expressing tumor slices compared to AR-negative slices, that did not respond to the intervention. Olaparib treatment significantly increased cell death in *BRCA2* mutated tumors slices as compared to slices from *BRCA2* wild type tumors.

Conclusions

Ex vivo treatment of PCa PDX tumor slices with enzalutamide and olaparib recapitulates responses previously observed *in vivo*. The faithful retention of tissue structure and function in this *ex vivo* model offers an ideal opportunity for treatment efficacy screening, thereby reducing costs and numbers of experimental animals.

1. Introduction

Prostate cancer (PCa) is the second most common cancer in men and the fourth most common tumor type worldwide (1). PCa remains a high burden in the current healthcare system, especially once it develops into castration resistant PCa (CRPC). Although therapeutic strategies have improved over the past decades, their gains are often transient and only marginally increase survival of CRPC patients. Therefore, there is a clear unmet clinical need for better treatment options and predictive markers for CRPC patients. Currently, a multitude of novel targets and compounds are in the pipeline for testing. In order to speed up the process from development towards clinical use, faster and better test models are urgently needed. When developing and testing novel therapies, it is essential to have a cancer model that is both reliable and representative.

Most preclinical studies of PCa depend heavily on immortalized cancer cell lines, which are grown in culture dishes as a two-dimensional model. These models do not recapitulate the complex architecture of tumors nor the important interaction between tumor cells and their microenvironment (2). They do therefore not always accurately predict treatment efficacy and these limitations could lead to a failure when transitioning a new drug from the bench to the clinic.

As an alternative, organotypic culture of tumor slices represent a solid model system for drug sensitivity testing due to its relatively short generation time and reflection of the tumor microenvironment (3-7). For example, several studies have shown that breast tumor tissue slices can be used to assess chemotherapy response in the context of personalized medicine (8-10). In recent years, efforts have been undertaken to establish such strategies to generate primary cultures from human prostate tumors and innovative complex culture systems. Unfortunately, the establishment of primary PCa organotypic cultures proved to be extremely challenging due to the slow-growing characteristics of the PCa cells; basal epithelial cells proliferate faster than tumor cells and often outgrow them during prolonged culture (11-13).

To allow testing of therapy responses in different genetics and functional background of PCa, we set out to develop an optimized tissue slice culture system. For that, we used well-established patient-derived xenograft (PDXs) models as a source for the tissue slices (14,15) and show that treatment outcome of these slices recapitulates responses previously found *in vivo*.

2. Materials and Methods

2.1 Reagents

Reagents were purchased from Sigma-Aldrich (Germany) unless otherwise specified.

2.2 Collection of PDX tumor tissue

PDXs of PCa (PC295, PC339 and PC310) were established by van Weerden et al. (14) and were routinely passaged by subcutaneous grafting of small fragments onto both shoulders of intact male athymic NMRI nu/nu mice (Taconic Biosciences, Germany). Characteristics of the different PDXs are summarized in Table 1. Fresh PDX tumors with volume of 500-1000 mm³ were obtained. After removal from mice, the tumors were kept on ice in Dulbecco's Modified Eagle Medium (DMEM; Lonza, Belgium).

2.3 Tissue slice and culture

Tumor slices were generated using a vibratome (Leica VT1200S; Leica, Germany) with a thickness set at 300 μm, vibration amplitude at 3.0 mm and slicing speed at 0.6 mm/sec. Slices were either submerged directly in 3 mL culture medium or placed on Falcon 40 μm Cell Strainers (Corning, NY, USA) or Millicell 0.4 μm Cell inserts (Merck Millipore, Bedford, USA) and then cultured in 3 mL culture medium in 6 well

plates. The culture media that were tested for quality assessment are summarized in Table II. Slices were put in culture within 3 h after the tumor was removed from the mouse. Culturing was performed at 5% CO₂ at 37°C and at atmospheric oxygen levels. Culture plates were standing still or were subjected to movement at 6 rpm using Luckham 4RT Rocking Table (Luckham 200 Ltd, West Sussex, UK). One third of medium was refreshed and collected daily. Slices were harvested at various time points and fixed in 10% neutral buffered formalin for at least 24 h at room temperature (RT). Subsequently, tumor slices were embedded in paraffin and 4 µm sections were made for further microscopy analysis (for practical setup, see Figure 1).

2.4 *Ex vivo* anti-androgen and PARP-1 inhibitor treatment

To test the response of anti-androgen and poly (ADP-ribose) polymerase-1 (PARP-1) inhibitor treatment, tissue slices were cultured under optimal conditions and treated with enzalutamide (1 µM, Sequoia Research Products, Pangbourne, UK), olaparib (10 µM, Selleck Chemicals, Munich, Germany) or with vehicle control (dimethyl sulfoxide, DMSO) for different time points.

2.5 Hematoxylin and eosin staining

Histological tumor architecture was examined by hematoxylin and eosin (H&E) staining. Briefly, sections were deparaffinized in xylene followed by rehydration in graded alcohols. They were then stained with hematoxylin for 1 minute, rinsed with tap water, stained with eosin for 1 minute, and rinsed again with tap water. The slides were then dehydrated with increasing concentration of ethanol successively followed by xylene and mounted with entellan.

2.6 Immunohistochemical and fluorescent procedures

Sections were deparaffinized in xylene followed by rehydration in graded alcohols. Antigen retrieval was performed with target retrieval buffer (Dako, Glostrup, Denmark). For diaminobenzidine (DAB) staining, endogenous peroxidase activity was blocked by using 3% hydrogen peroxide solution in methanol at RT for 20 min. 5% bovine serum albumin (BSA) in phosphate buffered saline (PBS, Lonza, Verviers, Belgium) was used to block nonspecific binding. Primary androgen receptor (AR) antibody (M4074, 1/200, SPRING Bioscience, CA, USA) and Ki67 antibody (ab16667, 1/200, Abcam, Cambridge, UK) diluted in blocking buffer were applied to the sections at 4°C overnight. Ki67 was detected with anti-rabbit Alexa Fluor 488 and mounted with Vectashield containing DAPI (Vector Laboratories, Burlingame, CA, USA). AR staining continues with a horseradish peroxidase (HRP)-conjugated anti-rabbit IgG secondary antibody (Dako, Glostrup, Denmark) at a 1:100 dilution for 1 h at RT. AR positive cells were visualized using DAB staining kit (Dako, CA, USA) followed by counterstaining with hematoxylin. Negative controls were performed for all samples by omitting the primary antibodies.

2.7 EdU incorporation and Click-iT™ reaction

5-ethynyl-2'-deoxyuridine (EdU, Invitrogen, USA) at a concentration of 3 µg/mL was added to the culture medium 2 h before fixation. For the Click reaction, tissue sections were deparaffinized in xylene followed by rehydration in graded alcohols and then blocked with PBS containing 1% BSA. After additional washing with PBS, sections were incubated with freshly made Click-iT Alexa Fluor 594 cocktail buffer for 30 min as previously reported (10). Samples were mounted using Vectashield mounting medium with DAPI.

2.8 TUNEL assay

Terminal deoxynucleotidyl transferase dUTP nick end-labeling (TUNEL) assay was performed using In Situ Cell Death Detection Kit (Roche Life Sciences, Penzberg, Germany) according to instruction of the manufacturer.

2.9 Medium Prostate-Specific Antigen (PSA) measurement

Tumor slices culture medium (1 mL) was collected daily for PSA measurement. The PSA concentration was measured using a PSA enzyme-linked immunosorbent assay (ELISA) kit (Abnova, Taiwan) according to the manufacturer instructions. The accumulated PSA concentration in the culture medium was calculated using the following formula (which corrects for medium removal each day):

$$\text{PSA total (d)} = \text{PSA measured (d)} * 3 + 1/3 \text{ PSA total (d-1)}$$

In which d = day of culture.

2.10 Image acquisition

AR staining was imaged using a light microscope (Olympus, Tokyo, Japan) and 4 fields (200x magnification) from each section were captured. For Ki67, EdU and TUNEL staining quantifications, 10 random images (400x magnification) from each tumor slice section were generated using a Leica fluorescence microscope (DM4000b, Germany) to represent the slice heterogeneity. Representative EdU and TUNEL photos were taken by using a Leica SP5 confocal microscope. Image size: 512x512 pixels, pixel size 0.7 μm , 200x magnification (Leica, Germany).

2.11 Image quantification

AR expression was quantified by Image J software to yield the pixel ratio of AR positive to total nuclei. To quantify the TUNEL microscopy images, all pictures were analyzed with the Fraction of overlap with Otsu's thresholding method: The DAPI and the TUNEL image were both thresholded according to Otsu's algorithm (16) which resulted into two binary images. The pixel number was measured and subsequently the Mander's M1 coefficient was used to calculate the fraction of TUNEL positive pixel overlapped with DAPI pixel (17). To quantify the fraction of EdU positive cells, the fraction of overlap of silhouette images method was used. This method relies on edge detection to obtain a binary image. For both the DAPI and EdU pictures, a gradient magnitude image was obtained from the image of entry. This binary image was created using a modified triangle-thresholding method in which black areas completely enclosed by white areas were filled (18). Next, a morphological dilation was applied using a circular structuring element with a radius of three pixels. All pixels that still had a value of one then constitute a newly formed gradient mask image. The same thresholding was applied to the original grayscale image. The intersection of this image and all pixels greater than the mean intensity of the original grayscale image formed the intensity mask image. A new image was obtained through seeded region growing, whereby the gradient mask served as a seed point image and the intensity mask as the target image. This newly formed image was subjected to a median filter with a 5x5 neighborhood and all pixels equal to one constitute the final binary image. Finally, Mander's M1 coefficient was calculated for the fraction of overlap.

2.12 Statistical analysis

Results are expressed as the mean \pm SEM or median \pm quartile in bar graph. Mann-Whitney test was used to analyze the differences between two groups. Statistical analysis and generation of graphs was performed using Graphpad Prism 6.0 (La Jolla, CA). $P < 0.05$ was considered statistically significant. * $P < 0.05$, ** $P < 0.01$, *** $P < 0.001$

3. Results

3.1 Culture condition selection

To establish the most optimal method for preservation of PCa tissue slice viability we developed a novel culture system and compared it to previously reported systems (19,20). Tumor slices from PC295, PC339 and PC310 PCa PDXs were generated using a vibratome and these slices were cultured in prostate growth medium (PGM) for 4 days under the different conditions in which we compared supporting materials (Figure 1). Furthermore, stationary condition and 3D orbital movement on a rocking table were compared as smooth 3D orbital movement could increase oxygen and nutrition exchange as reported previously (20). H&E stained sections of slices of all three tumors showed that slices cultured on cell strainers maintained tissue morphology, while slices cultured without support or on inserts lost tissue integrity and showed an increase in apoptotic nuclei and vacuolated structures over time (Figure 2A and Figure S1). Moreover, in contrast what was observed previously using inserts, we did not observe a viability gradient nor loco-regional changes in morphology (15).

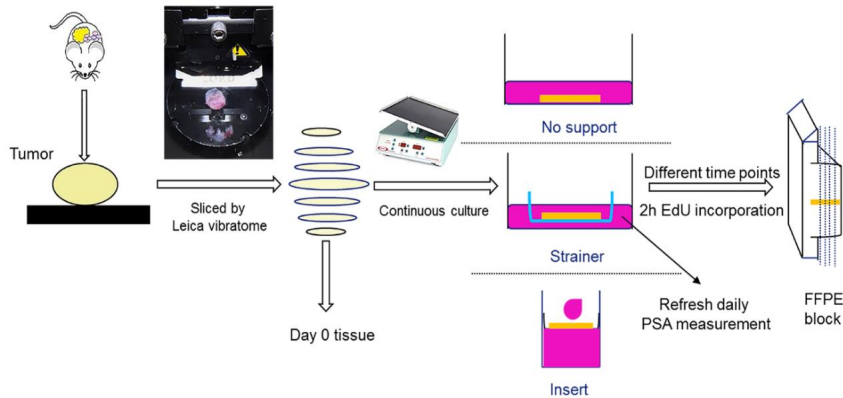


Figure 1. PDX tissue culture methodology.

The tumor was removed from the mice and sliced with a Leica Vibratome into 300 μm tumor slices. Slices were either submerged in culture medium, on Cell Strainers or on Cell Culture inserts. Culture dishes were then placed on a Rocking Table or incubated without movement. Slices were harvested at various time points and EdU was added 2 h before fixation. Subsequently, fixed tissue was embedded in paraffin (FFPE).

The thymidine analogue EdU was used as a real-time proliferation marker to assess tissue viability. We tested the reliability of our newly developed EdU quantification algorithm by comparing automatic counting with manual counting and a good correlation was observed (an R^2 of 0.922 and 0.841, respectively for 2 individuals compared to automatic counting; Figure S2). A large variability of EdU-positive cells was observed between individual image fields and, therefore, 10 fields of view were quantified per slice to provide a reliable assessment. Tissue slices cultured on cell strainers and under continuous 3D orbital movement outperformed the other tissue slice methods when looking at maintenance of proliferation at day 4 (Figure 2B and 2C). We further evaluated the induction of cell death during *ex vivo* culturing by TUNEL staining, which labels DNA strand breaks generated during apoptosis (21). In line with

the results on proliferation, slices cultured on cell strainers did not show an increase in apoptosis at 4 days of culture, while slices cultured under the other conditions showed enhanced apoptosis. No significant difference in TUNEL signal was observed between slices in the stationary condition and those cultured on a rocking table (Figure 2B and 2D). From these results, we concluded that cell strainer-support and continuous 3D orbital movement are optimal for maintenance of tissue slice morphology, proliferation and viability.

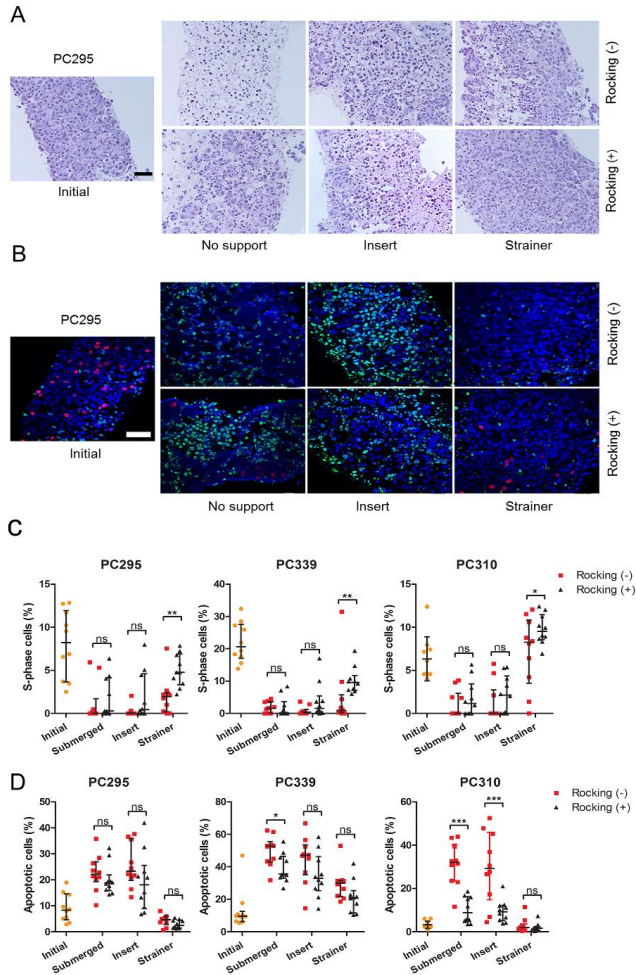


Figure 2. Effect of filter support and 3D orbital movement on PCa tissue slice morphology and viability.

A) Representative H&E images of PC295 tumor slice sections after 4 days of culturing under the different culture conditions, compared to an initial slice (day 0). Scale bar 50 μ m. B) Representative EdU/TUNEL/DAPI images of PC295 tumor slice sections after 4 days of culturing under the different culture conditions, compared to an initial slice (day 0) (blue=DAPI, red=EdU, green=TUNEL). Represented H&E and EdU/TUNEL images of PC339 and PC310 tumor slices can be found in Figure S1. Scale bar 50 μ m. C) Quantification of the fraction of EdU-positive cells in the tissue slices. D) Quantification of the fraction of TUNEL positive cells in the tissue slices. For

all graphs, 10 image fields were analyzed per tumor slice. Each point represents one image field, interquartile range and median values are indicated (results from 1 representative tumor per graph).

3.2 Optimal medium selection

The culture medium composition has vital impact on the viability of tissue slices. To select the optimal medium, we cultured tissue slices in 4 different culture media that have been reported previously for primary prostate cell or tumor culturing (Table 2) (19,20,22-24). Tissue morphology analysis showed that Prostate Growth Medium (PGM) (23) and aDMEM/F12K outperformed the other media tested (Figure S3).

Table 1. Overview of characteristics of different PDXs.

PDX	Origin ¹	AD ²	AR ³	PSA ⁴	BRCA	TD (days) ⁵	Pathology type
PC295	LN	+	+	+	WT ⁵	9-11	adenocarcinoma
PC339	TURP	-	-	-	WT	4-7	adenocarcinoma
PC310	PC	+	+	+	HD ⁶	9-11	adenocarcinoma

¹LN = lymph node metastasis, TURP = transurethral resection of the prostate, PC = primary prostate tumor; ²AD = androgen dependence (+); ³AR = androgen receptor; ⁴PSA = prostate specific antigen; ⁵WT = wild type; ⁶HD = homozygous deletion; ⁵TD = tumor doubling time

Table 2. Overview of the different medium compositions.

PGM	aDMEM/F12K	M199: K-SFM	DMEM
DMEM/Ham's F12 (1:1) BSA (0.01%) FCS (2%) Epidermal growth factor (10 ng/mL) Insulin-transferrin-selenium (1%) Hydrocortison (0.5 µg/mL) Triiodothyronine (1 nM) Phosphoethanolamine(0.1 mM) Cholera toxin (50 ng/mL) Fibronectin (100 ng/mL) Fetuin (20 µg/mL) R1881 (0.1 nM) Penicillin/streptomycin (100 U/mL, 100 µg/mL)	PFMR-4A (aDMEM/F12K) Penicillin/streptomycin (100U/mL, 100 µg/mL)	M199: K-SFM (1:1) Antibiotic/antimycotic solution	DMEM-high glucose Penicillin/streptomycin (100U/mL, 100 µg/mL)

We compared incubation of tissue slices from PC295 and PC339 to determine which medium preserved tumor cell viability most optimally. Average tissue proliferation remained constant for PC339 (average 10%) up to 6 days of culturing in both media while proliferation of PC295 reduced over time in both media (initial 10.7%, and 2.5% and 3.6% in PGM and aDMEM/F12K respectively after 6 days). There was no significant difference in performance between the two culture media for both PDXs (Figure 3A).

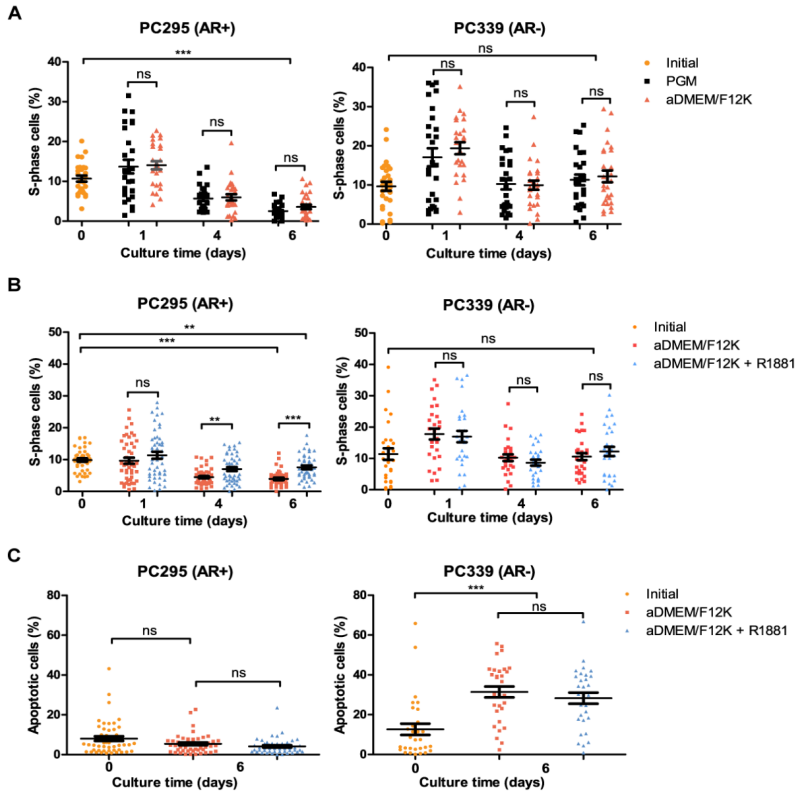


Figure 3. Optimization of culture medium.

A) Quantification of the fraction of EdU-positive cells of PC295 and PC339 slices cultured up to 6 days in PGM and aDMEM/F12K medium. B) Quantification of the fraction of EdU-positive cells for PC295 and PC339 slices cultured up to 6 days in aDMEM/F12K and aDMEM/F12K supplemented with R1881. C) Quantification of the fraction of TUNEL-positive cells for PC295 and PC339 slices cultured in aDMEM/F12K and aDMEM/F12K supplemented with R1881 at 6 days. For all graphs, 10 image fields were analyzed per tumor slice section. Each point represents one image field, average and SEM are indicated (Three independent experiments for each tumor type). ** $P < 0.01$, *** $P < 0.001$, ns = non-significant.

PGM constitutes 2% fetal calf serum (FCS) and is supplemented with the synthetic androgen R1881 (0.1 nM), while aDMEM/F12K devoid of FCS and does not contain R1881. The clear benefit of using serum-free medium led us to test the impact of addition of the same concentration of R1881 to the aDMEM/F12K medium. Three tumors of PC295 and PC339 each were cultured under optimal conditions in aDMEM/F12K or in aDMEM/F12K supplemented with R1881. We found a significantly higher proliferation rate of the PC295 slices cultured in aDMEM/F12K supplemented with R1881 compared to aDMEM/F12K without R1881 (1.9 folds at day 6) (Figure 3B). As expected, addition of R1881 did not affect proliferation rates of androgen independent PC339 slices (Figure 3B). Some increase in apoptosis was observed in PC339, while PC295 maintained its low apoptosis levels for up to 6 days of *ex vivo* culturing (Figure 3C).

To further assess tissue maintenance, we measured AR expression, a major characteristic of androgen dependent prostate tumors. Immunohistochemical stainings showed that AR expression was largely maintained during *ex vivo* culturing of PC295 slices, with a small but significant decrease of AR expression in slices cultured at 6 days in either PGM or aDMEM/F12K (Figure 4A and 4B). The addition of R1881 to aDMEM/F12K medium preserved AR levels up to 6 days of incubation (Figure 4C and 4D).

Because androgen stimulates PSA secretion from PCa cells, we measured PSA levels in the culture media. Medium from PC295 tumor slices was collected for up to 6 days and PSA accumulation was monitored. After normalization to initial PSA levels, we observed a continuous increase in PSA for up to 6 days in cultures supplemented with R1881 while slices cultured in aDMEM/F12K without R1881 showed a stabilization of PSA levels (Figure 4E). Altogether, we concluded that aDMEM/F12K plus R1881 is the optimal medium for maintenance of tissue slice morphology, viability, and AR-functionality.

3.3 Enzalutamide treatment of tissue slices

In order to validate the accuracy of the tissue slice system to reflect clinical responses to relevant therapies, we investigated the response to enzalutamide, a second generation anti-androgen which is currently being tested in a randomized phase III trial (25). PC295 (AR positive and androgen dependent) and PC339 (AR negative and androgen independent) slices were treated with enzalutamide with or without R1881. As shown in Figure 5A, we observed a significant drop in the fraction of EdU positive cells in PC295 slices treated with enzalutamide after 6 days of culturing (decreased by a factor of 5.5), while we did not observe a change in proliferation in PC339 slices. Simultaneously, a significant of 2.8 folds increase of TUNEL positive cells was observed in PC295 slices treated with enzalutamide, with no effect in the PC339 slices (Figure 5B). Presence of R1881 was unable to restore proliferation or revert apoptosis induced by enzalutamide treatment in PC295 slices (Figure 5A and 5B). AR staining of PC295 slices showed a dramatic reduction of 45% upon enzalutamide treatment at day 6 which could also not be reversed by the presence of R1881 (Figure 5C). PSA measurement in medium samples further confirmed the inhibitory effect of enzalutamide on AR positive tumor slices. After an initial rise in PSA at day 2, PSA secretion decreased after enzalutamide treatment, both in presence or absence of R1881 (Figure 5D). Similar anti-androgenic effects of enzalutamide were observed in tumor slices from the AR positive and androgen dependent PC310 PDX model (Figure S4)

3.4 Olaparib treatment of tissue slices

Mutations in the DNA repair gene *BRCA2* have been identified in PCa patients, and previous studies have shown that these specific patients benefit from treatment with olaparib, an inhibitor of poly(ADP-ribose) polymerase-1 (PARP-1) (26). We therefore assessed the response to olaparib treatment in PC295 (*BRCA2* wild type) and PC310 (*BRCA2* mutated) tumors. A significant drop in the fraction of S-phase cells was observed for both PC295 and PC310 tumor slices (decreased by a factor of 2.65 and 10, respectively) when treated with olaparib for 6 days, with a more pronounced reduction in cell proliferation for PC310 (Figure 6A). A significant increase of 10.9 fold of TUNEL positive cells was observed only in PC310 slices treated with olaparib, and not in PC295 tumor slices (Figure 6B). AR staining showed a significant reduction of AR positive tumor cells in PC310 tumor slices upon olaparib treatment, while only a slightly reduction of AR-positive tumor cell was observed in PC295 tumor slices (Figure 6C). PSA measurement revealed reduced PSA levels of both PC295 and PC310

slices (Figure 6D). In conclusion, both *BRCA2* deficient and proficient tumors are hampered by olaparib treatment, but only *BRCA2* deficiency causes induction of apoptotic cell death.

4. Discussion

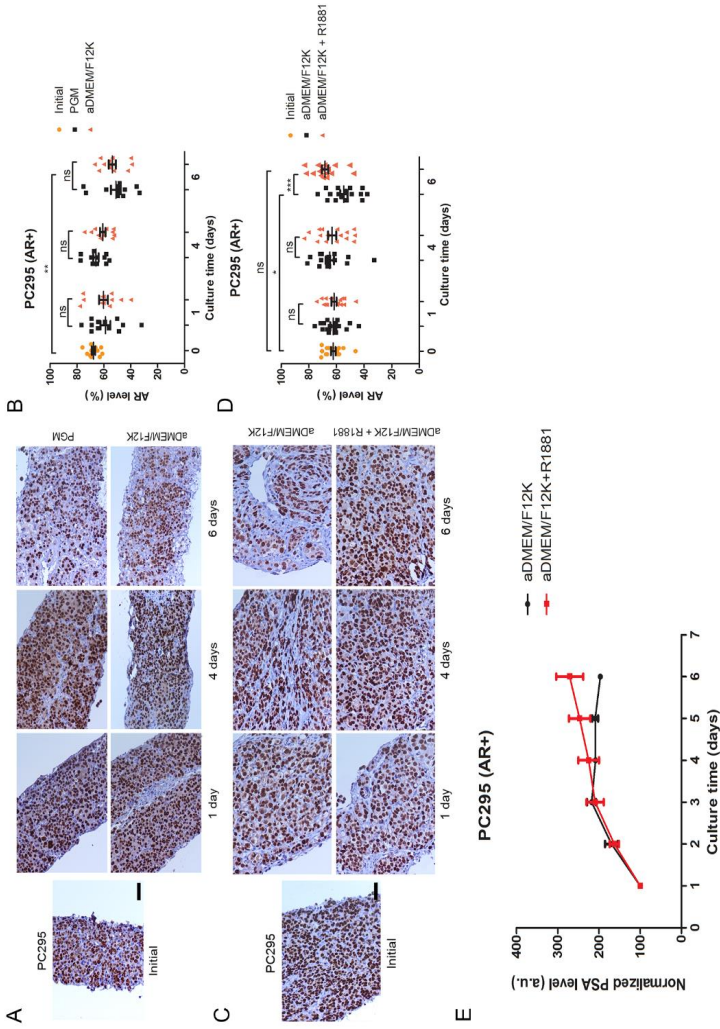
We have established an *ex vivo* tissue slice culture system using PCa PDXs. Under optimal culture conditions, tumor morphology, cell proliferation and prostatic characteristics are preserved for up to 6 days with minimal induction of cell death. Furthermore, we showed that this system is suitable for PCa drug testing: we observed responses to enzalutamide in androgen dependent tumor slices as well as to olaparib in *BRCA2* mutant tumor slices that reflect *in vivo* therapy responses.

An *ex vivo* tumor culture system should maintain cancer characteristics and tumor proliferating capacity during *ex vivo* culturing to allow reliable therapy response evaluation. Since the 1970s, various studies have been described that aim to establish an *ex vivo* culture system for PCa tumors. This has resulted in the development of different tumor culture methods, ranging from direct culturing of 1–2 mm³ human tissue samples in medium to more recently developed techniques to culture precision cut tissue slices on various scaffolds and supporting filters, like gelatin, collagen sponges or titanium mesh inserts (20,22,27-29). As reported in these studies, maintenance of prostate or PCa tissue slices for a week could be achieved, but maintenance of tissue structure and functionality was not always comprehensively reported with extensive variability in tissue origin and evaluation in the different studies. Application of the *ex vivo* culture system for drug testing was only reported in a few studies, describing reduced cell proliferation in response to genistein (28), cisplatin combined with a Bcl-2 antagonist (30), heat shock protein 90 inhibitors (27), PARP-1 inhibitors (31) and most recently published studies with bicalutamide (29) and docetaxel (32). However detailed cell cycle progression (proliferation) of the tumor cells was not investigated, making direct comparison to our studies difficult. Importantly, our study validates the response to different tumor genotypes, represented by different PDXs, and hence provide evidence that *ex vivo* drug testing can indeed predict *in vivo* responses.

Although *ex vivo* tumor cultures from other cancer types can be maintained for weeks or months (8,11,12,33-35), PCa tissue maintenance of primary tumors has been challenging probably due to the slow-growing characteristics and fast proliferation of basal cells (24,36,37). Also, obtaining aggressive metastatic PCa material is with limitations as metastatic disease is predominantly found in bone restricting easy excess. Nowadays, prostate-specific membrane antigen (PSMA) guided biopsy and salvage lymphadenectomy is reported (38-40), which may offer new opportunities for acquiring aggressive PCa material for *ex vivo* drug response tests. Our tissue slice culture platform for PCa defined in this study will be helpful to standardize ex-vivo culturing of patient material.

Figure 4. Prostate characteristics during prolonged *ex vivo* culturing.

A) Representative images of AR staining of PC295 tumor slice sections cultured in two media for different time points, compared to the stained section of the initial slice (day 0). **B)** Quantification of the AR staining. Four image fields were analyzed per tumor slice, each point represents one image field, average and SEM are indicated (Three independent experiments). **C)** Representative images of AR staining of PC295 tissue slice sections cultured in aDMEM/F12K and aDMEM/F12K supplemented with R1881 for different time points, compared to the stained section of the initial slice (day 0). **D)** Quantification of the AR staining. Four image fields were analyzed per tumor slice, each point represents one image field, average and SEM are indicated (Three independent experiments). **E)** Normalized accumulated PSA concentrations of PC295 aDMEM/F12K and aDMEM/F12K supplemented with R1881. Line represent mean values and bars indicates SEM (Three independent experiments). For all graphs scale bar 50 μm and * $P < 0.05$, ** $P < 0.01$, *** $P < 0.001$, ns = non-significant



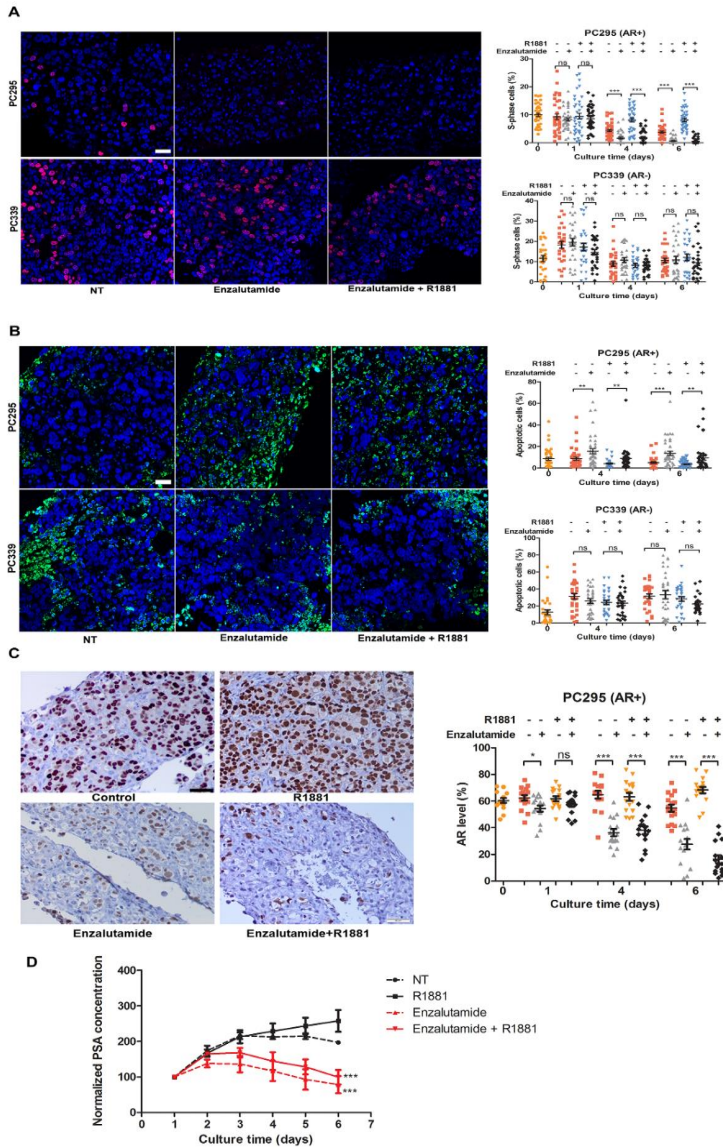


Figure 5. Response to *ex vivo* enzalutamide treatment.

A) Quantification of the fraction of EdU-positive cells for PC295 and PC339 slices at different time points. Scale bar 100 μ m. B) Quantification of the fraction of TUNEL-positive cells for PC295 and PC339 slices at different time points. Scale bar 100 μ m. C) Representative images of AR staining for PC295 tissue slice sections at day 6 and quantification of the AR stainings. Scale bar 50 μ m. D) Normalized accumulated PSA concentrations of PC295 and PC339 slices from day 1 to day 6 treated or not with Enzalutamide. Line represent mean values and bars indicates SEM. Ten image fields for EdU/TUNEL and 4 image fields for AR were analyzed per tumor slice section. Each point represents one image field, average and SEM are indicated, four independent experiments for each tumor type. * $P < 0.05$, ** $P < 0.01$, *** $P < 0.001$, ns = non-significant.

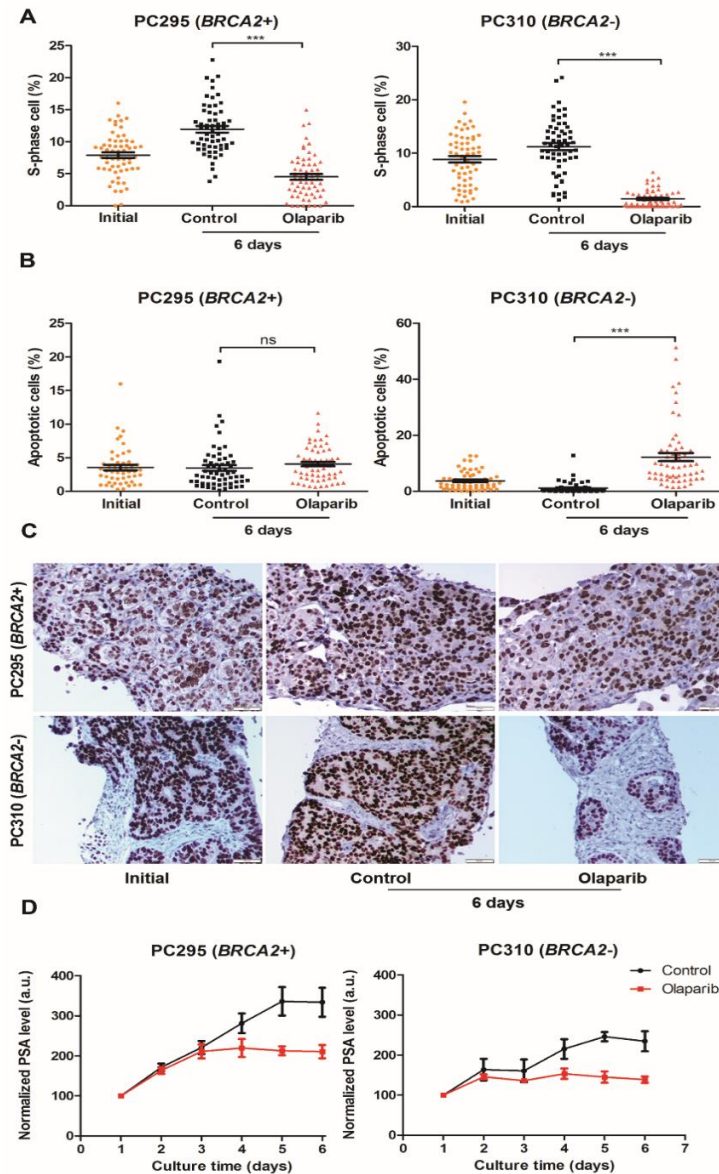


Figure 6. Response to *ex vivo* olaparib treatment.

A) Quantification of the fraction of EdU-positive cells of PC295 and PC310 slices treated with olaparib for 6 days. **B)** Quantification of the fraction of TUNEL positive cells of PC295 and PC310 slices treated with olaparib for 6 days. **C)** Representative images of AR staining of PC295 and PC310 slices treated with olaparib for 6 days. Scale bar 50 μm . **D)** Normalized accumulated PSA concentrations of PC295 and PC310 slices from day 1 to day 6 treated or not with olaparib. Ten image fields for EdU/TUNEL and 4 image fields for AR were analyzed per tumor slice section. Each point represents one image field, average and SEM are indicated, three independent experiments for each tumor. * $P < 0.05$, ** $P < 0.01$, *** $P < 0.001$, ns = non-significant.

We used PDX tumors to thoroughly evaluate the impact of different culture condition and the ability of tissue slices to recapitulate individual tumor responses. PDX tumors have limited intra-tumoral heterogeneity and high tumor content which also allow us for intensive technical studies. For lowering slices heterogeneity within the same tumor, slices were consecutive allocated to each experimental treatment. We were able to keep longevity of tumor slices by using serum-free aDMEM/F12K medium with the addition of synthetic androgen up to 6 days. This medium shares many similar ingredients with medium PFMR-4A which was reported previously for successful maintenance of benign and malignant prostate tissue slices for 5 days (20). Serum-free medium allows more precise evaluations of cellular function and better control over physiological responsiveness.

One of the strengths of this study is the use of EdU incorporation to assess cell proliferation, allowing real time measurement of DNA synthesis during replication. We believe that this is a more reliable way to measure early treatment effects compared to the commonly used Ki67 marker. Ki67 protein is present in all cycling cells, even for several days after cells have ceased to proliferate (41). Indeed, we observed a disparity between EdU ratio and Ki67 expression: after 6 days culturing EdU ratio dropped significantly while Ki67 only showed a slight reduction (Figure S5). In the majority of tumor slices from all three PDXs tested, we observed an increase of proliferation after one day of incubation, followed by constant homogenous maintenance of proliferation (PC339 and PC310) or slightly decrease of proliferation (PC295). The first-day proliferation boost might be a result of the availability of a high level of nutrients and oxygen. The initial high TUNEL level in PC339 slices is most likely due to a higher level of necrosis in the original tumor sample, since TUNEL assay is unable to distinguish necrosis and apoptosis (42).

We observed a marginal effect of androgen deprivation on tumor slice viability in androgen responsive PDX tissue slices. This might be caused by the presence of endogenous androgen maintained in the tumor slices and which is gradually released into the medium during culturing. Thus, endogenously present androgen can be used to maintain activation of AR signaling and proliferation for a few days. Similar observations were done by Zhou et al. in rat prostates that retained similar androgen tissue levels independent of the serum concentrations (43).

A clear anti-androgenic response to enzalutamide was observed in androgen dependent tissue slices. Our *ex vivo* response of tissue slices to enzalutamide are also supported by *in vivo* data reported by Guerrero et al. in which enzalutamide inhibits tumor growth significantly during the first 6 days of treatment compared with vehicle-treated mice (44). Additionally, we showed that olaparib induced cell death in the *BRCA2* mutant PC310 tumor slices, confirming the expected response when targeting DNA damage repair deficient tumors. This was in concordance with recent clinical studies, showing that that CRPC patients with somatic loss and germline mutation of *BRCA2* respond well to olaparib (26). Similar was reported by Beshiri et al. for PCa PDX organoid cultures in which *BRCA2* deficiency correlates with olaparib sensitivity (45). PARP-1 inhibitors with high PARP trapping potency, such as olaparib, can yield intense replication stress (46,47), which can explain the decrease of fraction of S-phase cells in the *BRCA2* wild type PC295 slices.

So far, several publications have suggested that tumor tissue slice culture can be utilized to predict drug response in breast cancer (8-10) and monitor cytotoxic drug effects in liver, intestine and lung (48-50). We have established dedicated tissue slice system for PCa that shows robust and specific anti-androgen and PARP-1 inhibition treatment effects and that can be extended to testing of novel compounds relevant to

PCa.

5. Conclusions

The faithful retention of tissue structure and function in our *ex vivo* culture system offers an opportunity to evaluate PCa response to therapeutic compounds making it an ideal system for low to medium throughput testing in drug discovery.

Acknowledgments

We thank Alex Nigg (Optical Imaging Center, Erasmus University Medical Center, Rotterdam, The Netherlands) for the AR quantification macro and Nikita Frehé for help during the development of the EdU quantification program.

Funding

This study was supported by the Chinese Scholarship Council (grant number 201506270172 (WZ)), by the Dutch Cancer Society (Alpe d'Huzes grant number EMCR 2014-7048 (TM and DvG)), by the gravitation program CancerGenomiCs.nl from the Netherlands Organization for Scientific Research (NWO) (RK), by the OncoCode Institute, which is partly financed by the Dutch Cancer Society (RK), and by the Daniel den Hoed Foundation (grant number 107235 (JN)).

References

1. Torre LA, Bray F, Siegel RL, Ferlay J, Lortet-Tieulent J, Jemal A. Global cancer statistics, 2012. *CA Cancer J Clin*. 2015;65(2):87-108.
2. Wilding JL, Bodmer WF. Cancer cell lines for drug discovery and development. *Cancer Res*. 2014;74(9):2377-84.
3. Gerlach MM, Merz F, Wichmann G, Kubick C, Wittekind C, Lordick F, et al. Slice cultures from head and neck squamous cell carcinoma: a novel test system for drug susceptibility and mechanisms of resistance. *Br J Cancer*. 2014;110(2):479-88.
4. Merz F, Gaunitz F, Dehghani F, Renner C, Meixensberger J, Gutenberg A, et al. Organotypic slice cultures of human glioblastoma reveal different susceptibilities to treatments. *Neuro Oncol*. 2013;15(6):670-81.
5. Koerfer J, Kallendrusch S, Merz F, Wittekind C, Kubick C, Kassahun WT, et al. Organotypic slice cultures of human gastric and esophagogastric junction cancer. *Cancer Med*. 2016;5(7):1444-53.
6. Hickman JA, Graeser R, de Hoogt R, Vidic S, Brito C, Gutekunst M, et al. Three-dimensional models of cancer for pharmacology and cancer cell biology: capturing tumor complexity in vitro/ex vivo. *Biotechnol J*. 2014;9(9):1115-28.
7. Meijer TG, Naipal KA, Jager A, van Gent DC. Ex vivo tumor culture systems for functional drug testing and therapy response prediction. *Future Sci OA*. 2017;3(2):FSO190.
8. Holliday DL, Moss MA, Pollock S, Lane S, Shaaban AM, Millican-Slater R, et al. The practicalities of using tissue slices as preclinical organotypic breast cancer models. *J Clin Pathol*. 2013;66(3):253-5.
9. van der Kuip H, Murdter TE, Sonnenberg M, McClellan M, Gutzeit S, Gerteis A, et al. Short term culture of breast cancer tissues to study the activity of the anticancer drug taxol in an intact tumor environment. *Bmc Cancer*. 2006;6:86.
10. Naipal KA, Verkaik NS, Sanchez H, van Deurzen CH, den Bakker MA, Hoesjmakers JH, et al. Tumor slice culture system to assess drug response of primary breast cancer. *Bmc Cancer*. 2016;16:78.
11. Nevalainen MT, Harkonen PL, Valve EM, Ping W, Nurmi M, Martikainen PM. Hormone regulation of human prostate in organ culture. *Cancer Res*. 1993;53(21):5199-207.
12. Parrish AR, Sallam K, Nyman DW, Orozco J, Cress AE, Dalkin BL, et al. Culturing precision-cut human prostate slices as an in vitro model of prostate pathobiology. *Cell Biol Toxicol*. 2002;18(3):205-19.
13. Gao H, Korn JM, Ferretti S, Monahan JE, Wang Y, Singh M, et al. High-throughput screening using patient-derived tumor xenografts to predict clinical trial drug response. *Nat Med*. 2015;21(11):1318-25.
14. van Weerden WM, de Ridder CM, Verdaasdonk CL, Romijn JC, van der Kwast TH, Schroder FH, et al. Development of seven new human prostate tumor xenograft models and their histopathological characterization. *Am J Pathol*. 1996;149(3):1055-62.
15. Davies EJ, Dong M, Gutekunst M, Narhi K, van Zoggel HJ, Blom S, et al. Capturing complex tumour biology in vitro: histological and molecular characterisation of precision cut slices. *Sci Rep*. 2015;5:17187.
16. Otsu N. A threshold selection method from gray-level histograms. *IEEE transactions on systems, man, and cybernetics*. 1979;9(1):62-6.
17. Manders EMM, Verbeek FJ, Aten JA. Measurement of Colocalization of Objects in Dual-Color Confocal Images. *J Microsc-Oxford*. 1993;169:375-82.
18. Soille P. *Morphological Image Analysis: Principles and Applications*: Springer-Verlag; 2003. 391 p.
19. De Hoogt R, Estrada MF, Vidic S, Davies EJ, Osswald A, Barbier M, et al. Protocols and characterization data for 2D, 3D, and slice-based tumor models from the PREDECT project. *Scientific data*. 2017;4:170170.

20. Maund SL, Nolley R, Peehl DM. Optimization and comprehensive characterization of a faithful tissue culture model of the benign and malignant human prostate. *Lab Invest.* 2014;94(2):208-21.
21. Loo DT. In situ detection of apoptosis by the TUNEL assay: an overview of techniques. *DNA Damage Detection In Situ, Ex Vivo, and In Vivo*: Springer; 2011. p. 3-13.
22. Papini S, Rosellini A, De Matteis A, Campani D, Selli C, Caporali A, et al. Establishment of an organotypic in vitro culture system and its relevance to the characterization of human prostate epithelial cancer cells and their stromal interactions. *Pathol Res Pract.* 2007;203(4):209-16.
23. Marques RB, van Weerden WM, Erkens-Schulze S, de Ridder CM, Bangma CH, Trapman J, et al. The human PC346 xenograft and cell line panel: a model system for prostate cancer progression. *Eur Urol.* 2006;49(2):245-57.
24. Blauer M, Tammela TL, Ylikomi T. A novel tissue-slice culture model for non-malignant human prostate. *Cell Tissue Res.* 2008;332(3):489-98.
25. Izumi K, Mizokami A, Namiki M, Inoue S, Tanaka N, Yoshio Y, et al. Enzalutamide versus abiraterone as a first-line endocrine therapy for castration-resistant prostate cancer (ENABLE study for PCa): a study protocol for a multicenter randomized phase III trial. *Bmc Cancer.* 2017;17.
26. Mateo J, Carreira S, Sandhu S, Miranda S, Mossop H, Perez-Lopez R, et al. DNA-Repair Defects and Olaparib in Metastatic Prostate Cancer. *N Engl J Med.* 2015;373(18):1697-708.
27. Centenera MM, Gillis JL, Hanson AR, Jindal S, Taylor RA, Risbridger GP, et al. Evidence for efficacy of new Hsp90 inhibitors revealed by ex vivo culture of human prostate tumors. *Clin Cancer Res.* 2012;18(13):3562-70.
28. Geller J, Sionit L, Partido C, Li L, Tan X, Youngkin T, et al. Genistein inhibits the growth of human-patient BPH and prostate cancer in histoculture. *Prostate.* 1998;34(2):75-9.
29. Centenera MM, Hickey TE, Jindal S, Ryan NK, Ravindranathan P, Mohammed H, et al. A patient-derived explant (PDE) model of hormone-dependent cancer. *Mol Oncol.* 2018;12(9):1608-22.
30. Bray K, Chen HY, Karp CM, May M, Ganesan S, Karantza-Wadsworth V, et al. Bcl-2 modulation to activate apoptosis in prostate cancer. *Mol Cancer Res.* 2009;7(9):1487-96.
31. Schiewer MJ, Goodwin JF, Han S, Brenner JC, Augello MA, Dean JL, et al. Dual roles of PARP-1 promote cancer growth and progression. *Cancer Discov.* 2012;2(12):1134-49.
32. van de Merbel AF, van der Horst G, van der Mark MH, van Uhm JIM, van Gennep EJ, Kloen P, et al. An ex vivo Tissue Culture Model for the Assessment of Individualized Drug Responses in Prostate and Bladder Cancer. *Frontiers in Oncology.* 2018;8(400).
33. Ahlgren H, Henjum K, Ottersen OP, Runden-Pran E. Validation of organotypical hippocampal slice cultures as an ex vivo model of brain ischemia: different roles of NMDA receptors in cell death signalling after exposure to NMDA or oxygen and glucose deprivation. *Cell Tissue Res.* 2011;345(3):329-41.
34. Meneghel-Rozzo T, Rozzo A, Poppi L, Rupnik M. In vivo and in vitro development of mouse pancreatic beta-cells in organotypic slices. *Cell Tissue Res.* 2004;316(3):295-303.
35. Behrsing HP, Vickers AE, Tyson CA. Extended rat liver slice survival and stability monitored using clinical biomarkers. *Biochem Biophys Res Commun.* 2003;312(1):209-13.
36. Centenera MM, Raj GV, Knudsen KE, Tilley WD, Butler LM. Ex vivo culture of human prostate tissue and drug development. *Nat Rev Urol.* 2013;10(8):483-7.
37. Varani J, Dame MK, Wojno K, Schuger L, Johnson KJ. Characteristics of nonmalignant and malignant human prostate in organ culture. *Lab Invest.* 1999;79(6):723-31.
38. Westenfelder KM, Lentz B, Rackerseder J, Navab N, Gschwend JE, Eiber M, et al. Gallium-68 HBED-CC-PSMA Positron Emission Tomography/Magnetic Resonance Imaging for Prostate Fusion Biopsy. *Clinical Genitourinary Cancer.* 2018.

39. Simopoulos DN, Natarajan S, Jones TA, Fendler WP, Sisk AE, Jr., Marks LS. Targeted Prostate Biopsy Using (68)Gallium PSMA-PET/CT for Image Guidance. *Urol Case Rep.* 2017;14:11-4.
40. Siriwardana A, Thompson J, van Leeuwen PJ, Doig S, Kalsbeek A, Emmett L, et al. Initial multicentre experience of 68Gallium-PSMA PET/CT guided robot-assisted salvage lymphadenectomy: acceptable safety profile but oncological benefit appears limited. *BJU international.* 2017.
41. van Oijen MGCT, Medema RH, Slootweg PJ, Rijksen G. Positivity of the proliferation marker Ki-67 in noncycling cells. *American journal of clinical pathology.* 1998;110(1):24-31.
42. Kraupp BG, RuttKay-Nedecky B, Koudelka H, Bukowska K, Bursch W, Schulte-Hermann R. In situ detection of fragmented DNA (TUNEL assay) fails to discriminate among apoptosis, necrosis, and autolytic cell death: a cautionary note. *Hepatology.* 1995;21(5):1465-8.
43. Korpál M, Korn JM, Gao X, Rakiec DP, Ruddy DA, Doshi S, et al. An F876L mutation in androgen receptor confers genetic and phenotypic resistance to MDV3100 (enzalutamide). *Cancer discovery.* 2013;3(9):1030-43.
44. Guerrero J, Alfaro IE, Gomez F, Protter AA, Bernales S. Enzalutamide, an androgen receptor signaling inhibitor, induces tumor regression in a mouse model of castration-resistant prostate cancer. *Prostate.* 2013;73(12):1291-305.
45. Beshiri ML, Tice CM, Tran C, Nguyen HM, Sowalsky AG, Agarwal S, et al. A PDX/organoid biobank of advanced prostate cancers captures genomic and phenotypic heterogeneity for disease modeling and therapeutic screening. *Clin Cancer Res.* 2018.
46. Parsels LA, Karnak D, Parsels JD, Zhang Q, Vélez-Padilla J, Reichert ZR, et al. PARP1 Trapping and DNA Replication Stress Enhance Radiosensitization with Combined WEE1 and PARP Inhibitors. *Molecular Cancer Research.* 2018;16(2):222-32.
47. Colicchia V, Petroni M, Guarguaglini G, Sardina F, Sahún-Roncero M, Carbonari M, et al. PARP inhibitors enhance replication stress and cause mitotic catastrophe in MYCN-dependent neuroblastoma. *Oncogene.* 2017;36(33):4682.
48. De Graaf IAM, Olinga P, De Jager MH, Merema MT, De Kanter R, Van De Kerkhof EG, et al. Preparation and incubation of precision-cut liver and intestinal slices for application in drug metabolism and toxicity studies. *Nature protocols.* 2010;5(9):1540.
49. Sauer UG, Vogel S, Aumann A, Hess A, Kolle SN, Ma-Hock L, et al. Applicability of rat precision-cut lung slices in evaluating nanomaterial cytotoxicity, apoptosis, oxidative stress, and inflammation. *Toxicol Appl Pharmacol.* 2014;276(1):1-20.
50. Draushuk AT, McGarrigle BP, Tai HL, Kitareewan S, Goldstein JA, Olson JR. Validation of precision-cut liver slices in dynamic organ culture as an *in vitro* model for studying CYP1A1 and CYP1A2 induction. *Toxicol Appl Pharmacol.* 1996;140(2):393-403.

Supplementary files

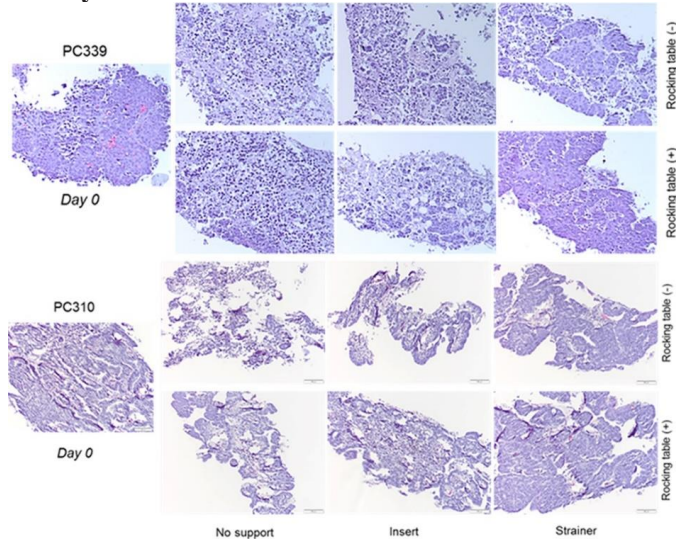


Figure S1. Effect of filter support and 3D orbital movement on PCa tissue slice morphology

Representative H&E images of PC339 and PC310 tumor slice sections after 4 days of culturing under the different culture conditions, compared to an initial slice (day 0).

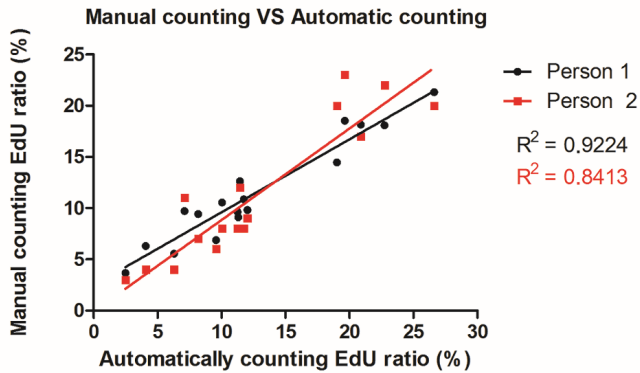


Figure S2. Correlation between manual counting and automatic counting.

EdU staining micrographs were randomly selected to test the reliability of the quantification algorithm. Manual counting results from two persons were compared to automatic counting results.

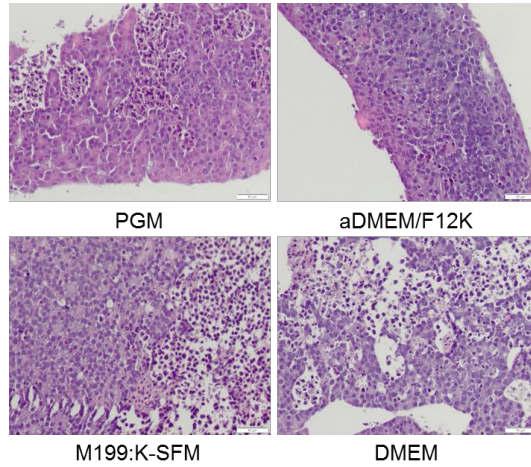


Figure S3. Effect of different media on tissue slice morphology.

Representative H&E images of PC295 tumor slice section after 4 days of culturing under different culture media.

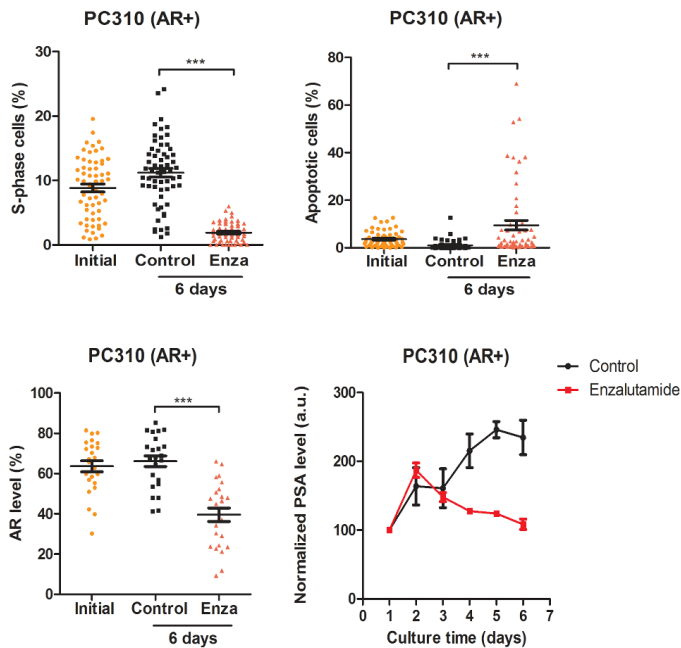


Figure S4. Ex-vivo Enzalutamide treatment effect on PC310 tumor

A). Quantification of the EdU-positive cell ratio of PC310 slices treatment with Enzalutamide, 10 image fields were analyzed per tumor slice. B) Quantification of the TUNEL-positive ratio of PC310 slices treated with Enzalutamide, 10 image fields were analyzed per tumor slice. C) Quantification of AR staining. Four image fields were analyzed per tumor slice (magnification $\times 100$). Each point represents one image field, average and SEM are indicated. D) Normalized PSA concentration in culture medium. (N=3). *** P < 0.001.

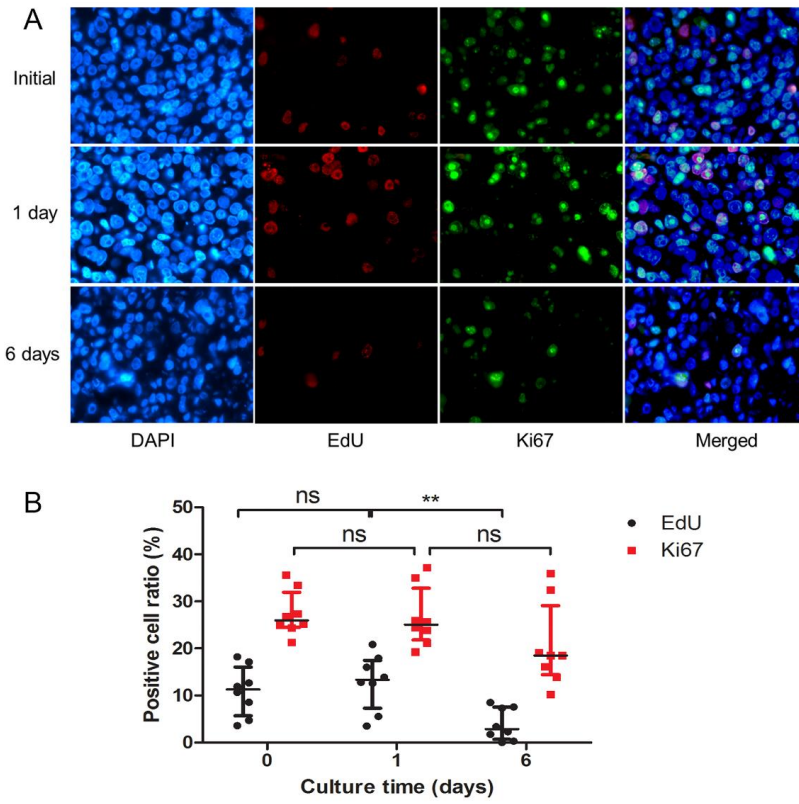
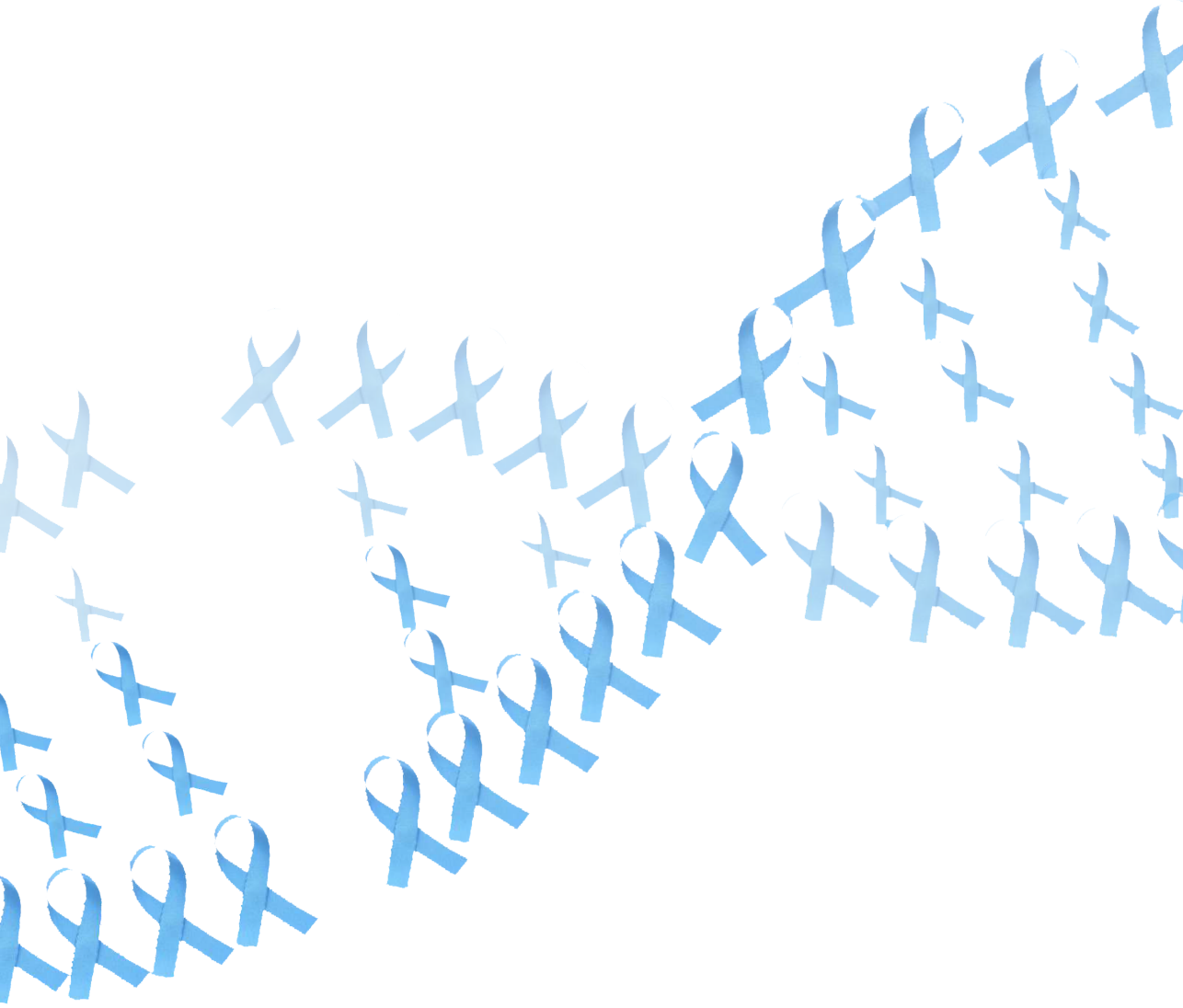


Figure S5. Double staining of Ki67 and EdU

Quantification of the Ki67 and EdU-positive cell ratio in PC295 slices cultured in aDMEM/F12K for different time points.



Chapter 4

Extracellular vesicle profiling for monitoring *ex vivo* prostate cancer therapy response

Wenhao Zhang¹, Sanjiban Chakrabarty¹, Natasja Dits³, Martin E. van Royen², Guido Jenster³, Julie Nonnekens^{1,4,5}, Wytske M. van Weerden³, Dik C. van Gent^{1,5}

¹Department of Molecular Genetics, Erasmus MC, Rotterdam, The Netherlands; ²Department of Pathology, Erasmus Optical Imaging Centre, Erasmus MC, Rotterdam, The Netherlands; ³Department of Urology, Erasmus MC, Rotterdam, The Netherlands; ⁴Dept of Radiology and Nuclear Medicine, Erasmus MC, Rotterdam, The Netherlands; ⁵Oncode Institute, Erasmus MC, Rotterdam, The Netherlands.

Manuscript in preparation

Abstract

Extracellular vesicles (EVs) are naturally occurring cell-derived vesicles which carry biomolecules such as lipids, proteins, and nucleic acids. EV-derived RNAs may serve as potential biomarkers for diagnosis, prognosis and therapeutic monitor of prostate cancer (PCa). We used a previously established *ex vivo* method to culture tissue slices from patient-derived xenografts (PDXs) of PCa to assess if EVs could be used to monitor responses to anti-androgen treatments. We analyzed treatment effects in tumor slices and in EVs secreted from these tissue slices in the culture medium, and characterized their abundance and RNA content. We detected abundant presence of EVs with high yield of RNAs in the tissue slice culture medium, which was sufficient for downstream analyses. As expected, tissue slices from hormone sensitive PDXs showed marked responses to the anti-androgen treatment. This response was reflected by changes in EV quantity and RNA profile. We reported that androgen receptor (AR)-regulated gene *FKBP5* and DNA damage response gene *BRCA1* and *RAD51* expression alterations after anti-androgen treatment in tumor slices is highly similar to that detected in EVs. This implies that EVs may reflect the biological effects on the original tissue and may thus be used as a biomarker for monitoring treatment response.

1. Introduction

Extracellular vesicles (EVs) are small membrane vesicles secreted by various types of cells into the extracellular environment to mediate cell communication (1, 2). They are enclosed by a phospholipid bilayer and contain DNA, RNA and proteins (3, 4). Different types of vesicles, such as exosomes, microvesicles and apoptotic bodies, were defined by biogenesis and roughly correlated with their size (5). Exosomes are small vesicles with a diameter generally in the range between 40 to 150 nm. They are released from cells upon fusion of an intermediate endocytic compartment, the multivesicular body, with the plasma membrane (1). Microvesicles are generally larger (100–1000 nm) and are formed by direct budding of the plasma membrane (6). Apoptotic bodies are released upon programmed cell death by membrane blebbing and the size can range from 50 nm up to 5 μ m in diameter (7). However, the classification of individual EVs is difficult and the origin of the individual EVs in cell culture medium and body fluids cannot yet be determined, we use here the term EVs as is the consent in the EVs community (8). Initially, EVs were regarded as cellular debris, however, in recent years several studies have proposed roles for EVs in physiological and pathogenic processes (9, 10). Particularly, recent work highlighted EV-mediated cell-to-cell communication in cancer, where transfer of EVs from the tumor to the tumor-microenvironment promotes cancer propagation (11), transfers phenotype (12), and modulates immune response (13) and cancer metastasis (14). EVs from cultured cells are released into the cell culture medium, and *in vivo* they are also found in body fluids. They may therefore serve as biomarkers for the development of sensitive and minimally invasive diagnostic alternatives in precision medicine as they may reflect the tumor cell origin in terms of content (protein, RNA, DNA) (15). However, despite the promising application of EVs in diagnosis, prognosis and therapy monitoring in cancer, their small sizes and the limited quantities that can usually be obtained from patient-derived samples pose a number of challenges to their isolation and characterization (16). So far, no clear consensus has been reached on the best method for the quantification and isolation of EVs from culture medium and biofluids (16). We used EVQuant which uses fluorescent lipophilic dyes and specific fluorescent labelled antibodies for visualizing and quantifying EVs. The advantage of this method is low sample input requirement (50 μ L), fast sample preparation, and short measurement time. There are numerous methods for EVs isolation and vesicles RNA extraction, such as precipitation, filtration, ultracentrifugation and affinity binding. We used a one-step affinity binding protocol, which is a rapid and simple procedure with high RNA yield (17).

Prostate cancer (PCa) is the most commonly diagnosed cancer and fifth leading cause of cancer-related death among men in western countries (18). Most preclinical studies of PCa depend heavily on immortalized cancer cell lines, which are grown in culture dishes as a two-dimensional (2D) model. These isolated cells do not adequately recapitulate important aspects of tissue function related to cell-cell communications *in vivo* and some important information may lose when studying EVs from cell culture system. This is the rationale to develop three-dimensional (3D) models which maintain the cellular relationships *ex vivo* (19). Previously, we have established an *ex vivo* method to culture tissue slices from patient-derived xenografts (PDX) of PCa for assessing responses to dedicated treatments (20). The faithful retention of tissue structure and function in this *ex vivo* model offers an ideal opportunity for treatment efficacy screening. Compared with animal studies, which require extensive resources, it reduces costs and numbers of experimental animals. Besides investigating treatment effect by directly assessing tumor slices, we further looked into the EVs secreted by

tissue slices, and studied whether EVs are feasible biomarkers in such an *ex vivo* setting to monitor treatment response. We characterized the tissue slice-derived EVs by using EVQuant, and we compared tissue slice and EV RNA profiles.

2. Material and methods

2.1 Reagents

Reagents were purchased from Sigma-Aldrich, unless otherwise specified.

2.2 Collection of PDX tumor

All animal experiments were approved by the Animal Welfare Committee of the Erasmus MC, and all experiments were conducted in accordance with accepted guidelines. Hormone sensitive PCa PDXs (PC310 and PC295) were established by van Weerden *et al.* (21) and were routinely passaged by subcutaneous grafting of small fragments onto both shoulders of intact male athymic NMRI nu/nu mice (Taconic Biosciences, Cologne, Germany). Fresh PDX tumors with volume of 500–1000 mm³ were obtained. After removal from mice, the tumors were kept on ice in Dulbecco's Modified Eagle Medium (DMEM; Lonza, Verviers Sprl, Belgium).

2.3 Tissue slice culture

Tissue slices were cultured as previously reported (20). Briefly, 300 µm slices were cultured on cell strainers (pore size 40 µm, Corning) in 3 mL serum-free advanced DMEM/F12 (ThermoFisher Scientific) medium in 6 well plates at 5% CO₂ and 37°C on a Rocking Table (Luckham 200 Ltd, West Sussex, UK). One third of medium was collected and refreshed daily. Collected medium was stored at -80 °C for later EV isolation. Slices were treated with enzalutamide (1 µM, Sequoia Research Products, Pangbourne, UK) or with vehicle control (dimethyl sulfoxide, DMSO) and cultured for different time points. Subsequently, slices were harvested and fixed in 10% neutral buffered formalin for 24 h at room temperature, embedded in paraffin and 4 µm sections were made for further analysis.

2.4 EVs detection and quantification

Isolated vesicles from tissue slice culture medium were quantified using the EVQuant method (unpublished method from M. E. van Royen (22)). Briefly, medium was first centrifuged at 3000 g for 10 min, then 50 µL of medium were incubated with Alexa fluor 647 labelled CD9 antibody (mouse, MEM-61, ThermoFisher scientific) and Alexa fluor 488 labelled CD63 antibody (mouse, MX49.129.5, Santa Cruz biotechnology) for 2 h, followed by fluorescently labelled rhodamine dye incubation for 10 min and immobilized in a polyacrylamide gel. The labeled vesicles are then detected and quantified by using the Opera Phenix high content screening system (PerkinElmer).

2.5 RNA isolation from exosomes

Exosome-derived RNA from tissue slice culture medium was isolated from 1 mL media using the exoRNeasy Midi kit (Qiagen, Hilden, Germany) according to manufacturer's protocol. Briefly, culture medium was first filtered by Millex®-AA syringe filters (Millipore) to exclude large particles and passed through a membrane-based affinity exoEasy spin column. Subsequently, a phenol/guanidine-based combined lysis and elution step recovered vesicular RNA from the exoEasy spin columns, which was followed by silica-membrane based purification of total RNA. After the lysis and elution step, the mixture was extracted using chloroform. The aqueous phase was collected in RNeasy MinElute spin column and washed with buffer twice. Finally, RNA was eluted in 14 µL RNase-free water.

2.6 RNA isolation from formalin-fixed, paraffin-embedded (FFPE) tissue sections from cultured tissue slices

Total RNA from the FFPE tissue slices was isolated by using RNeasy FFPE kit (Qiagen, Hilden, Germany) according to manufacturer's protocol.

2.7 RNA characterization

The RNA concentration was assessed using a NanoDrop 2000 spectrophotometer (Thermo Scientific, Waltham, MA, USA). Ranges of RNA concentration measurement with NanoDrop are between 20 and 500 ng/ μ L. The purity of RNA is indicated by measuring the absorbance ratios (260/280 and 260/230). A 260/280 and a 260/230 ratio of approximately 2 is usually interpreted as pure RNA. For highly precise analysis of RNA yield and size distribution, an Agilent 2100 Bioanalyzer with an RNA 6000 Pico kit (Agilent Technologies, Foster City, CA, USA) was employed according to the manufacturer's protocol.

2.8 Gene expression analysis

cDNA was synthesized from 500 ng total RNA by using First Strand cDNA Synthesis Kit (ThermoFisher scientific). Reverse transcription polymerase chain reaction (RT-PCR) was performed using TaqMan® Fast advanced RT-PCR Master Mix (ABI) in a 10 μ L reaction mixture containing 1 μ L cDNA template, 0.5 μ L TaqMan assay probe, 5 μ L TaqMan advanced master mix and 3.5 μ L H₂O. Amplification was performed on a CFX96 Touch™ Real-Time PCR Detection System (Bio-Rad) under the following conditions: 50 °C for 2 min, 95 °C for 20 sec followed by 40 cycles of 3 sec at 95 °C, 30 sec at 60°C. TaqMan probes were purchased from ThermoFisher Scientific. The gene expression level was analyzed by using the $2^{-\Delta\Delta C_t}$ method and relative mRNA expression was normalized to housekeeping gene *GAPDH*.

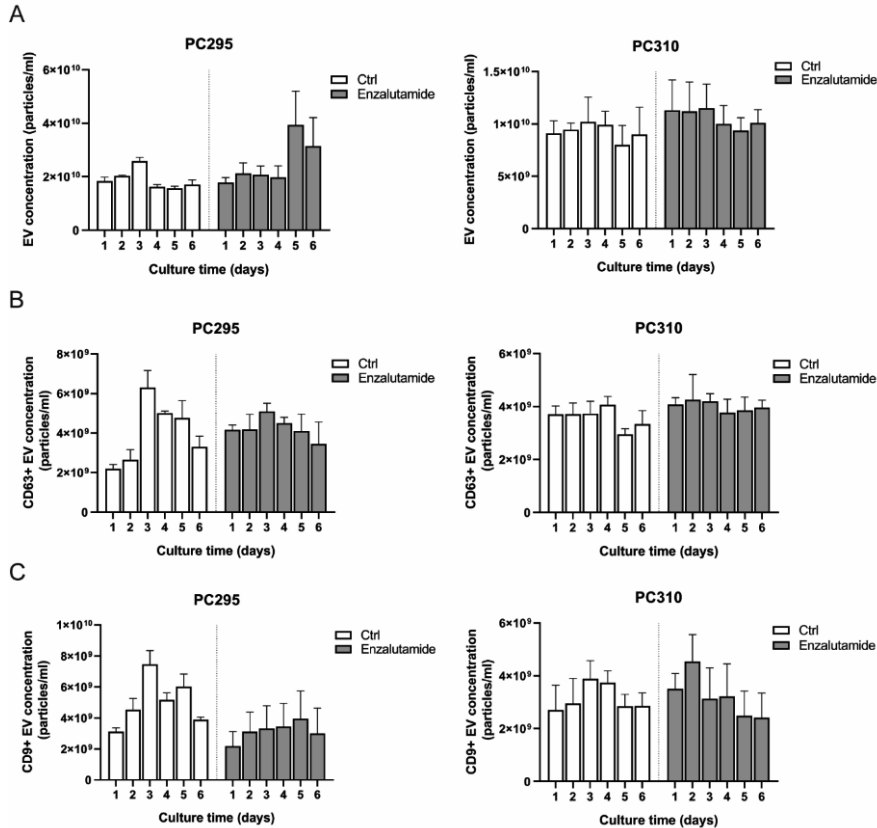
Gene symbol	Assay ID	Catalog number
Glyceraldehyde-3-phosphate dehydrogenase (<i>GAPDH</i>)	Hs02786624_g1	4331182
Breast Cancer 1 genes (<i>BRC1</i>)	Hs01556193_m1	4453320
RAD51 recombinase (<i>RAD51</i>)	Hs00947967_m1	4448892
FKBP prolyl isomerase 5 (<i>FKBP5</i>)	Hs01561006_m1	4331182

3. Results

3.1 Abundant EVs in tissue slices culture medium

Tumor slices were cultured and treated with the anti-androgen enzalutamide or control continuously for 6 days and we monitored the EV secretion during these days. Serum-free culture medium was used in our system, ensuring that only tissue slice-derived EVs were present in the media. We used an in house developed assay to quantify EVs (EVQuant). In short, EVs were labelled with lipophilic rhodamine dye as a probe for detecting all lipid bilayer structures in medium. As shown in Figure 1A and quantified as particle numbers, EVs are present in the tissue slice culture medium. After 24 h of culturing, around 10^{10} particles per mL were detected in the culture medium of both PC295 and PC310 tissue slices.

Figure 1.

**Figure 1 Quantification of EVs in tissue slices culture medium.**

The total amount of EVs (A), CD63 (B) and CD9 positive (C) EVs secreted from tissue slices were quantified by using EVQuant (n=3). Average and SEM are indicated.

This amount is much higher than detected in the culture medium of PCa cell lines, blood and urine samples reported by previous studies (17, 23). Enzalutamide-treated PC295 tumor slices have significantly increased EVs concentrations in the media after 5 days of treatment compared to the amount of EVs in previous days, which could be explained by substantial treatment-induced apoptosis (Supplementary Figure 1A) resulting in a release of large numbers of apoptotic bodies in the culture medium. This result from EVQuant is corroborated by the lack of enzalutamide induced EVs release in PC310 which showed much lower levels of treatment induced apoptosis in the tissue slices (Supplementary Figure 1A). To further confirm the existence of EVs in culture medium, we investigated the existence of EVs surface markers (CD9, CD63). Antibody incubation was combined with rhodamine dye to specifically detect EVs with CD9 and CD63 expression. Overall, we detected EVs with positive CD63 (Figure 1B) and CD9 (Figure 1C) expression in both PC295 and PC310 tumor slice culture medium. The quantity of the surface marker positive EVs was much less than total amount of EVs ($2-4 \times 10^9$ /mL) for both tumor types. This may be caused by many EVs have too few

CD9 or CD63 expression that cannot be visualized by fluorescent microscopy. The presence of marker positive EVs in PC295 fluctuated more during the culture than in PC310, but we did not observe an increase of EVs upon enzalutamide treatment, suggesting that EVs increase in PC295 upon enzalutamide treatment indeed reflected apoptosis.

3.2 Enriched RNA concentration in tissue slice culture medium

We were able to extract measurable amounts of RNA from 1 mL tissue slice culture medium for both PC295 (4992 ± 1778 ng) and PC310 (710 ± 278 ng). The much higher RNA concentration yielded from PC295 culture medium is mainly due to larger tissue slice size and higher EV counts. Total vesicle RNA recovery from tissue culture medium was further characterized by capillary electrophoresis using the Agilent 2100 Bioanalyzer, and RNA Pico chips (Figure 2). The majority of vesicle RNA from tissue culture medium was small (<200 nt), but there were variations in the RNA profiles between these two tumor types. We found that in PC295 RNA not only presented the main peak around 100 nt, but also showed some longer RNA species (500-1000 nt). However, PC310 only showed the clear small RNA (100 nt) with barely detectable longer RNA. Enzalutamide treatment did not alter the RNA quantity and size distribution (Figure 3). These data are in agreement with previous studies (24, 25), showing that small EVs primarily contain small RNA, such as miRNA, snRNA, snoRNA and broken mRNA, but also some full-length mRNA (more than 1kb long).

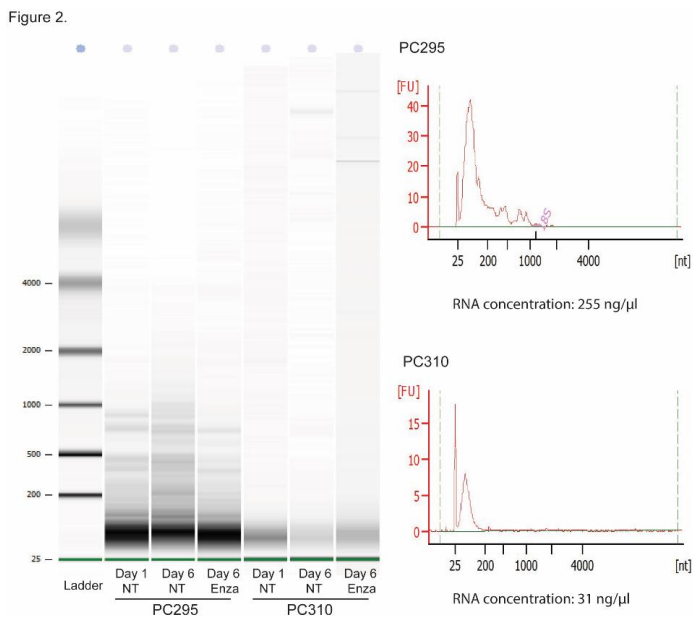


Figure 2 Bioanalyzer analysis of total EV RNA by Agilent RNA Pico chip.

The RNA ladder standard (in the first lane) contains six RNA fragments ranging in size from 0.2 to 6 kb. Representative bands of vesicle RNA from PC295 tissue slice (lane 2 to lane 4) and PC310 tissue slice (lane 5 to lane 7) were displayed. Almost all of the samples showed an obvious band in the small RNA area (25-200 nt).

3.3 Gene expression pattern in tissue RNA correlates with vesicle RNA

Finally, the gene expression levels of several mRNAs (*FKBP5*, *RAD51* and *BRCA1*), were analyzed by RT-qPCR and compared to the expression in the tissue slice of origin (Figure 3). Based on Ct values, 25-36 for all the genes tested, RNA isolation was efficient and the amount of material recovered is sufficient for standard PCR analysis. We compared the gene expression change after treatment between the EVs and tissue slices. RNA was extracted from FFPE tissue section and gene expression assays were performed. As expected, *FKBP5*, one of the key AR-signaling regulated genes, was significantly downregulated in both tumor tissues after 6 days of enzalutamide treatment. Interestingly, we observed a similarly dramatic decrease of *FKBP5* expression in EVs RNA after 6 days of treatment. Moreover, we found that reduction in viability and cell cycle blockade is less severe in PC310 compared with PC295 (Supplementary Figure 1B), probably due to difference in enzalutamide sensitivity. And this different sensitivity is also reflected by less dramatic changes in mRNA expression in slices as well as in EVs. Similarly, the expression of *BRCA1* and *RAD51* significantly dropped in tissue slices treated with enzalutamide, which also applied in EVs RNA expression from the same tissue slices. Taken together, these data suggest that RNA recovered from EVs in tissue slice culture medium is sufficient for downstream analysis and vesicle mRNA may be used as a proxy for gene expression changes in the original tissue slice.

Figure 3

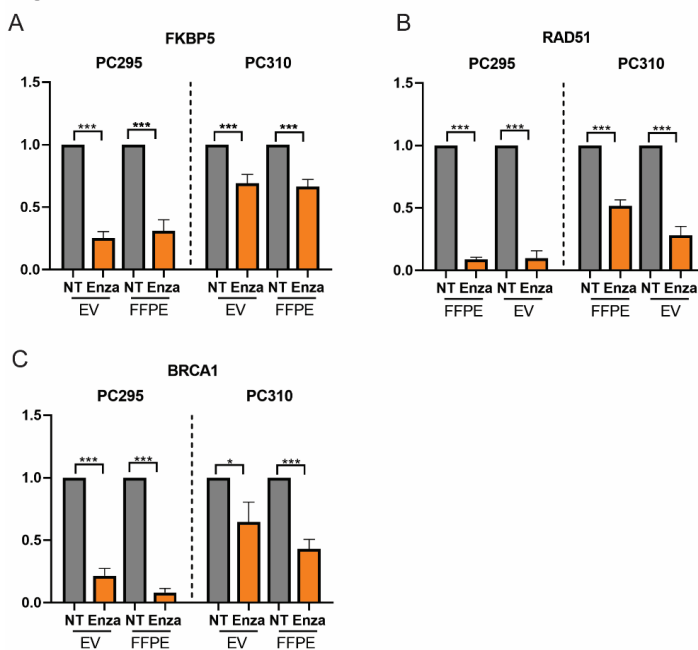


Figure 3 Gene expression pattern in tissue RNA correlates with EV RNA

Analysis of the mRNA levels from FFPE tissue section and EVs upon enzalutamide (Enza) or DMSO control (NT) treatment by qRT-PCR. Levels of three mRNAs (*FKBP5*, *RAD51*, *BRCA1*) were quantified by qRT-PCR using TaqMan assays and reagents. The gene expression level was analyzed by using the $2^{-\Delta\Delta Ct}$ method and relative mRNA expression was normalized to housekeeping

gene GAPDH. Average and SEM are indicated, *P < 0.05, **P < 0.01, ***P < 0.001.

4. Discussion

Here, we report the abundant presence of EVs derived from PCa tissue slices and high yield of RNA from those EVs which can be analyzed and reflects three tested gene expression alterations in tissue slices upon anti-androgen treatment.

The discovery of vesicle RNA as a signaling molecule has revolutionized our understanding of RNA in cell biology and has enormous translational potential for human disease. While significant advances have been achieved, the vesicle RNA field still faces challenges, especially, in isolating and analyzing vesicles RNAs from biological samples and the lack of faithful experimental models for mechanistic studies. By culturing a small tissue slice (surface area 50 - 150 mm², thickness 300 μm), the EV concentrations achieved are 10-100 folds higher than what is usually detected in 2D cell culture media. We could extract sufficient RNA from only 1 mL tissue slice culture medium for reliable downstream analysis. We propose several plausible explanations for such a high EVs concentration and RNA yield efficiency in our system. 1. Tissue slices contain more cells than monolayer cell culture. When roughly calculated: in a tissue slice (surface area 150 mm² and a single cell diameter 10 μm), there are 6 × 10⁷ cells, more than a confluent T-175 flask (2 × 10⁷ cells). 2. Tissue slices were cultured under 3D orbital movement condition, which may lead to more EVs release by mechanical force compared to conventional stationary condition. 3. The uptake of EVs by the cells in the slice can be different from monolayer cell culture.

Although the RNA inside EVs consists predominantly of small RNAs, vesicle have previously been shown to contain well-known PCa-associated transcripts as well, such as the kallikrein related peptidase 3 (*PSA*) and the transmembrane serine protease 2-ETS transcription factor ERG (*TMPRSS2-ERG*) fusion have been found in urinary EVs in men with PCa (26, 27). Measuring transcripts in PCa-derived EVs isolated from biofluids is expected to be a powerful method for the diagnosis, prognosis, and monitoring of PCa. However, it is uncertain that EVs from biofluid are tumor-associated. Microarray, RT-PCR and RNA sequencing studies published so far have only focused on miRNA from PCa-derived vesicles (28, 29). Since miRNAs are not PCa specific, the reliability and accuracy of these miRNAs as PCa biomarker can only be confirmed when they are specifically isolated from prostate/PCa-derived EVs.

In our study, by using serum-free culture condition, bovine EVs are excluded and human specific primers also guarantee that mouse EVs transcript from stroma are not detected, thus fully ensure the tumor-specific EVs transcript analysis. We detected *FKBP5*, *BRCA1* and *RAD51* transcripts in EVs from tissue slice culture medium, and the expression of all three genes have significantly downregulated upon enzalutamide treatment both in EVs and matched tissue slices. This data support for the hypothesis that mRNA from EVs reflects the status of the tissue of origin. *BRCA1* and *RAD51* play a crucial role in DNA homologous recombination (HR) and a previous study reported that enzalutamide suppressed the expression of those HR genes, thus creating HR deficiency in PCa cells (30). However, from our previous study (W. Zhang, chapter 6), we provide evidence that the significantly reduced S-phase cell ratio in treated tissue slices can explain the substantial decrease of *BRCA1* and *RAD51* expression instead of direct enzalutamide induced HR deficiency, since HR only happens in S/G2 phases of the cell cycle (Supplementary Figure 1B).

Current study opens a promising direction to implement tissue slice culture and

EVs in the context of personalized medicine. Tumor slices from PCa patients can be cultured in an *ex vivo* system or more advanced controlled system such as microfluidic organ-on-chip device, where we can monitor treatment responses by collecting culture medium and analyzing EVs content. For example: by looking at specific gene expression in compound targeted pathways or by performing RNA sequencing for wide transcriptome analysis.

In conclusion, we characterized the EVs from PCa tissue slice culture medium and detected abundant presence of EVs with high yield of RNAs with PCa specificity. We showed that similar gene expression alterations can be detected in tumor slices and their isolated secreted EVs after anti-androgen treatment. This data suggests that EVs may reflect the biological function of original cells and have the potential to be used to monitor treatment response in tissue slice culture system.

Acknowledgements

The authors thank D. Stuurman and C. de Ridder for their help in acquiring xenograft tumor samples.

Conflict of interest

We have nothing to disclose.

Funding

This work was supported by the Chinese Scholarship Council (grant number 201506270172 (WZ)), the IMMPROVE Alpe d’HuZes grant of the Dutch Cancer Society (EMCR2015-8022), Prostate Cancer UK grant (G2012-36).

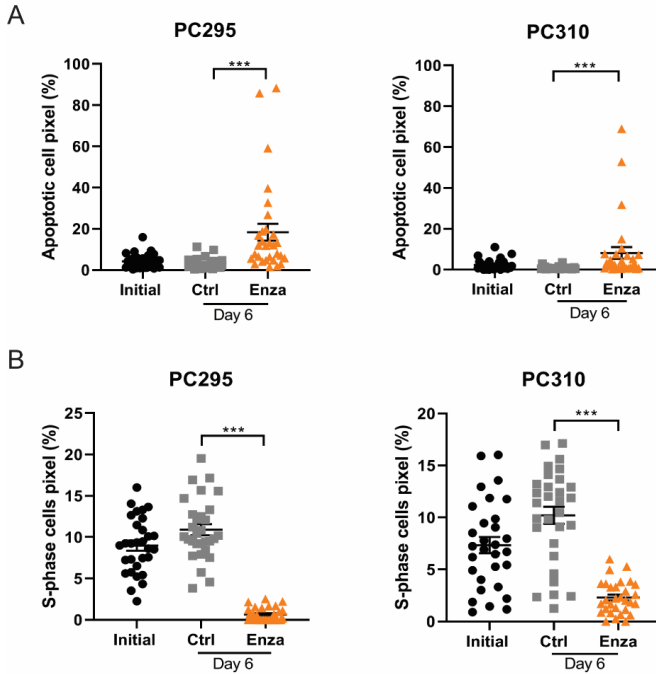
Reference

1. Colombo M, Raposo G, Thery C. Biogenesis, secretion, and intercellular interactions of exosomes and other extracellular vesicles. *Annu Rev Cell Dev Biol.* 2014;30:255-89.
2. Choi D, Lee TH, Spinelli C, Chennakrishnaiah S, D'Asti E, Rak J. Extracellular vesicle communication pathways as regulatory targets of oncogenic transformation. *Semin Cell Dev Biol.* 2017;67:11-22.
3. Février B, Raposo G. Exosomes: endosomal-derived vesicles shipping extracellular messages. *Current Opinion in Cell Biology.* 2004;16(4):415-21.
4. Raposo G, Stoorvogel W. Extracellular vesicles: exosomes, microvesicles, and friends. *J Cell Biol.* 2013;200(4):373-83.
5. van der Pol E, Böing AN, Harrison P, Sturk A, Nieuwland R. Classification, Functions, and Clinical Relevance of Extracellular Vesicles. *Pharmacological Reviews.* 2012;64(3):676-705.
6. Tricarico C, Clancy J, D'Souza-Schorey C. Biology and biogenesis of shed microvesicles. *Small GTPases.* 2017;8(4):220-32.
7. Hauser P, Wang S, Didenko VV. Apoptotic Bodies: Selective Detection in Extracellular Vesicles. *Methods Mol Biol.* 2017;1554:193-200.
8. Thery C, Witwer KW, Aikawa E, Alcaraz MJ, Anderson JD, Andriantsitohaina R, et al. Minimal information for studies of extracellular vesicles 2018 (MISEV2018): a position statement of the International Society for Extracellular Vesicles and update of the MISEV2014 guidelines. *J Extracell Vesicles.* 2018;7(1):1535750.
9. Bank IE, Timmers L, Gijsberts CM, Zhang YN, Mosterd A, Wang JW, et al. The diagnostic and prognostic potential of plasma extracellular vesicles for cardiovascular disease. *Expert Rev Mol Diagn.* 2015;15(12):1577-88.
10. Yoon YJ, Kim OY, Gho YS. Extracellular vesicles as emerging intercellular communicasomes. *BMB Rep.* 2014;47(10):531-9.
11. Skog J, Wurdinger T, van Rijn S, Meijer DH, Gainche L, Sena-Esteves M, et al. Glioblastoma microvesicles transport RNA and proteins that promote tumour growth and provide diagnostic biomarkers. *Nat Cell Biol.* 2008;10(12):1470-6.
12. Al-Nedawi K, Meehan B, Micallef J, Lhotak V, May L, Guha A, et al. Intercellular transfer of the oncogenic receptor EGFRvIII by microvesicles derived from tumour cells. *Nat Cell Biol.* 2008;10(5):619-24.
13. Huber V, Fais S, Iero M, Lugini L, Canese P, Squarcina P, et al. Human colorectal cancer cells induce T-cell death through release of proapoptotic microvesicles: role in immune escape. *Gastroenterology.* 2005;128(7):1796-804.
14. Luga V, Zhang L, Vitoria-Petit AM, Ogunjimi AA, Inanlou MR, Chiu E, et al. Exosomes mediate stromal mobilization of autocrine Wnt-PCP signaling in breast cancer cell migration. *Cell.* 2012;151(7):1542-56.
15. Junker K, Heinzlmann J, Beckham C, Ochiya T, Jenster G. Extracellular Vesicles and Their Role in Urologic Malignancies. *Eur Urol.* 2016;70(2):323-31.
16. Hartjes TA, Mytnyk S, Jenster GW, van Steijn V, van Royen ME. Extracellular Vesicle Quantification and Characterization: Common Methods and Emerging Approaches. *Bioengineering (Basel).* 2019;6(1).
17. Tang YT, Huang YY, Zheng L, Qin SH, Xu XP, An TX, et al. Comparison of isolation methods of exosomes and exosomal RNA from cell culture medium and serum. *Int J Mol Med.* 2017;40(3):834-44.
18. Ferlay J, Soerjomataram I, Dikshit R, Eser S, Mathers C, Rebelo M, et al. Cancer incidence and mortality worldwide: sources, methods and major patterns in GLOBOCAN 2012. *Int J Cancer.* 2015;136(5):E359-86.
19. Wilding JL, Bodmer WF. Cancer cell lines for drug discovery and development. *Cancer Res.* 2014;74(9):2377-84.

20. Zhang W, van Weerden WM, de Ridder CMA, Erkens-Schulze S, Schonfeld E, Meijer TG, et al. Ex vivo treatment of prostate tumor tissue recapitulates in vivo therapy response. *Prostate*. 2019;79(4):390-402.
21. Navone NM, van Weerden WM, Vessella RL, Williams ED, Wang Y, Isaacs JT, et al. Movember GAP1 PDX project: An international collection of serially transplantable prostate cancer patient-derived xenograft (PDX) models. *Prostate*. 2018;78(16):1262-82.
22. T H, D, Duijvesz, R, Van Der Meel, M, Vredenbregt, M, Bekkers, A, Houtsmuller, R, Schiffelers, G, Jenster, M, Van Royen. The Fifth International Meeting of ISEV, ISEV2016. *Journal of Extracellular Vesicles*. 2016;5:1, 31552. (Abstract OT16.4).
23. Cobbs A, Chen X, Zhang Y, George J, Huang M-b, Bond V, et al. Saturated fatty acid stimulates production of extracellular vesicles by renal tubular epithelial cells. *Molecular and Cellular Biochemistry*. 2019;458(1):113-24.
24. Valadi H, Ekstrom K, Bossios A, Sjostrand M, Lee JJ, Lotvall JO. Exosome-mediated transfer of mRNAs and microRNAs is a novel mechanism of genetic exchange between cells. *Nat Cell Biol*. 2007;9(6):654-9.
25. Zeringer E, Li M, Barta T, Schageman J, Pedersen KW, Neurauter A, et al. Methods for the extraction and RNA profiling of exosomes. *World J Methodol*. 2013;3(1):11-8.
26. Dijkstra S, Birker IL, Smit FP, Leyten GHJM, de Reijke TM, van Oort IM, et al. Prostate Cancer Biomarker Profiles in Urinary Sediments and Exosomes. *The Journal of Urology*. 2014;191(4):1132-8.
27. Donovan MJ, Noerholm M, Bentink S, Belzer S, Skog J, O'Neill V, et al. A molecular signature of PCA3 and ERG exosomal RNA from non-DRE urine is predictive of initial prostate biopsy result. *Prostate Cancer And Prostatic Diseases*. 2015;18:370.
28. Huang X, Yuan T, Liang M, Du M, Xia S, Dittmar R, et al. Exosomal miR-1290 and miR-375 as Prognostic Markers in Castration-resistant Prostate Cancer. *European Urology*. 2015;67(1):33-41.
29. Hessvik N, Sandvig K, Llorente A. Exosomal miRNAs as Biomarkers for Prostate Cancer. *Frontiers in Genetics*. 2013;4(36).
30. Li L, Karanika S, Yang G, Wang J, Park S, Broom BM, et al. Androgen receptor inhibitor-induced "BRCAness" and PARP inhibition are synthetically lethal for castration-resistant prostate cancer. *Sci Signal*. 2017;10(480):eaam7479.

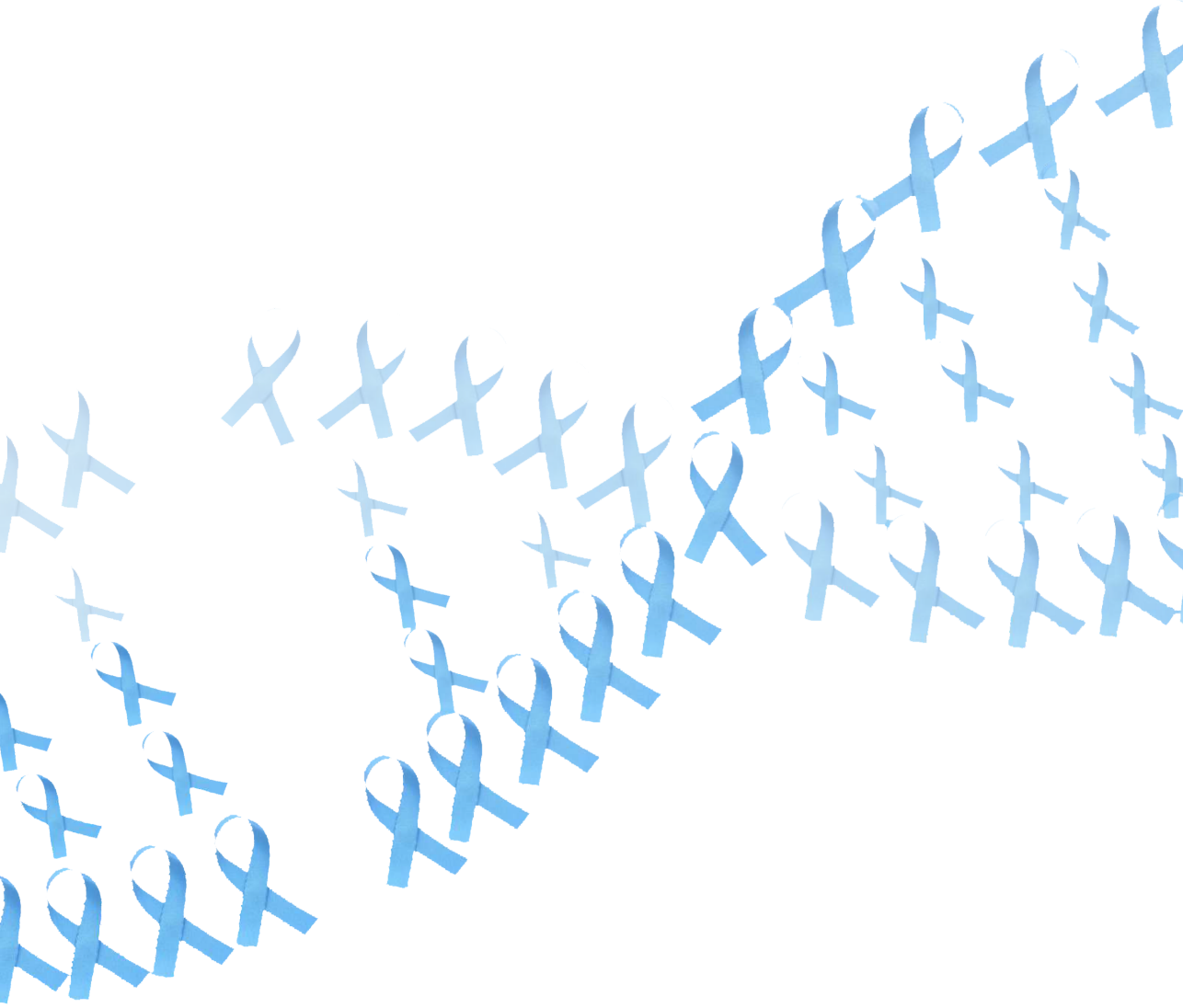
Supplementary file

Supplementary figure 1



Supplementary Figure 1 Response to *ex vivo* enzalutamide treatment

Quantification of the fraction of TUNEL-positive (A) and EdU-positive (B) cells for PC295 and PC310 slices after 6 days of enzalutamide (Enza) treatment. Line represents mean values and bars indicate SEM. Ten image fields for EdU/TUNEL were analyzed per tumor slice section. Each point represents one image field, average, and SEM are indicated (three independent biological replicates for each tumor type). * $P < 0.05$, ** $P < 0.01$, *** $P < 0.001$.



Chapter 5

Radiosensitivity of prostate cancer: assessment in patient-derived xenograft tissue slices and organoids

Wenhao Zhang ¹, Annelies Van Hemelryk ², Corrina MA de Ridder ², Sigrun Erkens-Schulze ², Debra Stuurman ², Dik C van Gent ^{1,3}, Julie Nonnekens ^{1,4}, Wytske M van Weerden².

¹Dept of Molecular Genetics, Erasmus University Medical Center, Rotterdam, The Netherlands; ²Dept of Urology, Erasmus University Medical Center, Rotterdam, The Netherlands; ³Oncode Institute, Erasmus University Medical Center, Rotterdam, The Netherlands; ⁴Dept of Radiology and Nuclear Medicine, Erasmus University Medical Center, Rotterdam, The Netherlands

Manuscript in preparation

Abstract

Radiotherapy is a standard treatment for localized prostate cancer (PCa). However, tumors might recur after radiotherapy and new combination strategies aiming to enhance treatment effect are under investigation. Traditional cell line models may not adequately recapitulate *in vivo* irradiation effect thus lead to a failure when transitioning newly tested treatments from bench to the clinic. Novel PCa organoids culture might circumvent this disadvantage while preserving the suitability for semi-high throughput screening approaches. We aim to evaluate the radiosensitivity of PCa, in organoids culture generated from patient-derived xenograft (PDX) with different *BRCA2* status and compared this with their matched tissue slices cultures. We ask whether PCa organoids can be a representative preclinical model for radiotherapy or radiotherapy-drug combinations testing. For this, tissue slices and organoids were irradiated with a dosage of 2 Gy X-ray. Cell proliferation, apoptosis and DNA damage repair were evaluated at different time points. PDX-derived PCa organoids were generated which maintained the morphology and AR signaling of the original PDX tumor. Direct comparison of organoids to tissue slices demonstrated the similarity between these two novel *in vitro* 3D models for evaluating irradiation response. Based on tested models, we were unable to elicit a relationship between *BRCA2* mutations and increased radiosensitivity. This result warrants further validation with more tumor models and treatments in order to obtain a complete view of similarities and differences between both culture models.

1. Introduction

Prostate Cancer (PCa) is the most common malignancy and the second most common cause of cancer-related death among men (1). Radical prostatectomy and external beam radiation therapy (EBRT) are first line treatments of localized PCa, but tumors can recur after treatment (2, 3). Currently, new combination strategies aiming to enhance irradiation effect are under investigation. In order to speed up the process of assessing the most promising combinations, faster and better preclinical models are urgently needed. As generally acknowledged (4), PCa research has been hampered by the lack of suitable *in vitro* model systems. Traditional cell line models may not adequately recapitulate *in vivo* irradiation effects as they neither recapitulate the complex architecture of tumors nor the important interaction between tumor cells. Together, this may lead to a failure when transitioning newly tested treatments from bench to the clinic. Although powerful *in vivo* models are available, these are often expensive and time-consuming.

Novel 3D culture technologies such as tissue slices and organoid cultures might circumvent this disadvantage while preserving the suitability for medium throughput screening approaches. Tissue-derived adult stem cells can be embedded in a 3D matrix and grown into self-organizing organotypic structures, termed organoids (5). Similar technology allows 3D culture of tumor cells in spheroid structures - often referred to as tumor organoids. Organoid cultures can represent (part of) the heterogeneity of the original tumor with a good chance for *ex vivo* expansion of primary tumor cells. However, it is not completely clear how well these tumor organoids recapitulate structural and functional aspects of their *in vivo* counterpart tumors.

Ionizing radiation (IR) damages DNA by inducing base damages, single-strand breaks and double-strand breaks (DSBs). DSBs are the most critical lesions and faulty repair or lack of repair of these lesions could lead to substantial chromosomal instability. Cells exhibit complex signal transduction, cell cycle checkpoints and repair pathways to respond to DNA damage and maintain the genomic integrity. Homologous recombination (HR) and non-homologous end-joining (NHEJ) are the two major DSB repair pathways. These two mechanisms act at different phases of the cell cycle. Breast cancer 2 (*BRCA2*) is a tumor-suppressor gene located at chromosome 13 which has been implicated in HR repair and cell cycle control (6). Given the biologic role of the *BRCA2* genes, mutation carriers might have increased sensitivity to IR due to inefficient DNA repair and defective G2/M checkpoint activation in response to DNA damage. However, up to now, there is conflicting evidence as to whether cells with *BRCA2* mutations show increased radiosensitivity and clinical data do not indicate a clear correlation between *BRCA2* gene status and enhanced radiotherapy effect (7-11).

In this study, we investigated whether organoids can be used as a reliable novel 3D model for the testing of IR effects. We evaluated the radiosensitivity of PCa organoids with different *BRCA2* status, comparing them to tissue slice cultures derived from the same patient derived xenograft (PDX) tumor.

2. Material and methods:

2.1 Reagents

Reagents were purchased from Sigma-Aldrich, unless otherwise specified.

2.2 Irradiation

Organoids and tissue slices were irradiated using an Xstrahl Cabinet Irradiator RS320 (195 kV, 10 mA, Thoraeus filter, 1 Gy in 36 s, Xstrahl Ltd.).

2.3 Collection of PDX tumor

All animal experiments were approved by the Animal Welfare Committee of the Erasmus MC, and all experiments were conducted in accordance with accepted guidelines. PDXs of PCa (PC310, PC82, PC295) were established by van Weerden et al. (12) and were routinely passaged by subcutaneous grafting of small fragments onto both shoulders of intact male athymic NMRI nu/nu mice (Taconic Biosciences, Cologne, Germany). Characteristics of the different PDXs are summarized in Table 1. Fresh PDX tumors with volume of 500–1000mm³ were obtained. After removal from mice, the tumors were kept on ice in Dulbecco's Modified Eagle Medium (DMEM; Lonza, Verviers Sprl, Belgium).

2.4 Tissue slice culture

Tissue slices were cultured as previously reported (13). Briefly, 300 µm slices were cultured on 40 µm cell strainers (Corning) in 3 mL advanced DMEM/F12 (ThermoFisher Scientific) medium in 6 well plates at 5% CO₂ and 37°C on a Rocking Table (Luckham 200 Ltd, West Sussex, UK). One third of medium was refreshed daily. Slices were irradiated with a dose of 2 Gy and cultured for various time points. Subsequently, slices were harvested and fixed in 10% neutral buffered formalin for 24 h at room temperature (RT), embedded in paraffin and 4 µm sections were made for further analysis.

Table 1. Overview of characteristics of PDXs

PDX	Origin ¹	AR ²	PSA ³	BRCA2	Histology
PC310	PC	+	+	HD ⁴	adenocarcinoma
PC82	PC	+	+	WT ⁵	adenocarcinoma
PC295	LN	+	+	WT ⁵	adenocarcinoma

¹PC, primary prostate tumor; ²AR, androgen receptor; ³PSA, prostate-specific antigen; ⁴HD, homozygous deletion; ⁵WT, wild type; ⁶LN, lymph node metastasis.

2.5 Organoids culture

PDX tumor tissue was dissociated mechanically using a scalpel or scissors and subsequently digested enzymatically in advanced DMEM/F12 medium supplemented with collagenase A (2 mg/mL, Roche Diagnostics) and Y-27632 (10 µM, AbMole BioScience) for 1 h at 37°C. Next, an additional digestion step was performed using TrypLE™ Express Enzyme (ThermoFisher Scientific) and Y-27632 (10µM) for 10 min at 37°C. Dissociated material was passed through a 100 µm cell strainer (ThermoFisher Scientific) and the flow through was washed twice using advanced DMEM/F12 medium. Remaining single cells and small cell clumps were plated in NovioGel (NovioCell, Oss, The Netherlands) as 30 µL droplets in a 24-well plate. Organoids were cultured in 500 µL of prostate growth medium (PGM) (14) and medium adapted from Drost et al. (15) for PC310 and PC82 organoids respectively. Medium was changed every 3 or 4 days. Organoids were passaged every 1 or 3 weeks, depending on density. First and second organoid passages were used for further experiments. Organoids were irradiated with a dose of 2 Gy and cultured for various time points. Subsequently, organoids were fixed in 4% paraformaldehyde for 2 h at 37°C, harvested and embedded in low melting agarose. Next, processed organoids were embedded in paraffin and 4 µm sections were made for further analysis.

2.6 Medium prostate-specific antigen (PSA) detection

Organoid culture medium (500 μ L) was first collected after 3 days of culturing and then collected every 3 days and stored in -20°C for later PSA measurement. The PSA concentration was measured using a PSA enzyme-linked immunosorbent assay (ELISA) kit (Abnova, Taipei City, Taiwan) according to the manufacturer instructions.

2.7 Hematoxylin & eosin (H&E) staining

Histological tumor architecture was examined by H&E staining as previously described (13). Briefly, sections were deparaffinized in xylene followed by rehydration in graded alcohols and staining with hematoxylin and eosin.

2.8 Immunofluorescent staining of tissue sections

53BP1 staining was performed as previously described (16). Briefly, sections were deparaffinized in xylene followed by rehydration in graded alcohols. Antigen retrieval was performed with target retrieval buffer (pH 6, Dako). Following permeabilization and blocking, sections were incubated with anti-53BP1(1:1000, NB100-904, Novus Biologicals) for 1h at RT, followed by anti-mouse Alexa Fluor 488 secondary antibodies.

2.9 TUNEL and EdU assays

EdU at a concentration of 3 $\mu\text{g}/\text{mL}$ was added to the tissue slice or organoid culture medium 2 h before fixation. Simultaneous TUNEL and EdU staining was performed as described previously (17). Briefly, tissue sections were deparaffinized in xylene followed by rehydration in graded alcohols and then blocked with PBS 3% BSA. TUNEL reaction was performed using In Situ Cell Death Detection Kit (Roche Life Sciences), after which the sections were incubated with Click-iT Alexa Fluor 594 cocktail buffer for 30 min.

2.10 Immunohistochemical staining

Sections were deparaffinized in xylene followed by rehydration in graded alcohols. Antigen retrieval was performed with target retrieval buffer (pH 6, Dako). Sections were treated with 3% hydrogen peroxide solution in methanol at RT for 20 min, followed by incubation in 5% BSA in PBS for 30 min at RT. Sections were incubated with anti-AR antibody (1:200, M4074, SPRING Bioscience) overnight, and horseradish peroxidase (HRP)-conjugated anti-rabbit IgG secondary antibody (1:100, Dako) for 1 h at RT. AR positive cells were visualized using diaminobenzidine (DAB) staining kit (Agilent, Santa Clara, CA) and hematoxylin counter staining.

2.11 Image acquisition and quantification

For tissue slice EdU and TUNEL staining quantifications, 10 random images (400x magnification) from each tumor slice section were generated using a Leica fluorescence microscope (DM4000b, Germany). For organoid EdU and TUNEL quantifications, 10 organoid images from at least 3 sections were captured using the above mentioned microscope. TUNEL and EdU positive ratio in tissue slices was quantified automatically as previously reported (13) while this was counted manually for organoids. For the fluorescent foci analysis, Z-stack images were made (Z-distance $1\mu\text{m}$, 1024×1024 pixels, 630x magnification) using a Zeiss LSM700 confocal microscope (Carl Zeiss Microimaging Inc). Three random images per tumor slice section were taken in the DAPI channel and in total 10 organoids images from several organoid sections were captured. Fluorescent foci were quantified by a self-designed automated script in Image J (unpublished data). Briefly, after making a Max Projection of the Z-stack, the nuclei were segmented by thresholding the DAPI channel (Median $r = 1$, Auto Threshold Huang dark, Smooth, Convert to Mask, Threshold). Overlapping

nuclei were separated using an adjusted watershed and regions of interest outside the range of 20-150 pixels were excluded. With a For-loop over all nuclei, the number of foci inside each nucleus was counted with the Find Maxima function (noise tolerance of 60 for 53BP1foci). The results were stored in a single spreadsheet file per image. The different spreadsheets were combined to a single file in R.

2.12 Statistical analysis

Experiments were performed 3 times for both organoids and tissue slices. Results are expressed as the mean \pm SD or SEM. Unpaired student's t-test was used to analyze the differences between two groups. Statistical analysis and generation of graphs was performed using Graphpad Prism 6.0 (La Jolla, CA). $P < 0.05$ was considered statistically significant. * $P < 0.05$, ** $P < 0.01$, *** $P < 0.001$.

3. Results

3.1 Development of patient-derived PCa xenograft organoids

Fresh tumor tissue from PC82 (*BRCA2* wild type), PC310 (*BRCA2* deficient) and PC295 (*BRCA2* wild type) were either sliced using a vibratome and cultured as previously reported (13) or were dissociated, seeded into Noviolgel and cultured in stemness stimulated media as tumor organoids (Figure 1A). PC82 and PC310 succeeded in multiple organoid passages, while PC295 did not. Each organoid showed a solid structure with an adenocarcinoma histology type resembling the epithelial structures of original tissues (Figure 1B). Since both PDXs show AR expression, we confirmed AR expression of these organoids (Figure 1B). To test if AR signaling is functionally active, we measured the PSA concentration in the organoid culture medium and both organoids are secreting PSA (Figure 1C). These results show that PDX-derived organoids recapitulate aspects of the histology and functional ARsignaling of the original PDX tumor.

Figure 1

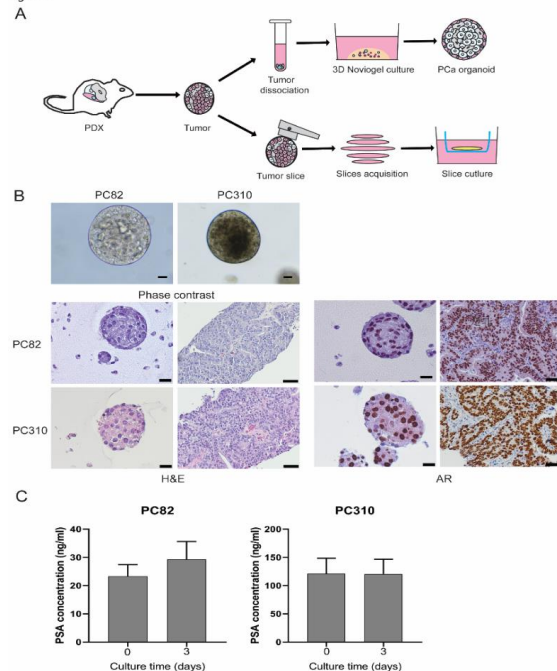


Figure 1. Establishment of PDX-derived PCa organoids.

(A). Schematic experimental design of two 3D culture system using PDX-derived PCa tumor. (B). Representative images of organoids under phase contrast microscope (scale bar 20 μ m) after 7 days of culturing. Representative H&E images of organoids (scale bar 20 μ m) and tissue slices (scale bar 50 μ m). Representative images of AR expression of organoids (scale bar 20 μ m) and tissue slices (scale bar 50 μ m). (C). PSA concentrations in medium of organoids from day 0 and day 3. Colum represent mean values and bars indicates SEM (three organoids from 2 independent experiments).

3.2 Similar response to irradiation in tissue slices and organoids

In order to study if organoids reflect *ex vivo* response of tissue slice to IR, we used two PDX models with different *BRCA2* status. Tissue slices and organoids cultured from PC82 (*BRCA2* wild type) and PC310 (*BRCA2* deficient) models were treated with 2 Gy of X-ray. As shown in Figure 2A, we observed a significant drop in the fraction of EdU-positive cells in slices from PC82 treated with IR after 1 and 3 days of culturing. At both days, very few proliferating cells could be detected. In parallel, we observed an identical response to IR in PC82 organoids: almost no EdU-positive nuclei could be detected at day 1 and day 3 days post-IR (Figure 2B). Simultaneously, a significant 6-fold increase of TUNEL positive cells was observed after 3 days in PC82 slices treated with 2 Gy X-ray. This effect was also detected in PC82 organoids already at day 1, with a similar fold increase in TUNEL signal (Figure 2A&B).

Figure 2.

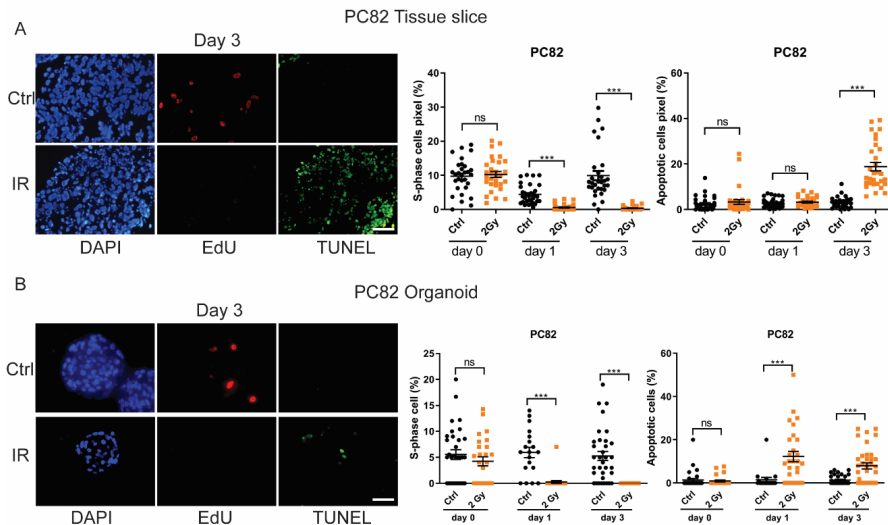


Figure 2. Response to IR treatment of PC82 *in vitro* 3D model

(A). Representative EdU/TUNEL/DAPI images of PC82 tumor slice sections after 3 days of culturing under the different conditions (scale bar 20 μ m). Quantification of the fraction of EdU-positive cells and TUNEL-positive cells in the tissue slices. For all graphs, 10 image fields were analyzed per tumor slice. Each point represents one image field, average and SEM values are indicated. (B). Representative EdU/TUNEL/DAPI images of PC82 organoids sections after 3 days of culturing under the different conditions (scale bar 20 μ m). Quantification of the fraction of EdU-positive cells and TUNEL-positive cells in the organoids sections. For all graphs, 10 organoids from several sections were analyzed. Each point represents one organoid, average and SEM values are indicated.

Same experiments were performed for the PC310 tissue slices and organoids. As expected from its genetic background, a significant drop in the fraction of S-phase cells was observed for both tissue slices and organoids (decreased by a factor of 1.35 and 1.61, respectively) when treated with IR for 1 day (Figure 3A&B), with a more pronounced reduction at 3 days post-IR (both decreased by a factor 2). Likewise, the proliferation inhibition effect of IR was less in PC310 compared with PC82. A significant increase of 2.6 folds of TUNEL positive cells was observed in PC310 slices

treated with IR, and 5.4 folds in PC310 tumor organoids at day 3 post-IR (Figure 3A&B). In addition, we tested the IR effect on PC295 (*BRCA2* wild type) tumor slices. As shown in Figure 4A&B, at both day 1 and day 3, there was neither a reduction of proliferation cells nor an increase of apoptosis upon IR exposure compared to untreated controls. These data showed that the response to IR treatment for *BRCA2* wild type tumors can be divergent. In contrast to what was expected based on the *BRCA2* status of the xenografts, PC310 has medium radiosensitivity among these three PDXs. Importantly, these effects were observed in PDX-derived organoids and recapitulated the response of tissue slices derived from the same tumor.

Figure 3.

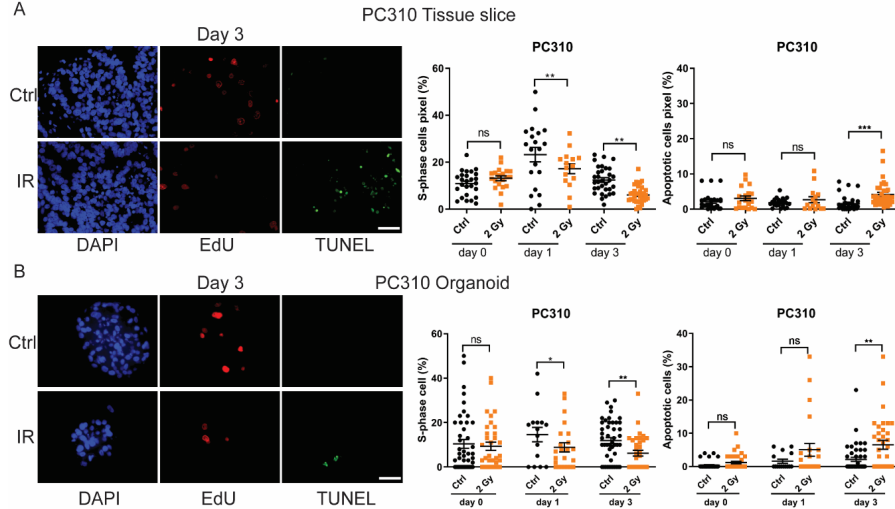


Figure 3. Response to IR treatment of PC310 *in vitro* 3D model

(A). Representative EdU/TUNEL/DAPI images of PC310 tumor slice sections after 3 days of culturing under the different conditions (scale bar 20 μ m). Quantification of the fraction of EdU-positive cells and TUNEL-positive cells in the tissue slices. For all graphs, 10 image fields were analyzed per tumor slice. Each point represents one image field, average and SEM values are indicated. (B). Representative EdU/TUNEL/DAPI images of PC310 organoids sections after 3 days of culturing under the different conditions (scale bar 20 μ m). Quantification of the fraction of EdU-positive cells and TUNEL-positive cells in the organoid sections. For all graphs, 10 organoids from several sections were analyzed. Each point represents one organoid, average and SEM values are indicated.

Figure 4.

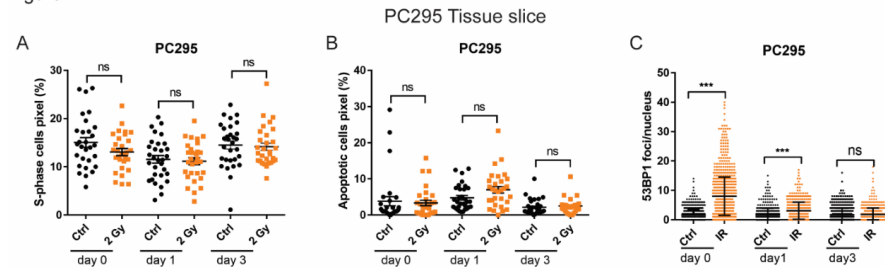


Figure 4. Response to IR treatment of PC295 tissue slices model

(A). Quantification of the fraction of EdU-positive cells in the tissue slice. (B). Quantification of the fraction of TUNEL-positive cells in the tissue slices. For all graphs, 10 image fields were analyzed per tumor slice. Each point represents one image field, average and SEM values are indicated. (C). Quantification of the 53BP1 foci per nucleus in the tissue slices sections. Three random fields of tissue slice section were analyzed. Each point represents one cell, average and SD values are indicated.

3.3 Differential DNA damage repair kinetics after IR-exposure

Previous studies have shown that downregulation of *BRCA2* leads to inhibition of DSBs repair (18, 19). We therefore investigated whether *BRCA2* homozygous deletion could delay IR-induced DNA damage repair by measuring the capacity of tissue slices and organoids to repair DSBs, using 53BP1 foci formation as DSBs marker. 53BP1 colocalization with IR-induced DSBs remains in cells at relatively long times post-IR and thus can be used as a readout for monitoring repair kinetic (20). In the *BRCA2* proficient PC82 derived organoids and tissue slices, IR exposure resulted in rapid induction of DSBs, measured by 53BP1 foci (Figure 5A&B). At 24 h post-IR, slices and organoids exposed to IR showed significant higher numbers of foci than their respective untreated control. The foci number gradually returned to basic level at 72 h post-IR, suggesting that DSB repair has been completed, although we cannot exclude that cells with high damage load may have entered into apoptosis at this time point (Figure 5A&B). Similar repair kinetics were observed in PC295 tissue slices (Figure 4C). In the *BRCA2* deficient PC310 model, we observed similar repair kinetics at 24 h post-IR, with a significantly higher amount of foci detected compared to the untreated counterpart both in tissue slices and organoids (Figure 6A&B). However, unlike PC82, we found that the foci had not disappeared at 72 h post-IR in organoids and tissue slices, indicating remaining unrepaired DNA damage (Figure 6A&B). Taken together, we detected different DNA damage repair kinetics between PC82 and PC295 compared to PC310, which could be attributed to their *BRCA2* status, however, a high level of apoptosis induced by IR in PC82 may have biased the results. Importantly, similar repair kinetics between tissue slices and organoids from the same tumor type were observed, supporting the equal value of these *in vitro* systems for IR response assessment.

Figure 5.

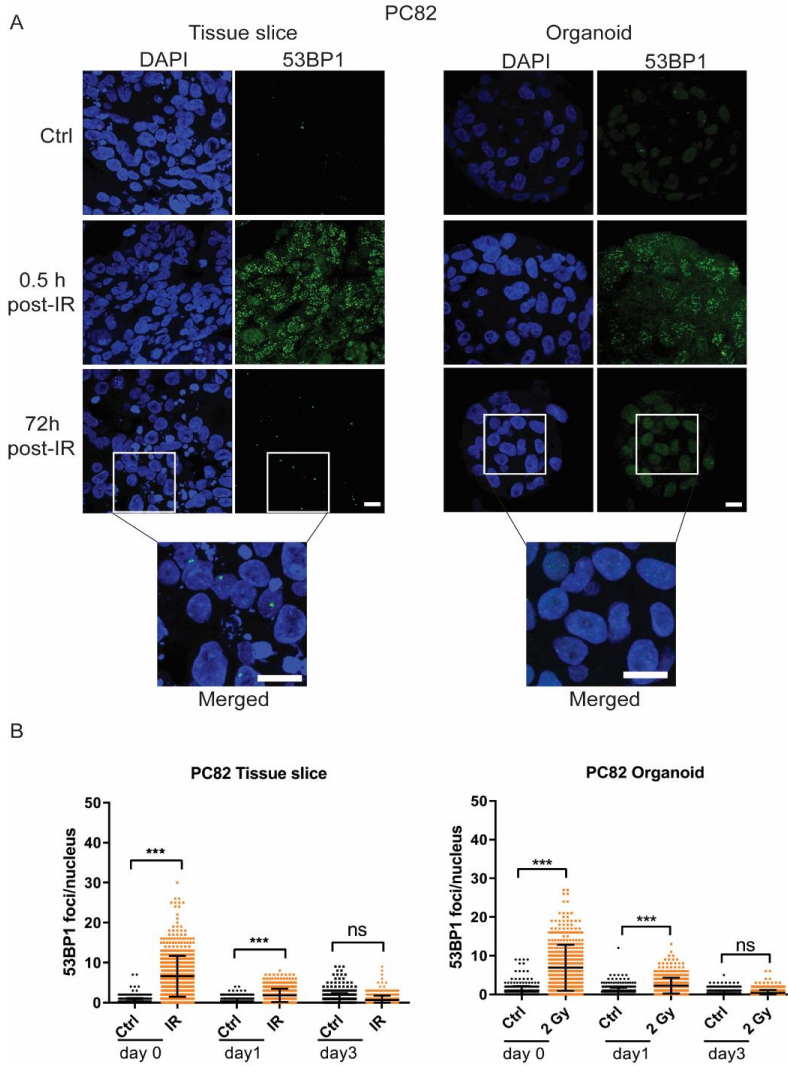


Figure 5. DNA damage repair kinetics of PC82 *in vitro* 3D model after IR treatment

(A). Representative 53BP1/DAPI images of PC82 organoids and tissue slice sections after 0.5 h and 72 h of culturing under the different conditions (scale bar 10 μm). (B). Quantification of the 53BP1 foci per nucleus in the organoids and tissue slices sections. Three random fields of tissue slice section and 10 organoids from several sections were analyzed. Each point represents one cell, average and SD values are indicated.

Figure 6.

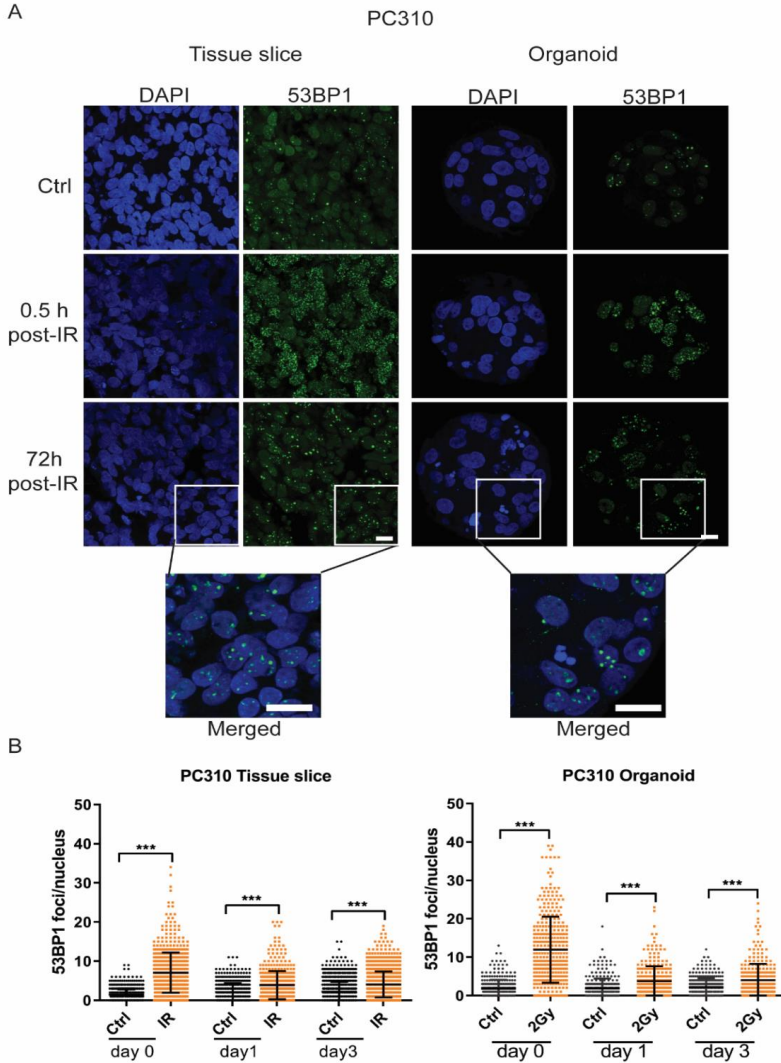


Figure 6. DNA damage repair kinetics of PC310 *in vitro* 3D model after IR treatment

(A). Representative 53BP1/DAPI images of PC310 organoids and tissue slice sections after 0.5 h and 72 h of culturing under the different conditions (scale bar 10 μ m). (B). Quantification of the 53BP1 foci per nucleus in the organoids and tissue slices sections. Three random fields of tissue slice section and 10 organoids from several sections were analyzed. Each point represents one cell, average and SD values are indicated.

4. Discussion

Although substantial progression has been made in the treatment of PCa, curative therapeutic options for advanced disease are limited. Meanwhile, clinicians still face the difficulty that biomarkers for selection of patients that will benefit from EBRT or EBRT based combination therapy are still lacking. The recent advances in *in vitro* 3D

culture technologies, such as precision-cut tumor slice cultures or organoid cultures, have opened new avenues for the development of more reliable cancer models. The discovery of growing healthy human adult stem cells into organoids brings up the opportunity to grow organoids from tumor tissues (5). However, whether these tumor organoids recapitulate structural and functional aspects of their *in vivo* counterpart tumors is still unclear. Few initial studies have demonstrated the feasibility of drug screening on patient-derived tumor organoids (21, 22). One study using patient-derived PCa organoids demonstrated that organoids with chromodomain helicase DNA binding protein 1 (*CHDI*) deletion sensitized to DNA damaging agents, and that these patients were subsequently successfully treated with carboplatin (23).

In the current study, we set up PDX-derived PCa organoid cultures and compared them to tissue slice cultures, a system previously established in our laboratory. We used PDXs as our starting material as PDX tumors have limited intra-tumoral heterogeneity and high tumor content, which allows for intensive technical studies and guarantees reproducibility. We investigated the irradiation effects on PCa organoids. After comparison of organoids to tissue slices head-to-head, we found similar responses to IR in regard to cell proliferation, apoptosis and DNA damage repair kinetics between these models, thus may indicate the reliability of PCa organoids and its recapitulation of the tumor itself. Compared to the tissue slice model, the organoid model is not restricted to short-term culture and limited proliferation capacity and therefore allows for larger-scale screening once organoid lines have been established. Nevertheless, organoids also have their limitations, as they still lack stroma and immune cells, while this may partly be preserved in tissue slices. Compared to organoids, assays based on tissue slices can be done within a few days to weeks after obtaining material, which is compatible with regular clinical decision making and could be incorporated into the diagnostic routine before start of treatment. Thus, models should be chosen based on the specific situation and research question.

BRCA2 is a tumor-suppressor gene which was identified in families at high risk for breast and ovarian cancers. *BRCA2* gene functions are known to play a role in DNA HR repair and cell cycle control. When the HR pathway is defective, DNA repair is re-routed through error-prone NHEJ pathways and is less efficient. The issue of a possible higher radiosensitivity in *BRCA2*-associated tumors was addressed for the first time by Sharan *et al.*(24), they reported that inactivation of the *BRCA2* gene in mouse embryonic cells could cause irreparable radiation-induced DNA damage. In the recent past, few translational research studies showed higher radiosensitivity levels in *BRCA2* mutation carriers (7-9). However, other investigators were unable to elicit a relationship between *BRCA2* mutations and radiosensitivity and not all these inconsistencies could be explained by differences in detection methods (10, 11). So far, no evidence has been acquired to show *BRCA2* mutated PCa patients are more sensitive to radiotherapy, only one retrospective study showed that metastatic PCa patients with DNA repair mutations (including *BRCA2*) have a greater benefit from radium-223 radionuclide therapy compared to patients without these mutations (25). Our results were unable to demonstrate a link between radiosensitivity and *BRCA2* status. Two *BRCA2* wild type tumors, PC295 and PC82, showed completely different responses to IR, with the *BRCA2* deficient tumor had medium radiosensitivity among three tumors tested. When we looked into DNA repair kinetics, it seems that the data support *BRCA2* wild type status of these tumors, however, due to the high level of IR-induced apoptosis in PC82, the repair kinetics could be biased as repair foci could not be detected when cells enter into apoptosis. In PC310 tumors, we detected residual DNA damage foci even at 72 h

post-IR both in tissue slices and organoids. Previous studies using tumor cells and human fibroblasts cell harboring heterozygous (26) or homozygous (27) *BRCA2* mutation showed a reduced DSB repair capacity with residual DNA damage foci in G2 phase at late time point (8 h post-IR). These data may partially explain the residual foci in PC310, however, whether this long-lasting IR-induced DNA damage effect in tissue slices and organoids is caused by the difference between 3D and 2D models warrants further investigation.

In summary, we generated PDX-derived PCa organoids which maintained the morphology and AR signaling of the original PDX tumor. Direct comparison of organoids to tissue slices demonstrated the similarity and reliability of this novel *in vitro* 3D model for evaluating IR response. Based on PDXs tested, we were unable to elicit a relationship between *BRCA2* mutations and increased radiosensitivity. This result warrant further validation with more tumor models and *in vitro* response should be compared to *in vivo* effect in order to get a more complete view of similarities and differences between both culture models.

Acknowledgments

We thank Christine van Tuy and Danny Feijtel for sharing the 53BP1 foci quantification macro.

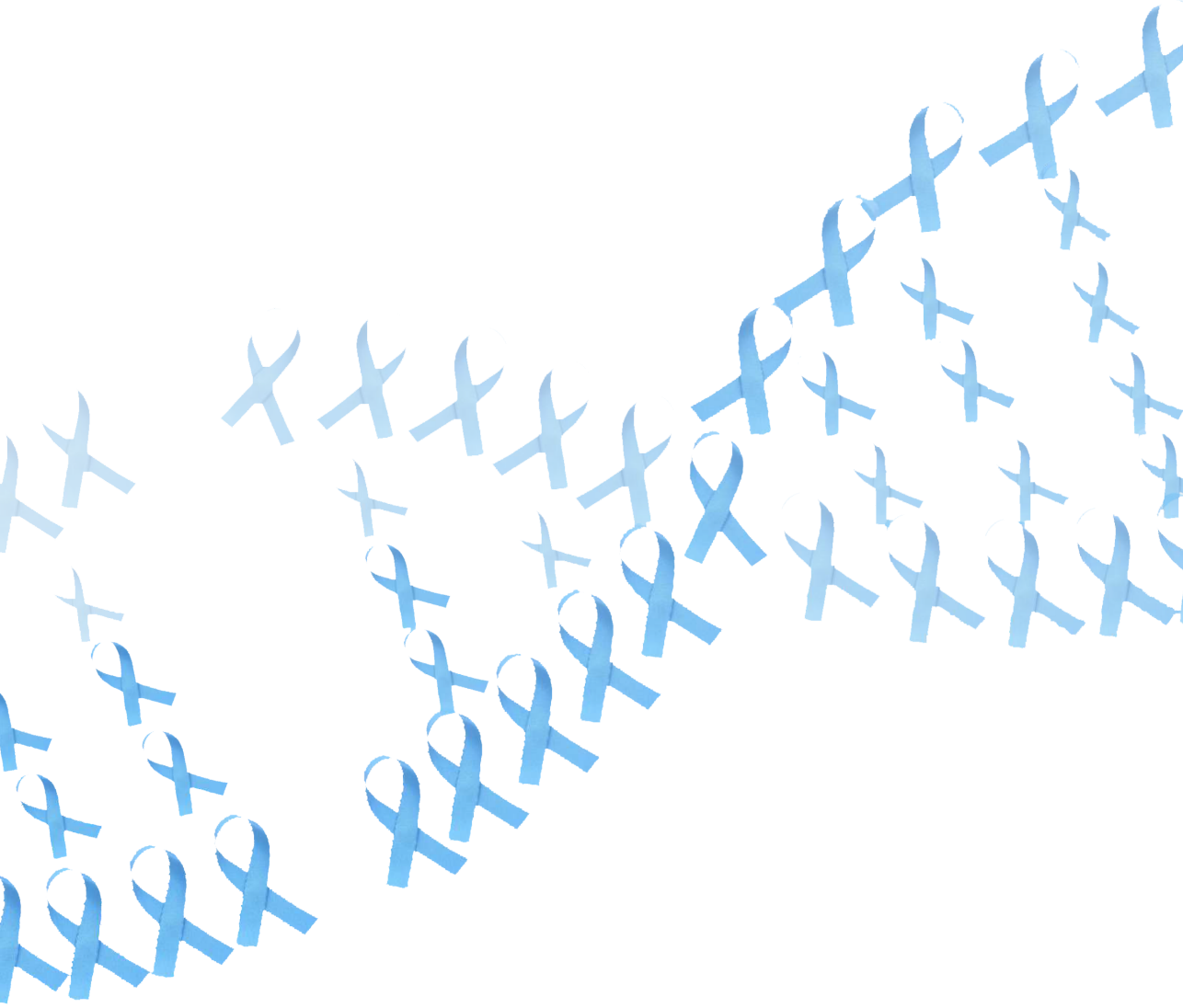
Funding source

This work was supported by the Chinese Scholarship Council (WZ, grant number 201506270172) and EU Horizon 2020 research and innovation program under the Marie Skłodowska-Curie grant agreement (AvH, grant number 721746 (TransPot)).

Reference

1. Siegel RL, Miller KD, Jemal A. Cancer statistics, 2018. *CA Cancer J Clin.* 2018;68(1):7-30.
2. Djavan B, Moul JW, Zlotta A, Remzi M, Ravery V. PSA progression following radical prostatectomy and radiation therapy: new standards in the new Millennium. *Eur Urol.* 2003;43(1):12-27.
3. Khan MA, Han M, Partin AW, Epstein JI, Walsh PC. Long-term cancer control of radical prostatectomy in men younger than 50 years of age: update 2003. *Urology.* 2003;62(1):86-91; discussion -2.
4. Wilding JL, Bodmer WF. Cancer cell lines for drug discovery and development. *Cancer research.* 2014;74(9):2377-84.
5. Tuveson D, Clevers H. Cancer modeling meets human organoid technology. *Science.* 2019;364(6444):952-5.
6. Ceccaldi R, Rondinelli B, D'Andrea AD. Repair Pathway Choices and Consequences at the Double-Strand Break. *Trends Cell Biol.* 2016;26(1):52-64.
7. Ernestos B, Nikolaos P, Koulis G, Eleni R, Konstantinos B, Alexandra G, et al. Increased Chromosomal Radiosensitivity in Women Carrying BRCA1/BRCA2 Mutations Assessed With the G2 Assay. *International Journal of Radiation Oncology*Biophysics.* 2010;76(4):1199-205.
8. Barwell J, Pangon L, Georgiou A, Kesterton I, Langman C, Arden-Jones A, et al. Lymphocyte radiosensitivity in BRCA1 and BRCA2 mutation carriers and implications for breast cancer susceptibility. *International Journal of Cancer.* 2007;121(7):1631-6.
9. Buchholz TA, Wu X, Hussain A, Tucker SL, Mills GB, Haffty B, et al. Evidence of haplotype insufficiency in human cells containing a germline mutation in BRCA1 or BRCA2. *International Journal of Cancer.* 2002;97(5):557-61.
10. Baeyens A, Thierens H, Claes K, Poppe B, De Ridder L, Vral A. Chromosomal radiosensitivity in BRCA1 and BRCA2 mutation carriers. *International Journal of Radiation Biology.* 2004;80(10):745-56.
11. Nieuwenhuis B, Assen-Bolt AJV, A. W. H. Van Waarde-Verhagen M, Sijmons RH, Hout AHVd, Bauch T, et al. BRCA1 and BRCA2 heterozygosity and repair of X-ray-induced DNA damage. *International Journal of Radiation Biology.* 2002;78(4):285-95.
12. Navone NM, van Weerden WM, Vessella RL, Williams ED, Wang Y, Isaacs JT, et al. Movember GAP1 PDX project: An international collection of serially transplantable prostate cancer patient-derived xenograft (PDX) models. *Prostate.* 2018;78(16):1262-82.
13. Zhang W, van Weerden WM, de Ridder CMA, Erkens-Schulze S, Schonfeld E, Meijer TG, et al. Ex vivo treatment of prostate tumor tissue recapitulates in vivo therapy response. *Prostate.* 2019;79(4):390-402.
14. Marques RB, Erkens-Schulze S, de Ridder CM, Hermans KG, Waltering K, Visakorpi T, et al. Androgen receptor modifications in prostate cancer cells upon long-term androgen ablation and antiandrogen treatment. *International Journal of Cancer.* 2005;117(2):221-9.
15. Drost J, Karthaus WR, Gao D, Driehuis E, Sawyers CL, Chen Y, et al. Organoid culture systems for prostate epithelial and cancer tissue. *Nat Protoc.* 2016;11(2):347-58.
16. Nonnekens J, Chatalic KL, Molkenboer-Kuennen JD, Beerens CE, Bruchertseifer F, Morgenstern A, et al. (213)Bi-Labeled Prostate-Specific Membrane Antigen-Targeting Agents Induce DNA Double-Strand Breaks in Prostate Cancer Xenografts. *Cancer Biother Radiopharm.* 2017;32(2):67-73.
17. Naipal KAT, Verkaik NS, Sánchez H, van Deurzen CHM, den Bakker MA, Hoeijmakers JHJ, et al. Tumor slice culture system to assess drug response of primary breast cancer. *BMC Cancer.* 2016;16(1):78.
18. Yu D, Sekine E, Fujimori A, Ochiya T, Okayasu R. Down regulation of BRCA2 causes radiosensitization of human tumor cells in vitro and in vivo. *Cancer Sci.* 2008;99(4):810-5.

19. Yu VP, Koehler M, Steinlein C, Schmid M, Hanakahi LA, van Gool AJ, et al. Gross chromosomal rearrangements and genetic exchange between nonhomologous chromosomes following BRCA2 inactivation. *Genes Dev.* 2000;14(11):1400-6.
20. Marková E, Schultz N, Belyaev IY. Kinetics and dose-response of residual 53BP1/ γ -H2AX foci: Co-localization, relationship with DSB repair and clonogenic survival. *International Journal of Radiation Biology.* 2007;83(5):319-29.
21. Gao D, Vela I, Sboner A, Iaquinta PJ, Karthaus WR, Gopalan A, et al. Organoid cultures derived from patients with advanced prostate cancer. *Cell.* 2014;159(1):176-87.
22. van de Wetering M, Francies HE, Francis JM, Bounova G, Iorio F, Pronk A, et al. Prospective derivation of a living organoid biobank of colorectal cancer patients. *Cell.* 2015;161(4):933-45.
23. Shenoy TR, Boysen G, Wang MY, Xu QZ, Guo W, Koh FM, et al. CHD1 loss sensitizes prostate cancer to DNA damaging therapy by promoting error-prone double-strand break repair. *Annals of Oncology.* 2017;28(7):1495-507.
24. Sharan SK, Morimatsu M, Albrecht U, Lim DS, Regel E, Dinh C, et al. Embryonic lethality and radiation hypersensitivity mediated by Rad51 in mice lacking Brca2. *Nature.* 1997;386(6627):804-10.
25. Isaacsson Velho P, Qazi F, Hassan S, Carducci MA, Denmeade SR, Markowski MC, et al. Efficacy of Radium-223 in Bone-metastatic Castration-resistant Prostate Cancer with and Without Homologous Repair Gene Defects. *Eur Urol.* 2019;76(2):170-6.
26. Beucher A, Deckbar D, Schumann E, Krempler A, Frankenberg-Schwager M, Lohrich M. Elevated radiation-induced gammaH2AX foci in G2 phase heterozygous BRCA2 fibroblasts. *Radiotherapy and oncology : journal of the European Society for Therapeutic Radiology and Oncology.* 2011;101(1):46-50.
27. Beucher A, Birraux J, Tchouandong L, Barton O, Shibata A, Conrad S, et al. ATM and Artemis promote homologous recombination of radiation-induced DNA double-strand breaks in G2. *The EMBO journal.* 2009;28(21):3413-27.



Chapter 6

Apalutamide sensitizes prostate cancer to ionizing radiation via inhibition of non-homologous end-joining DNA repair

Wenhao Zhang¹, Chen-Yi Liao², Hajar Chatatou², Luca Incrocci³, Dik C. van Gent^{1,4},
Wytske van Weerden², Julie Nonnekens^{1,4,5#}

1. Department of Molecular Genetics, Erasmus MC, Rotterdam, The Netherlands 2. Department of Experimental Urology, Erasmus MC, Rotterdam, The Netherlands 3. Department of Radiation Oncology, Erasmus MC Cancer Institute, Rotterdam, The Netherlands 4. OncoCode Institute, Erasmus MC, Rotterdam, The Netherlands 5. Department of Radiology and Nuclear Medicine, Erasmus MC, Rotterdam, The Netherlands

Published in *Cancers* 2019, 11, 1593.

Abstract

Androgen-deprivation therapy was shown to improve treatment outcome of external beam radiation therapy (EBRT) for locally advanced prostate cancer (PCa). DNA damage response (DDR) was suggested to play a role in the underlying mechanism, but conflicting results were reported. This study aims to reveal the role of the androgen receptor (AR) in EBRT-induced DDR and to investigate whether next-generation AR inhibitor apalutamide can radiosensitize PCa. PCa cell lines and tissue slices were treated with anti-androgen alone or combined with EBRT. The effect of treatments on cell growth, tissue viability, DDR, and cell cycle were investigated. RAD51 and DNA-dependent protein kinase catalytic subunit (DNA-PKcs) levels were determined by Western blotting. Homologous recombination (HR) capacity was measured with the directed repeats-green fluorescent protein (DR-GFP) assay. We report the radiosensitizing effect of anti-androgens, which showed synergism in combination with EBRT in AR-expressing tumor slices and cell lines. Moreover, a compromised DDR was observed in AR-expressing cells upon AR suppression. We found that AR inhibition downregulated DNA-PKcs expression, resulting in reduced non-homologous end-joining repair. DDR through HR was a secondary effect due to cell-cycle change. These data provide a mechanistic explanation for the combination regimen and support the clinical use of apalutamide together with EBRT for localized PCa patients.

1. Introduction

Prostate Cancer (PCa) is the most common malignancy and the second cause of cancer-related death among men (1). External beam radiation therapy (EBRT) is the first line of treatment for locally advanced PCa, but unfortunately tumors frequently recur after treatment (2, 3). The combination of EBRT with androgen-deprivation therapy (ADT), the first line systemic treatment for advanced PCa, has shown to improve the overall therapeutic outcome compared to EBRT alone (4-6). Blocking activation of the androgen receptor (AR) signaling pathway by ADT is highly effective in reducing PCa tumor growth, therefore, preclinical studies and clinical trials have not been able to assess whether the addition of ADT to EBRT induces a synergistic or additive effect. Moreover, conflicting results have been reported on the underlying cellular mechanisms causing this effect. Interestingly, recent studies have indicated that AR signaling can activate DNA repair pathways, which may contribute to radioresistance (7, 8).

Ionizing radiation (IR) induces DNA double-strand breaks (DSBs), which can be repaired by two main pathways: non-homologous end-joining (NHEJ) and homologous recombination (HR). NHEJ involves recruitment of DNA dependent protein kinase catalytic subunit (DNA-PKcs) to DNA ends by the Ku70/80 heterodimer, followed by coupling of the DNA ends. HR is mediated by the RAD51 protein in combination with many other factors such as breast cancer 1 and 2 (BRCA1 or 2) (9). AR activation promotes upregulation of DNA-PKcs, Ku70/80 and RAD51, however it is unclear whether AR directly regulates expression of these genes and previous studies contain conflicting findings on DNA repair pathway regulation (7, 8, 10, 11).

Apalutamide (ERLEADA®) is a next-generation AR inhibitor which has been approved in 2018 for treatment of non-metastatic castration-resistant prostate cancer (CRPC). Apalutamide blocks AR activation by competing with androgen binding and preventing AR translocation to the nucleus. It has a 5- to 10- fold higher binding affinity than the first-generation anti-androgen bicalutamide, which has been widely used for PCa patient treatment (12). Also, apalutamide showed a greater efficacy compared to the second-generation anti-androgen enzalutamide (12), which was shown in preclinical studies to have radiosensitizing capacities (13). Ongoing clinical trials are testing the efficacy of combination treatment of apalutamide and EBRT; however, preclinical data are yet to be presented to support this combination.

Here, we compared the radiosensitizing capacity of apalutamide to ADT and enzalutamide in PCa cell and *ex vivo* patient-derived xenograft (PDX) tissue slice models. Furthermore, we identified NHEJ downregulation as the underlying mechanism of apalutamide-enhanced radiosensitivity in AR-expressing PCa models.

2. Results

2.1. AR suppression enhances IR-induced cell killing

The impact of AR suppression treatments on PCa cell response to IR exposure was studied by applying ADT, enzalutamide or apalutamide 24 hours prior to IR. The IR dose per cell lines was chosen such that cell proliferation was not fully inhibited (data not shown). AR suppression alone reduced the total cell number with 50% in LNCaP and 40% in PC346C cells 7 days post-IR, and IR treatment alone reduced the total cell number with 20% in LNCaP and 35% in PC346C cells (Fig. 1A). The combination treatment resulted in a further reduction of the total cell number of 65% and 70% for LNCaP and PC346C cells, respectively. As expected, AR suppression did not affect cell number in AR-negative DU145 and PC346C-DCC cells, and the addition of AR suppression to IR exposure did not cause additional sensitivity (Fig. 1B). In AR-overexpressing PC346C-Flu1 cells, AR suppression did not affect cell growth,

reflecting the CRPC nature of this cell line. Interestingly, combining AR suppression and IR treatments resulted in a small, but significant reduction of the total cell number with 40% at 7 days post-IR compared to IR alone (20%) (Fig. 1C). No significant difference was observed between the different AR suppression treatments. These data suggest that there is an additional effect of the combination treatment compared to IR alone, which is dependent on the AR status of the tumor cells.

2.2. Apalutamide enhances PCa tissue slice IR sensitivity

Subsequently, we investigated the effects of apalutamide on IR sensitivity in androgen-dependent, AR-positive PC295 *ex vivo* tumor slices (14). Tumor slices retained morphology 6 days post IR-exposure, while treatment with apalutamide resulted in tissue integrity loss, loss of AR-expression (Fig. 2A-B) and significantly reduced tissue slice viability with reduced fraction of S-phase cells and increased number of apoptotic cells (Fig. 2C-E). 2 Gy of IR had no effect on tissue slice viability, with neither a reduction of S-phase cells nor an increase of apoptotic cells at any time point. Combination of IR and apalutamide, significantly reduced the level of S-phase cells and increased the level of apoptotic cells already at day 1 after IR at which no effect of the single treatments can be detected, indicating a synergy between these two treatments. This effect became more prominent over time (Fig. 2C-E). The combination treatment did not further reduce AR expression level compared to apalutamide treatment alone (Fig. 2A-B). Together, these data show the synergistic effect of IR and apalutamide treatment in this PCa tumor model.

2.3. AR suppression inhibits DNA damage repair

Next, we investigated whether AR suppression treatment enhanced IR sensitivity could result from a DSB repair defect by measuring DSB repair kinetics of PCa cells. AR suppression treatment alone did not increase DSB foci numbers compared to untreated controls (Fig. S1). IR exposure resulted in rapid induction of DSBs, measured by γ H2AX and 53BP1 foci staining, in all 3 cell lines tested (Fig. 3A-B). At 1 and 24 hours after IR, cells in the combination therapy groups showed significantly more DSB foci than cells treated with IR alone, indicative of a slower repair of DSBs or higher level of DNA damage (Figure 3A-B). An alternative explanation for the increase of foci numbers could be the increased DNA content per nucleus in the S/G2 phase of the cell cycle. Therefore, we analyzed the cell cycle distribution 24 hours post-IR. The fraction of S/G2 cells was not increased by AR suppression treatment in PC346C and PC346C-Flu1 cells (Fig. S2), while LNCaP cells displayed an even higher fraction of G1 phase cells, a cell phase with less DNA content, excluding a cell cycle effect.

In addition to indirect measurement of the level of DSBs using γ H2AX and 53BP1 foci quantifications, we also measured the number of DNA breaks by PFGE. AR suppression as single treatment did not cause increased levels of broken DNA, while IR exposure did. No difference was observed between control and AR suppression treatment directly after IR exposure, indicating that the same level of DNA breaks was induced (Fig. 3C-D). When allowing cells to repair the DNA damage for 1 hour, a significantly higher level of DNA breaks was observed in AR suppression treated cells compared with control group (Fig. 3C-D). This effect is robust in both androgen-dependent and CRPC AR-expressing cells, but was absent in AR-negative DU145 cells (Fig. 3C-D). Combined, these data indicate that AR suppression inhibits repair of IR-induced DSBs and that this effect is dependent on AR-expression.

Figure 1

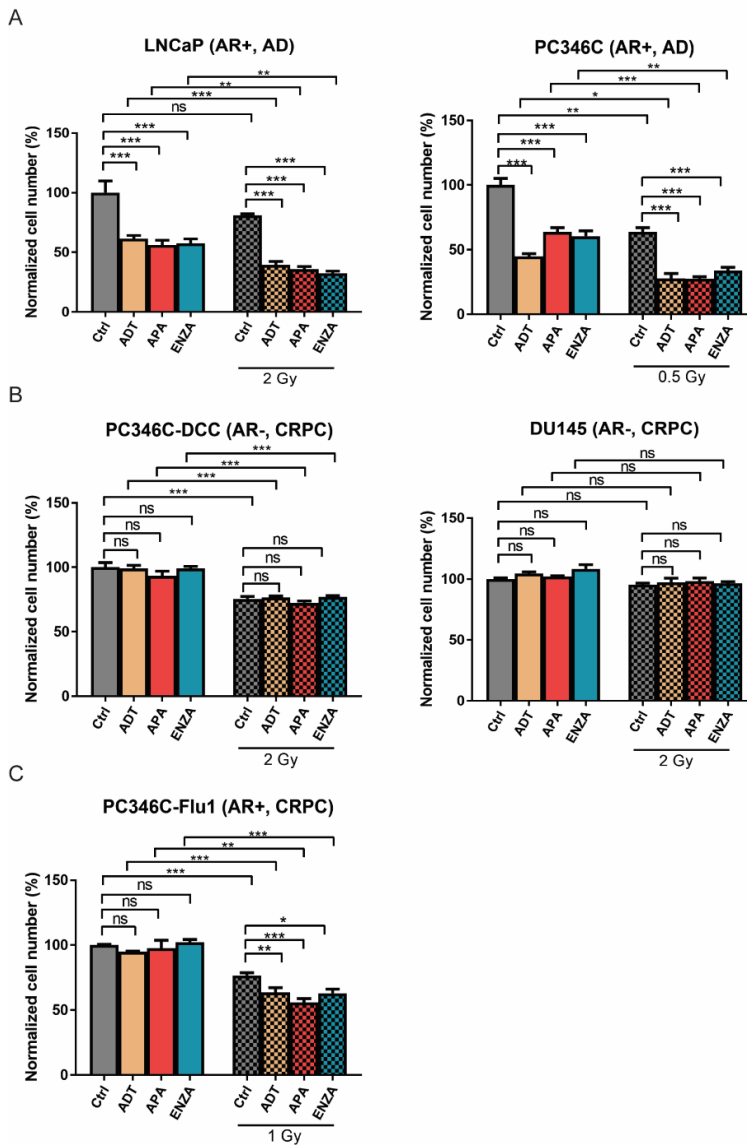


Figure 1. AR suppression treatment inhibits cell growth cooperatively with IR treatment in AR-positive PCa cells.

Cells were pretreated with AR suppression or DMSO control for 24 h followed by IR treatment. The cell number was measured at day 7 post-treatment with a sulforhodamine beta (SRB) assay and set relative to initial cell number followed by normalized to untreated control. (a) Androgen receptor (AR)-positive and androgen-dependent (AD) LNCaP and PC346C. (b) AR-negative, castration-resistant prostate cancer (CRPC) PC346C-DCC and DU145 cells. (c) AR-positive and CRPC PC346C-Flu1 cells. Average and SEM are indicated, * $P < 0.05$, ** $P < 0.01$, *** $P < 0.001$. ns, non-significant, ADT, androgen-deprivation treatment; APA, apalutamide; ENZA, enzalutamide.

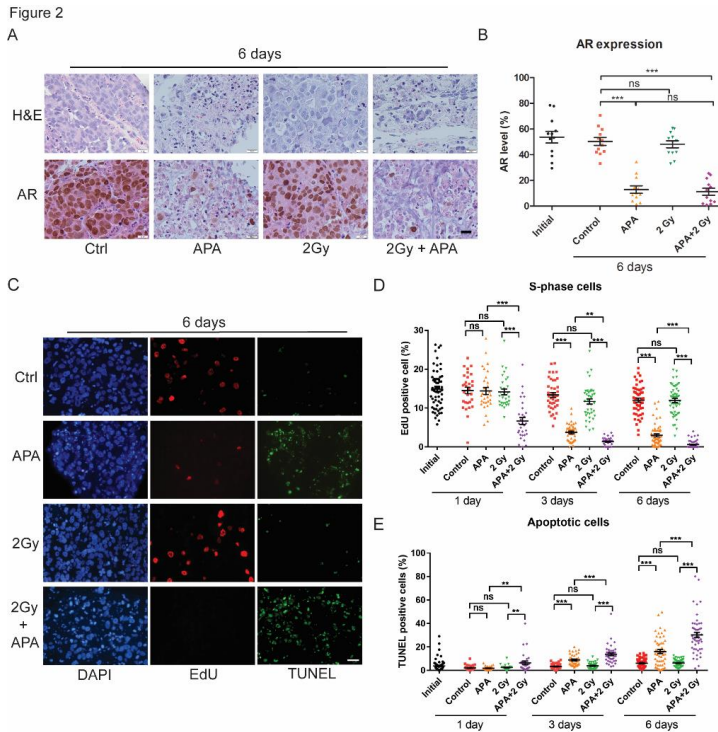


Figure 2. Apalutamide radiosensitizes PCa tissue slices *ex vivo*.

Androgen receptor (AR)-positive, androgen-dependent PC295 PDX slices were pretreated with apalutamide (APA) for 2 h followed by 2 Gy IR treatment. (a) Representative H&E and AR immunostaining images of tumor slice sections after 6 days of culturing under different conditions. Scale bar 20 μ m. (b) Quantification of AR expression. Four image fields were analyzed per tumor slice, each data point represents one image field, average and SEM are indicated. (c) Representative DAPI/EdU/TUNEL images of tumor slice sections after 6 days of culturing under different conditions, scale bar 20 μ m. (d) Quantification of the fraction of EdU-positive cells in the tissue slices. (e) Quantification of the fraction of TUNEL positive cells in the tissue slices. For EdU and TUNEL graphs, 10 image fields were analyzed per tumor slice. Each data point represents one image field, average and SEM are indicated. ** $P < 0.01$, *** $P < 0.001$, ns, non-significant.

2.4. Reduced HR efficiency provoked by AR suppression results from cell cycle alterations

Subsequently, we investigated whether AR suppression directly affected HR. Since previous studies have reported reduced RAD51 expression after enzalutamide treatment (10), we measured change in the RAD51 protein level after the different AR suppression treatments. In LNCaP cells, a reduction of RAD51 expression was detected upon AR suppression (statistically significant after ADT and enzalutamide treatment) (Fig. 4A-B). However, PC346C and PC346C-Flu1 cells did not show similar decrease in RAD51 levels after AR suppression treatment (Fig. 4A-B). Cell cycle analysis revealed a significant reduction of the fraction of S-phase cells in LNCaP cells, while no change was observed in PC346C and PC346C-Flu1 cells (Fig. 4C). Since RAD51 is

only expressed in S/G2 phase cells, this suggests that reduced RAD51 levels may be secondary to cell cycle distribution changes. To further substantiate this finding, the effect of apalutamide treatment on HR was directly assessed using the DR-GFP assay. Apalutamide treatment caused 50% reduction of HR in LNCaP cells (Fig. 4D), while PC346C-Flu1 cells were not affected. As a control, knockdown of the BRCA1 protein successfully reduced HR capacity more than 50% in both cell lines (Fig. 4D). Since HR functionality was reduced upon apalutamide treatment only in LNCaP cells, these data suggest again that this may be caused by a reduced fraction of S/G2 cells (Fig. 4C). To confirm that HR capacity was not affected in S/G2 cells, we measured HR functionality by RAD51 foci formation in EdU-positive cells. RAD51 foci formation in S-phase cells was not changed by AR suppression in both LNCaP and PC346C-Flu1 cells (Fig. 4E-F). Taken together, these data indicate that HR efficiency is not directly inhibited by AR suppression, but only a secondary effect of cell cycle alteration.

2.5. NHEJ inhibition by AR suppression contributed to radiosensitization

After excluding the HR pathway as the direct cause of AR suppression induced radiosensitization, we investigated the involvement of the NHEJ pathway. Previously, Goodwin et al. showed that the AR pathway regulates the NHEJ factor DNA-PKcs (7). Therefore, we analyzed DNA-PKcs protein expression after AR suppression treatment. A significant reduction of the DNA-PKcs protein level was observed in all 3 cell lines (Fig. 5A-B). On average, all AR suppression modalities reduced DNA-PKcs levels to 30-60 %. We further investigated whether these reduced DNA-PKcs levels were sufficient to explain the observed DSB repair defects (Fig. 3). To this end, PC346C-Flu1 cells were treated with small interfering RNA (siRNA) to reduce DNA-PKcs expression. This cell line was selected since HR was shown to be unaffected, allowing us to determine if reduction of NHEJ repair could explain the observed synergistic therapy response. DNA-PKcs expression was reduced to approximately 50% by siRNA treatment, similar to DNA-PKcs levels observed after AR suppression. A significantly decreased ability to repair DSBs was observed at 24 hours after IR compared to control cells (Fig. 5C-D). DNA-PKcs knockdown did show significant difference in γ H2AX and 53BP1 foci levels at 1 hour post-IR as was observed for AR suppression treatments. Furthermore, PFGE analysis also showed a higher level of DNA breaks at 1 hour after IR in cells with reduced DNA-PKcs levels compared to control cells (Fig. 5E-F). The functional consequences of DNA-PKcs reduction were directly assessed and these cells showed a significant reduced cell number after IR treatment compared to cells with normal levels of DNA-PKcs (Fig. 5G). These results indicate that reduced DNA-PKcs expression caused by AR suppression treatment can at least partially account for the observed delay in DSB repair and the associated radiosensitization.

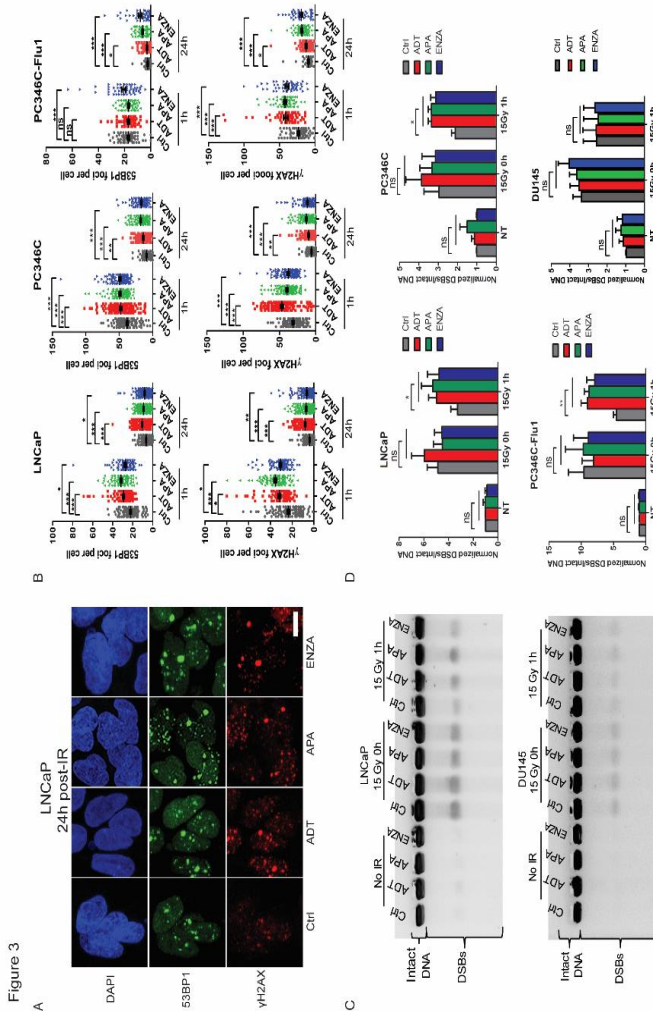


Figure 3. AR suppression treatment suppresses DNA damage repair.

(a) Cells were treated with AR suppression for 24 h followed by 2 Gy IR treatment. Representative images of γ H2AX and 53BP1 staining 24 h post-IR of LNCaP cells (scale bar 10 μ m). (b) Quantification of γ H2AX and 53BP1 foci from different cell lines. Each data point represents one cell, average and SEM are indicated. (c) Representative pulsed-field gel electrophoresis (PFGE) image of PC346C and DU145 cells under different conditions. (d) DNA break signals were quantified using ImageJ and normalized to unsaturated signals of intact DNA. Average and SD are indicated, * $p < 0.05$, ** $p < 0.01$, *** $p < 0.001$, ns, non-significant. ADT, androgen-deprivation treatment; APA, apalutamide; ENZA, enzalutamide.

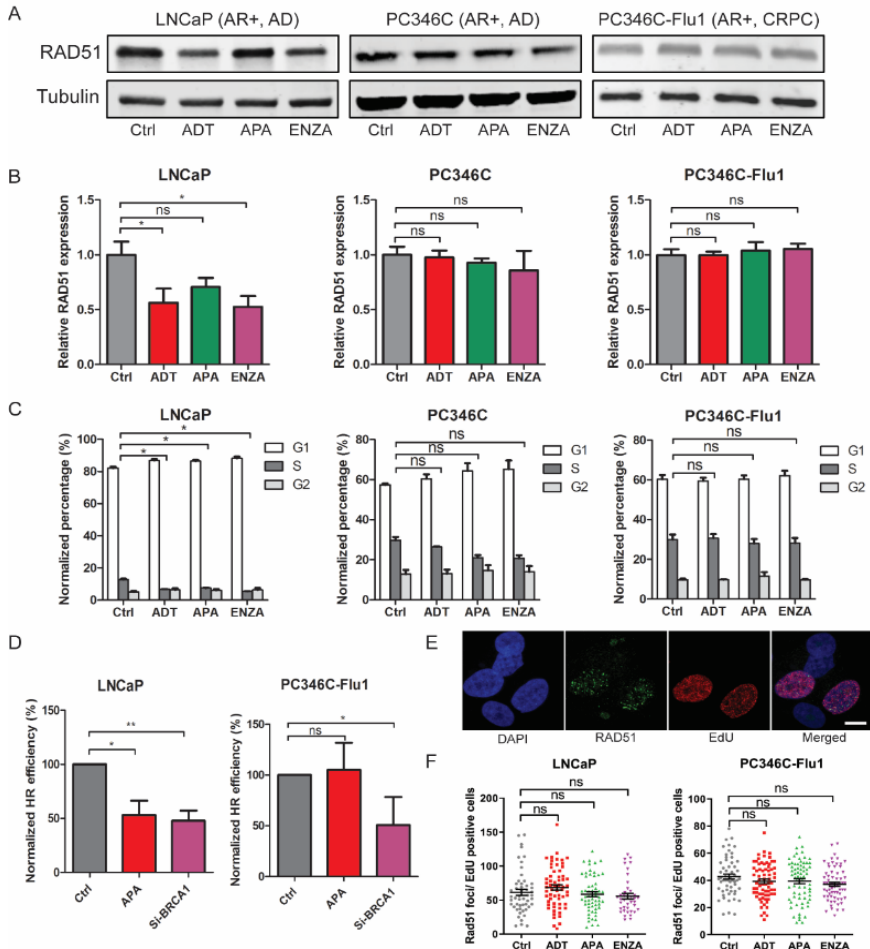


Figure 4. Reduced HR efficiency provoked by AR suppression treatment results from cell cycle alterations.

(a) LNCaP, PC346C and PC346C-Flu1 cells were treated with AR suppression for 48 h and RAD51 expression was analyzed by Western blotting. Tubulin is used as loading control. Full blots can be found in supplementary Figure 3. (b) Quantification of RAD51 protein levels compared to loading control and normalized to untreated (Ctrl). Average and SEM are indicated. (c) The same cell samples from a were incubated with EdU for 30 min before fixation and the cell cycle profile was determined by flow cytometry. Average and SD are indicated. (d) Transient DR-GFP assay was performed in LNCaP and PC346C-Flu1 cells treated with apalutamide for 48 h. Cells transfected with siRNA against BRCA1 transcript for 72 h were used as positive control. GFP positive cells were scored by flow cytometry and quantified. Average and SD are indicated. (e) Representative images of double staining of EdU-positive and RAD51 foci and their colocalization in LNCaP cells at 2 h after 5 Gy IR treatment (scale bar 10 μ m). (f) Quantification of RAD51 foci numbers in EdU-positive cells. Each data point represents one cell, average and SEM are indicated. * $P < 0.05$, ** $P < 0.01$, ns,

non-significant. ADT, androgen deprivation treatment; APA, apalutamide; ENZA, enzalutamide.

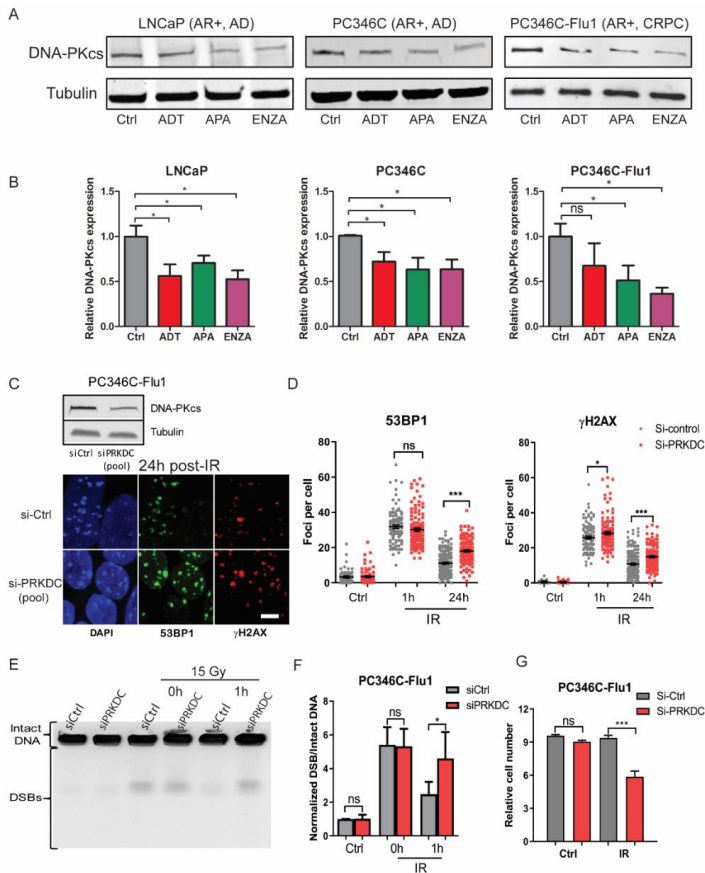


Figure 5. NHEJ suppression is regulated by AR signaling and contributes to radiosensitization.

(a) LNCaP, PC346C and PC346C-Flu1 cells were treated with AR suppression for 48 h and DNA-PKcs protein levels were analyzed by Western blotting. Tubulin is used as loading control. Full blots can be found in supplementary Figure 3. (b) Quantification of DNA-PKcs protein levels compared to loading control and normalized to untreated (Ctrl). Average and SEM are indicated. (c) PC346C-Flu1 cells were transfected with a pool of siRNAs against the DNA-PKcs or non-targeting siRNA for 48 h then treated with 2 Gy IR treatment. Representative images of γ H2AX and 53BP1 stainings 24 h post-IR (scale bar 10 μ m). (d) Quantification of γ H2AX and 53BP1 foci. Each data point represents one cell, average and SEM are indicated. (e) Representative pulsed-field gel electrophoresis (PFGE) image of PC346C-Flu1 cells were treated as in C but following treated with 15 Gy IR. (f) DNA break signals were quantified by ImageJ and normalized to unsaturated signals of intact DNA. Average and SD are indicated. (g) PC346C-Flu1 were treated as in C but followed with 1 Gy IR treatment, and cells were counted 7 days after treatment by sulforhodamine beta (SRB) assay and cell number set relative to initial cell number. * $P < 0.05$, ** $P < 0.01$, *** $P < 0.0001$,

ns, non-significant. ADT, androgen deprivation treatment; APA, apalutamide; ENZA, enzalutamide.

3. Discussion

Here, we demonstrate that different forms of AR suppression treatment can act as a radiosensitizer in AR-expressing androgen-dependent and CRPC preclinical PCa models. The mechanism of action causing this radiosensitization involves regulation of the NHEJ DNA repair pathway.

We and others found that AR suppression and IR treatment have an additive effect on cell proliferation in AR-expressing PCa (7, 13). Based on these data, AR suppression treatments were reported to have a radiosensitizing effect. However, the observed effects could also be explained by additivity of both modalities. Previous reports come to opposing conclusions regarding the radiosensitizing effect of AR suppression in CRPC models, with studies showing a synergistic effect (7, 15) or no effect (13, 16). Our *in vitro* CRPC cells and *ex vivo* androgen-dependent PCa tissue slices experiments provide new evidence that AR suppression can act as radiosensitizer in both AR-expressing hormone-sensitive PCa (which represents the majority of patients receiving EBRT) and AR-expressing CRPC. Although no synergy could be demonstrated in cell growth assays, our DSB repair kinetic assays showed a clear synergy between IR and AR suppression treatment for AR-expressing PCa cells. We found similar effects of apalutamide, enzalutamide and ADT, showing that various methods of AR suppression have similar efficacy *in vitro*. We conclude that patients with AR-expressing PCa can benefit from apalutamide or other AR suppressing treatment in addition to EBRT.

Previous preclinical studies have investigated the molecular mechanism of radiosensitization by ADT and discovered an interplay between AR-signaling and the DNA repair machinery (7, 8, 10, 11, 16). However, opposing conclusions were drawn from these studies about the DNA repair pathways that cause the radiosensitization. Studies reported a functional link between AR-signaling and HR repair and synthetic lethality in combinations of AR inhibitors and PARP inhibitors in PCa. Enzalutamide suppressed the expression of the HR protein RAD51 in androgen-dependent PCa cells (10) and HR efficiency, measured by a functional HR assay, was indeed significantly reduced by AR suppression (10, 11, 16). We found that reduced RAD51 expression and compromised HR could be explained by a reduced fraction of S/G2 phase cells. Such cell cycle analyses were not included in their studies, which precludes definitive conclusions. Asim et al. showed that IR-induced RAD51 foci formation in Ki67-positive PCa cells were strongly decreased in patient biopsies who received ADT (11). This is seemingly in contrast with our results that equal numbers of RAD51 foci were detected in EdU-positive cells after AR suppression. However, this discrepancy can be explained by the difference in detection of proliferating cells: EdU labels only S-phase cells, whereas Ki67 is present in all cycling cells. It has even been reported to persist for several days after cells have ceased to proliferate (17). Ki67 positive cells may thus be primarily G1 phase cells that do not form RAD51 foci nor perform HR. Together, our data indicate that the HR pathway is not directly regulated by AR-signaling, but HR might be reduced on a cell population level caused by a change of the cell cycle

profile.

After excluding AR regulated HR repair, we further investigated the NHEJ repair pathway. A previous study discovered that AR directly regulates the level and function of the NHEJ factor DNA-PKcs (7). Our data confirmed this observation and showed that AR suppression reduced DNA-PKcs levels in both androgen-dependent and CRPC cells. Downregulation of DNA-PKcs is further supported by the low staining intensity of DNA-PKcs in PCa tissue after combined castration and radiotherapy when compared with radiotherapy alone (18). These data were further confirmed by siRNA knockdown of DNA-PKcs indeed resulted in a similar level of radiosensitization and delayed DNA repair in AR-expressing cells. We conclude that NHEJ is directly regulated by AR-signaling and that downregulation of DNA-PKcs expression contributes to the radiosensitization induced by AR suppression.

Previous preclinical studies reported the synthetic lethality between AR inhibitors and PARP inhibitors (10, 11). Unfortunately, the first randomized multicenter clinical trial failed to show a significant difference in prostate-specific antigen response rate and median progression-free survival between patients treated with abiraterone plus the PARP inhibitor veliparib compared to abiraterone acetate plus prednisone alone (19). This combination was based of the rationale that tumors with loss-of-function mutations in *BRCA1/2* are deficient in HR repair, which makes them highly sensitive to PARP inhibition treatment (20, 21). Based on our finding that AR suppression causes reduced NHEJ, not HR, one would indeed expect a lack of efficacy from this combination treatment in an unselected PCa patient population. On the other hand, PCa patients harboring *BRCA1/2* mutations could possibly benefit to a greater degree from combination of apalutamide and EBRT compared to *BRCA1/2* wild type patient, as intrinsic HR repair defects in these patients plus compromised NHEJ repair by apalutamide will render the tumor cells exquisitely vulnerable to IR.

Emerging preclinical and clinical studies show that AR variants (AR-Vs) can play an important role in the development of resistance to AR suppression treatment (22, 23). AR-Vs lack the ligand-binding domain, and therefore are constitutively active, which constitutes a mechanism of resistance when androgen ligands are very low under ADT (22). Recently, studies reported that in genetically engineered R1-D567 cells (only expressing AR-Vs), and 22Rv1 cell line (expressing both AR and high AR-V7), combination of IR and AR suppression treatment, could not increase radiosensitivity via altering the AR mediated DDR (24). These studies imply that the expression of AR-Vs in PCa cells may counteract the AR suppression-induced radiosensitization and patients with AR-V expression might not be eligible for such a combination regimen. It remains to be investigated whether a certain level of AR expression is a prerequisite for achieving radiosensitization by AR suppression treatments. These issues warrant further investigation with more PCa models.

We did not find significant differences in response between ADT, enzalutamide and apalutamide treatment, probably because ADT in an *in vitro* setting is a simplified and optimal scenario, while effects in patients are less optimal due to adrenal androgen production being unaffected under ADT. Apalutamide has recently received FDA approval for the treatment of non-metastatic CRPC. Several clinical trials are underway

to test the efficacy of apalutamide with EBRT (NCT03488810, NCT03503344, NCT02531516). The preclinical data presented here fully support the ongoing clinical trials. Furthermore, our study showed benefit of the combination in AR-expressing CRPC cells, a situation also found in patients with advanced metastatic disease that are progressive on ADT. Therefore, we propose that an alternative treatment approach should be considered for these patients, consisting of apalutamide in combination with prostate-specific membrane antigen (PSMA)-targeted radioligand therapy (25). The decreased DNA repair effectivity in the tumor, but not the normal tissue, should increase the therapeutic ratio in this setting.

4. Materials and Methods

4.1. Reagents

Reagents were purchased from Sigma-Aldrich, unless otherwise specified. The following antibodies were used: AR (1:200, M4074, SPRING Bioscience, Pleasanton, CA, USA), RAD51 (1:10000, homemade, (26)), DNA-PKcs (1:1000, homemade (27)), phospho-histone H2AX (ser139) (γ -H2AX) (1:500, JBW301, Millipore, Darmstadt, Germany), 53BP1 (1:1000, NB100-904, Novus Biologicals, Novus Biologicals, Littleton, CO, USA), α -tubulin (1:10000, B-5-12, Sigma-Aldrich, Darmstadt, Germany), anti-rabbit/mouse Alexa Fluor 488/594 (1:1000, Life Technologies, Carlsbad, CA, USA). Apalutamide was a gift from Janssen-Cilag B.V., enzalutamide was purchased from Axon Medchem (Groningen, The Netherlands). Both compounds were diluted in dimethyl sulfoxide (DMSO) and used at a final concentration of 1 μ M.

4.2. Cell lines

DU145 and LNCaP cells were purchased from American Type Culture Collection (Manassas, VA, USA) and cultured as described (28, 29). PC346C, PC346C-DCC and PC346C-Flu1 cells were established in our laboratory and cultured as previously described (30). Composition of the cell culture medium and characteristics of each cell line can be found in supplementary table 1. All cells lines were authenticated for AR expression by western blot. Cells were regularly tested for mycoplasma infection, and kept into culture for maximum 25 passages after initiating the hormone sensitive/castration resistance phenotype.

4.3. Irradiation (IR)

Cells and tissue slices were irradiated with different X-ray doses using Xstrahl Cabinet Irradiator RS320 (195 kV, 10 mA, 1.67 Gy/min, Xstrahl Ltd. Camberley, UK).

4.4. Cell growth assay

Cell growth was measured using the sulforhodamine beta (SRB) assay. Briefly, all cells were plated in FNC coating mix (Athena Environmental Sciences) coated 96-well plates in 100 μ l steroid-stripped medium (medium with dextran-coated charcoal-treated FCS: DCC). The next day, 100 μ l of culture medium were added either alone (ADT condition) or supplemented with R1881 (0.1 nM, control condition) or R1881 (0.1 nM) plus apalutamide/enzalutamide (1 μ M, apalutamide or enzalutamide condition) 24 h before irradiation (IR). Cells were allowed to grow until different time points, and fixed

and stained with SRB as previously described (31). Absorbance was measured at 560 nm using a GloMax®-Multi Detection System (Promega, Madison, WI, USA).

4.5. Immunofluorescent staining on cells

γ -H2AX and 53BP1 staining was performed as previously described (31). Briefly, cells were seeded in DCC medium overnight on coverslips and treated with various antiandrogen or control (R1881) treatments for 24 h before IR. Cells were fixed with 2% paraformaldehyde (PFA) after 1 h and 24 h. Following permeabilization and blocking, cells were incubated with anti- γ H2AX and anti-53BP1 antibodies overnight, and secondary antibodies. EdU/RAD51 co-staining was done as previous reported (32). Briefly, 5-ethynyl-2'-deoxyuridine (EdU, Thermo Fisher Scientific, Carlsbad, CA, USA) at a concentration of 3 μ g/ml was added to the cells 30 min before fixation. Pre-extraction was performed in Triton X-100 buffer (0.5% Triton X-100, 20 mM Hepes-KOH, pH 7.9, 50 mM NaCl, 3 mM MgCl₂, 300 mM sucrose) at room temperature (RT) for 1 min before fixation. After permeabilization and blocking, cells were incubated with anti-RAD51 antibody and subsequently incubated with secondary antibody followed by Click-iT Alexa Fluor 594 cocktail buffer for 30 min.

4.6. Cell cycle analysis

Cell cycle distribution was measured by flowcytometry (33). Briefly, cells were seeded in DCC medium overnight and treated with various antiandrogen treatments for 24 h before IR. EdU at a concentration of 3 μ g/ml was added to the culture medium 30 min before fixation and cells were fixed with ice-cold 70% ethanol 24 h post-IR. Cells were washed with phosphate-buffered saline (PBS) and permeabilized in 0.1% Triton X-100 in PBS for 5 min at RT. Subsequently cells were incubated in Click-iT Alexa Fluor 594 cocktail buffer for 30 min, and then cells were resuspended in 1 μ g/ml DAPI and 0.1 mg/ml RNase (Roche Life Sciences, Mannheim, Germany) in PBS. Cell cycle distribution was measured using a LSRFORTESSA FACS machine (BD Bioscience, San Jose, CA, USA).

4.7. Tissue slice culture

All animal experiments were approved by the Animal Welfare Committee of the Erasmus MC, and all experiments were conducted in accordance with accepted guidelines (permit AVD101002017867, 25 September 2017). PC295 PDXs were previously established in our laboratory (34). PDX tumors were excised, sliced and cultured as previously reported (14). Briefly, 300 μ m slices were cultured in advanced DMEM/F12 (ThermoFisher Scientific, Carlsbad, CA, USA) medium in 6 well plates on a Rocking Table (Luckham 200 Ltd., West Sussex, UK) and one third of medium was refreshed daily. Slices were pretreated with apalutamide or DMSO control for 2 h and subsequently irradiated with a dose of 2 Gy. At different time points, slices were harvested and fixed in 10% neutral buffered formalin for 24h at RT, embedded in paraffin and 4 μ m sections were made for further analysis. EdU (3 μ g/ml) was added to the tissue slice culture medium 2 h before fixation.

4.8. Tissue section TUNEL and EdU Click-iT assays

EdU at a concentration of 3 μ g/ml was added to the tissue slice culture medium 2 h

before fixation. Simultaneous TUNEL and EdU staining was performed as described previously (35). Briefly, tissue sections were deparaffinized in xylene followed by rehydration in graded alcohols and then blocked with PBS 3% BSA. TUNEL reaction was performed using In Situ Cell Death Detection Kit (Roche Life Sciences, Penzberg, Germany) after which the sections were incubated with Click-iT Alexa Fluor 594 (Invitrogen, Carlsbad, CA, USA) cocktail buffer for 30 min.

4.9. Tissue section Hematoxylin & eosin (H&E)

Histological tumor architecture was examined by H&E staining as previously described (14). Briefly, sections were deparaffinized in xylene followed by rehydration in graded alcohols and staining with hematoxylin and eosin (14).

4.10. Tissue section immunohistochemical staining

Sections were deparaffinized in xylene followed by rehydration in graded alcohols. Antigen retrieval was performed with target retrieval buffer (pH 6, Dako, Glostrup, Denmark). Sections were treated with 3% hydrogen peroxide solution in methanol at RT for 20 min, followed by incubation in 5% BSA in PBS for 30 min at RT. Sections were incubated with anti-AR antibodies overnight, and horseradish peroxidase (HRP)-conjugated anti-rabbit IgG secondary antibody (1:100, Dako) for 1 h at RT. AR positive cells were visualized using diaminobenzidine (DAB) staining kit (Agilent, Santa Clara, CA, USA) and hematoxylin counter staining.

4.11. Pulsed-field gel electrophoresis

Pulsed-field gel electrophoresis (PFGE) was performed as previously described (36). Briefly, cells were embedded in 2% agarose plugs and lysed following 15 Gy of IR (15 Gy is commonly used for the PFGE assay since 2 Gy is too low to detect clear bands of DSBs). Electrophoresis was performed at 14 °C in 0.9% pulse-field certified agarose (Bio-Rad, Hercules, CA, USA) in a Bio-Rad Chef DR III system (Bio-Rad, La Jolla, CA, USA). The gel was stained with ethidium bromide and imaged on a UVITEC gel documentation system (UVItec, Cambridge, UK). DSBs bands were quantified using ImageJ (version 1.52, open source software via <https://imagej.nih.gov/ij/index.html>) with background subtracted and normalized to unsaturated signals of intact DNA. For each treatment, these values were normalized against their respective untreated controls to obtain the fold-change in DSBs.

4.12. HR assay

DR-GFP assay was performed to measure HR as previous described (33). Briefly, cells were transfected with 1.5 µg of DR-GFP plasmid and an I-SceI expression vector or empty vector according to the manufacturer's protocol (FuGENE HD (Promega) for LNCaP and Lipofectamine 3000 (Invitrogen) for PC346C-Flu1). Transfected cells were cultured in medium containing apalutamide or DMSO control for 48 h. BRCA1 knockdown was used as a positive control. GFP expression was analyzed by flow cytometry (LSRFORTESSA, BD Bioscience, San Jose, CA, USA).

4.13. Western blot

Cells were lysed and lysates were resolved by sodium dodecyl sulfate polyacrylamide gel electrophoresis (SDS-PAGE) (Bio-Rad, Hercules, CA, USA), transferred to

polyvinylidene difluoride membranes, and analyzed using antibodies described above. Quantification was conducted using ImageJ software.

4.14. RNA Interference

PC346C-Flu1 cells were transfected with either control or DNA-PKcs siRNA (Dharmacon, Lafayette, CO, USA) using Lipofectamine RNAi MAX (Life Technologies, Carlsbad, CA, USA). Transfected cells were cultured for 48 h and then treated as specified.

4.15. Image acquisition and quantification

For 53BP1, γ H2AX, RAD51 foci quantification, at least 3 random fields of view of Z-stack images were captured with a LSM700 confocal microscope (Zeiss, Oberkochen, Germany) and quantified as previously described (32). AR and H&E was imaged with a light microscope (Olympus, Tokyo, Japan) and 4 fields of view from each section were analyzed. For EdU and TUNEL quantification, 10 random images from each tissue slice section were generated using a Leica fluorescence microscope (DM4000b, Wetzlar, Germany) and quantified using the Otsu's algorithm in a Matlab based software as previous reported (14). AR expression was quantified by using Image J software as previous described (14).

4.16. Statistical analysis

Experiments were performed in duplicate (foci kinetics) or triplicate (all other experiments). One-way ANOVA test was used to compare more than two groups and unpaired student's t-test was used to analyze the differences between two groups. Statistical analysis and generation of graphs was performed using GraphPad Prism 6.0 (GraphPad, La Jolla, CA, USA).

5. Conclusions

In summary, we demonstrate for the first time that the next-generation AR inhibitor apalutamide acts as a radiosensitizer in AR-expressing androgen-dependent PCa and CRPC models. This radiosensitization is caused by inhibition of DNA repair by NHEJ, not HR. Our results suggest that apalutamide can not only be used in combination with EBRT for the treatment of androgen-dependent localized PCa, but also for AR-expressing CRPC patients.

Author Contributions: Conceptualization (WZ, LI, DvG, WvW, JN); Data curation (WZ); Formal analysis (WZ, CL, HC); Funding acquisition (LI, DvG, WvW, JN); Investigation (WZ, CL, HC); Supervision (DvG, WvW, JN); Writing - original draft (WZ, JN); Writing-review & Editing (WZ, DvG, WvW, JN).

Funding: This study was supported by the Chinese Scholarship Council (grant number 201506270172 (WZ)), by the Dutch Cancer Society (Alpe d'Huzes grant number EMCR 2014-7048 (DvG) and grant number 10317 (DvG and JN)), and by the Daniel den Hoed Foundation (JN).

Acknowledgments: The authors thank D. Stuurman and C. de Ridder for their help in acquiring xenograft tumor samples, Dr. A. Ray Chaudhuri and M. Manolika for their help during PFGE experiments and Calvin S.Y. Lo for his help during flow cytometry experiments. Fluorescent imaging was performed in collaboration with the optical imaging center (OIC) of the Erasmus MC.

Conflicts of Interest: Apalutamide was a gift from Janssen-Cilag B.V. (collaborative project of LI and WvW). The authors declare no conflict of interest.

Ethical statement: All animal experiments were approved by the Animal Welfare Committee of the Erasmus MC and all experiments were conducted in accordance with accepted guideline (AVD101002017867)0.

References

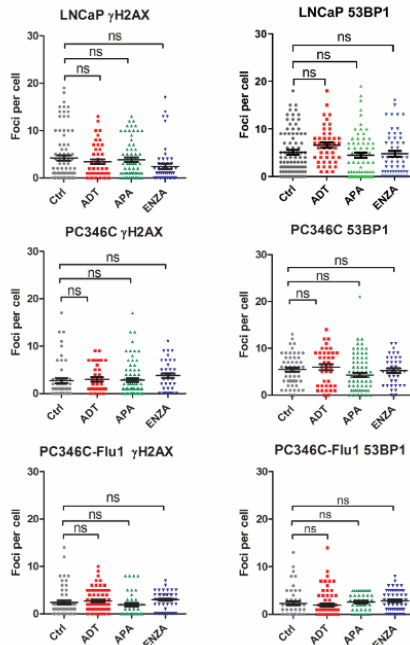
1. Siegel RL, Miller KD, Jemal A. Cancer statistics, 2018. *CA Cancer J Clin*. 2018;68(1):7-30.
2. Djavan B, Moul JW, Zlotta A, Remzi M, Ravery V. PSA progression following radical prostatectomy and radiation therapy: new standards in the new Millennium. *Eur Urol*. 2003;43(1):12-27.
3. Khan MA, Han M, Partin AW, Epstein JI, Walsh PC. Long-term cancer control of radical prostatectomy in men younger than 50 years of age: update 2003. *Urology*. 2003;62(1):86-91; discussion -2.
4. Schmidt-Hansen M, Hoskin P, Kirkbride P, Hasler E, Bromham N. Hormone and radiotherapy versus hormone or radiotherapy alone for non-metastatic prostate cancer: a systematic review with meta-analyses. *Clin Oncol (R Coll Radiol)*. 2014;26(10):e21-46.
5. Jones CU, Hunt D, McGowan DG, Amin MB, Chetner MP, Bruner DW, et al. Radiotherapy and Short-Term Androgen Deprivation for Localized Prostate Cancer. *New England Journal of Medicine*. 2011;365(2):107-18.
6. D'Amico AV, Manola J, Loffredo M, Renshaw AA, DellaCroce A, Kantoff PW. 6-Month Androgen Suppression Plus Radiation Therapy vs Radiation Therapy Alone for Patients With Clinically Localized Prostate Cancer A Randomized Controlled Trial. *Jama*. 2004;292(7):821-7.
7. Goodwin JF, Schiewer MJ, Dean JL, Schrecengost RS, de Leeuw R, Han S, et al. A hormone-DNA repair circuit governs the response to genotoxic insult. *Cancer discovery*. 2013;3(11):1254-71.
8. Polkinghorn WR, Parker JS, Lee MX, Kass EM, Spratt DE, Iaquina PJ, et al. Androgen receptor signaling regulates DNA repair in prostate cancers. *Cancer discovery*. 2013;3(11):1245-53.
9. Ceccaldi R, Rondinelli B, D'Andrea AD. Repair Pathway Choices and Consequences at the Double-Strand Break. *Trends Cell Biol*. 2016;26(1):52-64.
10. Li L, Karanika S, Yang G, Wang J, Park S, Broom BM, et al. Androgen receptor inhibitor-induced "BRCAness" and PARP inhibition are synthetically lethal for castration-resistant prostate cancer. *Sci Signal*. 2017;10(480).
11. Asim M, Tarish F, Zecchini HI, Sanjiv K, Gelali E, Massie CE, et al. Synthetic lethality between androgen receptor signalling and the PARP pathway in prostate cancer. *Nat Commun*. 2017;8(1):374.
12. Clegg NJ, Wongvipat J, Joseph JD, Tran C, Ouk S, Dilhas A, et al. ARN-509: a novel antiandrogen for prostate cancer treatment. *Cancer research*. 2012;72(6):1494-503.
13. Ghashghaei M, Niazi TM, Heravi M, Bekerat H, Trifiro M, Paliouras M, et al. Enhanced radiosensitization of enzalutamide via schedule dependent administration to androgen-sensitive prostate cancer cells. *Prostate*. 2018;78(1):64-75.
14. Zhang W, van Weerden WM, de Ridder CMA, Erkens-Schulze S, Schonfeld E, Meijer TG, et al. Ex vivo treatment of prostate tumor tissue recapitulates in vivo therapy response. *Prostate*. 2019;79(4):390-402.
15. Sekhar KR, Wang J, Freeman ML, Kirschner AN. Radiosensitization by enzalutamide for human prostate cancer is mediated through the DNA damage repair pathway. *PLoS One*. 2019;14(4):e0214670.

16. Chou F-J, Chen Y, Chen D, Niu Y, Li G, Keng P, et al. Preclinical study using androgen receptor (AR) degradation enhancer to increase radiotherapy efficacy via targeting radiation-increased AR to better suppress prostate cancer progression. *EBioMedicine*. 2019;40:504-16.
17. van Oijen MG, Medema RH, Slootweg PJ, Rijksen G. Positivity of the proliferation marker Ki-67 in noncycling cells. *Am J Clin Pathol*. 1998;110(1):24-31.
18. Tarish FL, Schultz N, Tanoglidis A, Hamberg H, Letocha H, Karasz K, et al. Castration radiosensitizes prostate cancer tissue by impairing DNA double-strand break repair. *Science translational medicine*. 2015;7(312):312re11.
19. Hussain M, Daignault-Newton S, Twardowski PW, Albany C, Stein MN, Kunju LP, et al. Targeting Androgen Receptor and DNA Repair in Metastatic Castration-Resistant Prostate Cancer: Results From NCI 9012. *J Clin Oncol*. 2018;36(10):991-9.
20. Bryant HE, Schultz N, Thomas HD, Parker KM, Flower D, Lopez E, et al. Specific killing of BRCA2-deficient tumours with inhibitors of poly(ADP-ribose) polymerase. *Nature*. 2005;434(7035):913-7.
21. Farmer H, McCabe N, Lord CJ, Tutt AN, Johnson DA, Richardson TB, et al. Targeting the DNA repair defect in BRCA mutant cells as a therapeutic strategy. *Nature*. 2005;434(7035):917-21.
22. Lu J, Van der Steen T, Tindall DJ. Are androgen receptor variants a substitute for the full-length receptor? *Nature reviews Urology*. 2015;12(3):137-44.
23. Antonarakis ES, Lu C, Wang H, Lubner B, Nakazawa M, Roeser JC, et al. AR-V7 and resistance to enzalutamide and abiraterone in prostate cancer. *The New England journal of medicine*. 2014;371(11):1028-38.
24. Yin Y, Li R, Xu K, Ding S, Li J, Baek G, et al. Androgen Receptor Variants Mediate DNA Repair after Prostate Cancer Irradiation. *Cancer research*. 2017;77(18):4745-54.
25. Afshar-Oromieh A, Babich JW, Kratochwil C, Giesel FL, Eisenhut M, Kopka K, et al. The Rise of PSMA Ligands for Diagnosis and Therapy of Prostate Cancer. *J Nucl Med*. 2016;57(Suppl 3):79S-89S.
26. Essers J, Hendriks RW, Wesoly J, Beerens CE, Smit B, Hoeijmakers JH, et al. Analysis of mouse Rad54 expression and its implications for homologous recombination. *DNA Repair (Amst)*. 2002;1(10):779-93.
27. Weterings E, Verkaik NS, Bruggenwirth HT, Hoeijmakers JH, van Gent DC. The role of DNA dependent protein kinase in synapsis of DNA ends. *Nucleic Acids Res*. 2003;31(24):7238-46.
28. Moll JM, Kumagai J, van Royen ME, Teubel WJ, van Soest RJ, French PJ, et al. A bypass mechanism of abiraterone-resistant prostate cancer: Accumulating CYP17A1 substrates activate androgen receptor signaling. *Prostate*. 2019;79(9):937-48.
29. Stone KR, Mickey DD, Wunderli H, Mickey GH, Paulson DF. Isolation of a human prostate carcinoma cell line (DU 145). *Int J Cancer*. 1978;21(3):274-81.
30. Marques RB, Erkens-Schulze S, de Ridder CM, Hermans KG, Waltering K, Visakorpi T, et al. Androgen receptor modifications in prostate cancer cells upon long-term androgen ablation and antiandrogen treatment. *International Journal of Cancer*. 2005;117(2):221-9.
31. Nonnekens J, van Kranenburg M, Beerens CE, Suker M, Doukas M, van Eijck CH, et al. Potentiation of Peptide Receptor Radionuclide Therapy by the PARP Inhibitor Olaparib. *Theranostics*. 2016;6(11):1821-32.

32. van den Tempel N, Laffeber C, Odijk H, van Cappellen WA, van Rhoon GC, Franckena M, et al. The effect of thermal dose on hyperthermia-mediated inhibition of DNA repair through homologous recombination. *Oncotarget*. 2017;8(27):44593.
33. Ray Chaudhuri A, Callen E, Ding X, Gogola E, Duarte AA, Lee J-E, et al. Replication fork stability confers chemoresistance in BRCA-deficient cells. *Nature*. 2016;535(7612):382-7.
34. van Weerden WM, de Ridder CM, Verdaasdonk CL, Romijn JC, van der Kwast TH, Schroder FH, et al. Development of seven new human prostate tumor xenograft models and their histopathological characterization. *Am J Pathol*. 1996;149(3):1055-62.
35. Naipal KAT, Verkaik NS, Sánchez H, van Deurzen CHM, den Bakker MA, Hoeijmakers JHJ, et al. Tumor slice culture system to assess drug response of primary breast cancer. *BMC Cancer*. 2016;16(1):78.
36. Ray Chaudhuri A, Hashimoto Y, Herrador R, Neelsen KJ, Fachinetti D, Bermejo R, et al. Topoisomerase I poisoning results in PARP-mediated replication fork reversal. *Nature Structural & Molecular Biology*. 2012;19:417.

Supplementary Materials:

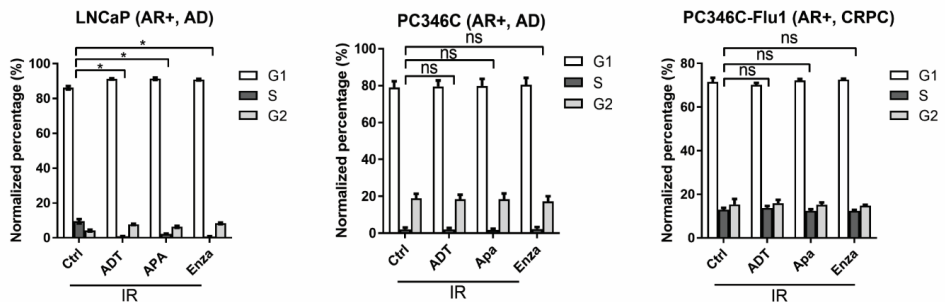
Supplementary Figure 1



Supplementary Figure 1.

Quantification of γ H2AX and 53BP1 foci in cell lines treated with AR suppression for 48 h. Each data point represents one cell, average and SEM are indicated, ns, non-significant. ADT, androgen deprivation treatment; APA, apalutamide; ENZA, enzalutamide.

Supplementary Figure 2

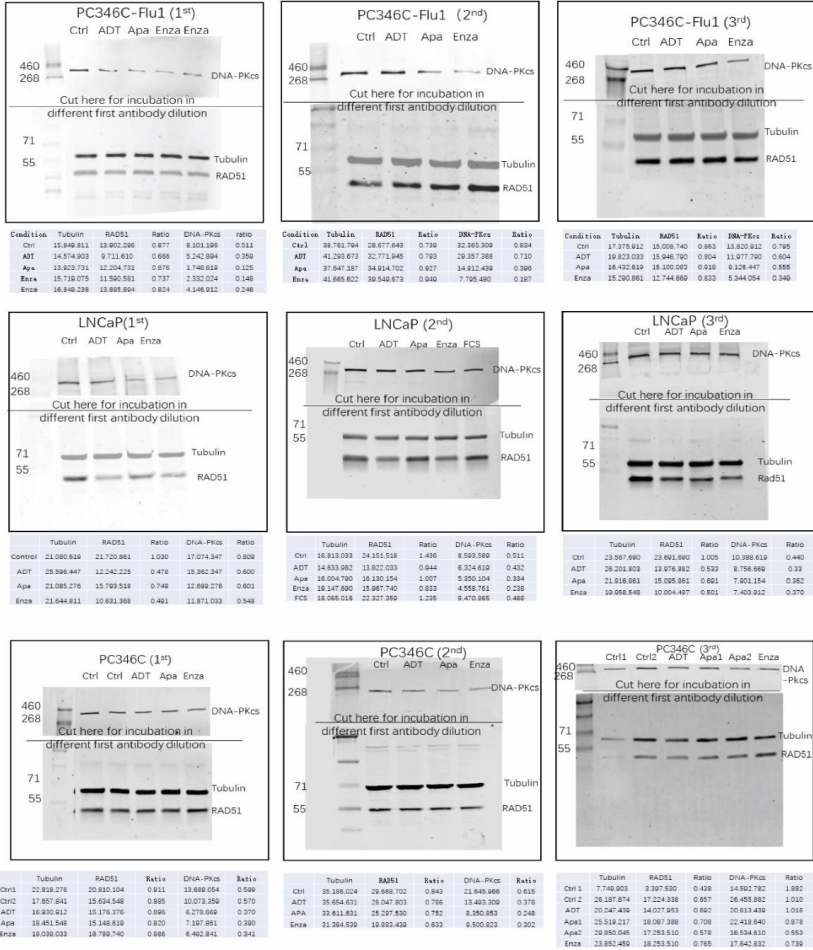


Supplementary Figure 2.

LNCaP, PC346C and PC346C-Flu1 cells were treated with AR suppression for 24 h followed by IR (2 Gy). Cell samples were collected 24 h post-IR and cell cycle was determined by flow

cytometry. Average and SD were indicated. *P < 0.05, ns, non-significant. ADT, androgen deprivation treatment; APA, apalutamide; ENZA, enzalutamide.

Supplementary Figure 3



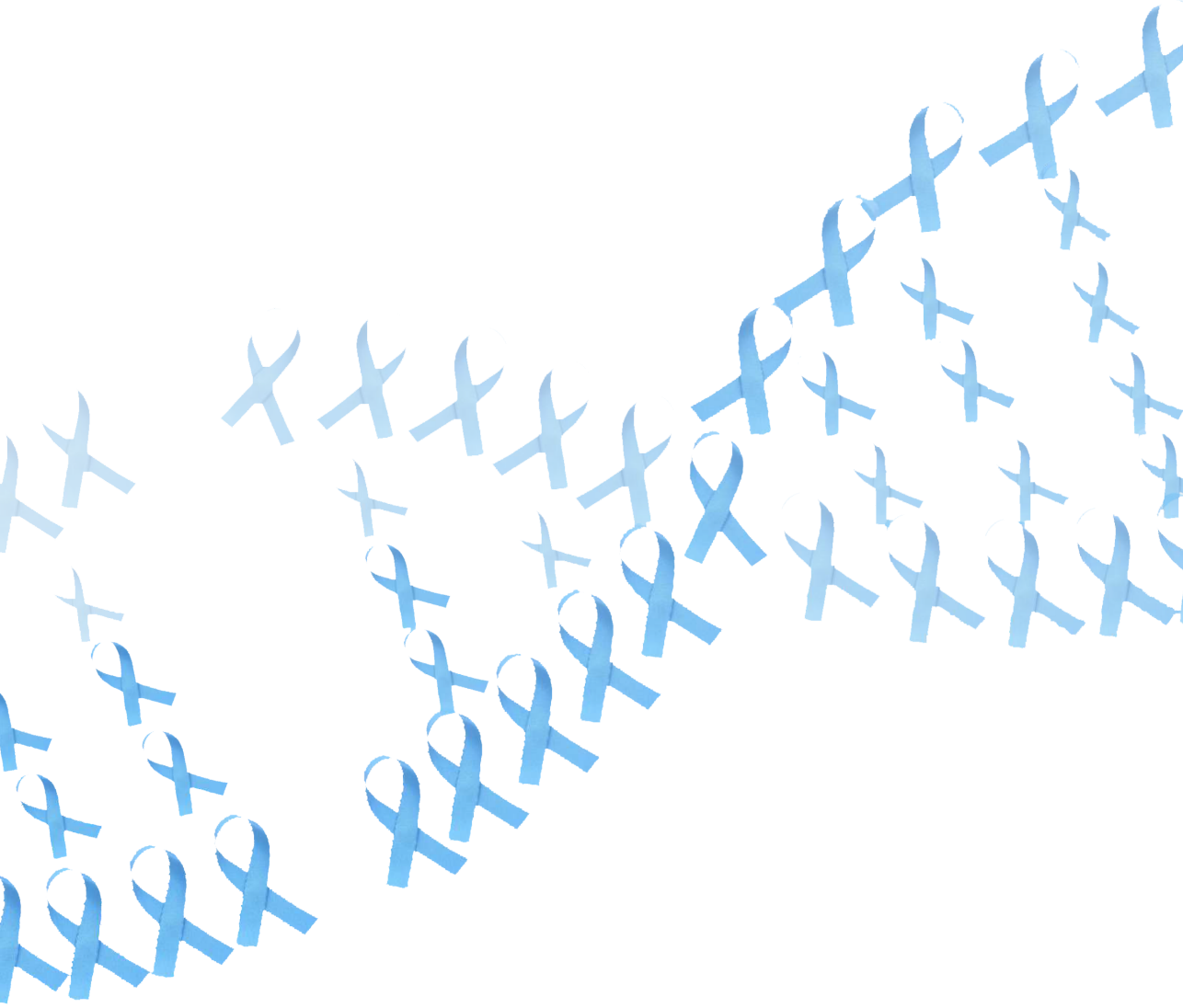
Supplementary Figure 3.

Full blots and quantification of the band of the western blot experiments shown in Figure 4A and 5A.

Supplementary Table 1

Cell lines	DU145	LNCaP	PC346C	PC346C-DCC	PC346C-Flu1
Culture	RPMI	RPMI	DMEM/Ham's F12	DMEM/Ham's F12	PC346C-DCC
Medium	1640	1640	BSA (0.01%)	BSA (0.01%)	medium
	FCS	FCS	FCS (2%)	DCC (2%)	plus
	(10%)	(10%)	Epidermal growth factor (10 ng/mL)	Epidermal growth factor (10 ng/mL)	OH-flutamide
	PS	PS	Insulin-transferrin-selenium (1%)	Insulin-transferrin-selenium (1%)	(1 μM)
			Hydrocortison (0.5 μg/mL)	Hydrocortison (0.5 μg/mL)	
			Triiodothyronine (1 nM)	Triiodothyronine (1 nM)	
			Phosphoethanolamine (0.1 mM)	Phosphoethanolamine (0.1 mM)	
			Cholera toxin (50 ng/mL)	Cholera toxin (50 ng/mL)	
			Fibronectin (100 ng/mL)	Fibronectin (100 ng/mL)	
			Fetuine (20 μg/mL)	Fetuine (20 μg/mL)	
			R1881 (0.1 nM)	R1881 (0.1 nM)	
			PS	PS	
AR	-	+	+	-	++
p53	Missense Mutation	Silent	WT	WT	WT
BRCA2	Missense Mutation	WT	WT	WT	WT
PTEN	WT	Frame Shift Deletion	Nonsense mutation	Nonsense mutation	Nonsense mutation

AR: androgen receptor; BRCA2: breast cancer 2; PTEN: Phosphatase and tensin homolog; PS: Penicillin/streptomycin (100 U/mL, 100 μg/mL); FCS: Fetal calf serum; DCC: charcoal dextran-stripped serum; WT: wild type. For DU145 and LNCaP, data was acquired from The Cancer Cell Line Encyclopedia (CCLE) <https://portals.broadinstitute.org/ccle>.



Chapter 7

Summary, considerations and conclusions

Prostate cancer (PCa) remains a heavy burden in current healthcare as it is the most common non-skin cancer and fifth leading cause of cancer-related death in males. Despite progress in understanding the biology of PCa and developing new drugs and therapeutic strategies, advanced stage PCa continues to be incurable and development of drug resistance remains a crucial issue. Extensive research has aimed to further understand PCa, including developing more reliable preclinical models, increasing treatment efficacy, selecting best patients for certain treatment regimens and predicting treatment response. The role of the DNA damage response (DDR) has drawn particular attention in recent years as an increasing number of PCa patients harboring DDR defect is being identified. These findings may have important implications for their treatment, since new DDR-targeting compounds show great potential for precision medicine. Furthermore, the recently discovered crosstalk between the DDR machinery and androgen receptor (AR) signaling opens a new array of possible strategies to enhance treatment efficacy.

This thesis describes the development of novel 3D *in vitro* PCa models, analysis of DNA double-strands break (DSB) repair in PCa and how the DDR may impact PCa treatment. Preclinical research of PCa depends heavily on a limited number of conventional 2D cell lines. Although their homogeneity and ease of handling makes them valuable models for high-throughput experiments, lack of complex architecture and cell interaction makes them “unrepresentative” models and may lead to a failure when transitioning a new treatment from bench to clinic. To overcome this, two distinct methods to culture 3D PCa tumor *in vitro* are being discussed in this thesis. The first method involves the generation and culture of organotypic PCa tumor slices (chapter 3). Organotypic indicates these tumor slices retain morphology and function of the tumor of origin *in vivo*. Culture conditions have been optimized such that tissue viability, proliferation capacity and prostatic characteristics have been maintained up to at least 6 days. Robust marker and analytical tools for cell proliferation and cell apoptosis were used as surrogates to assess response to *ex vivo* anti-androgen and poly(ADP-ribose) polymerase (PARP) inhibitor treatment. Importantly, the response to different tumor genotypes, represented by different PDXs were validated, and hence provide evidence that *ex vivo* drug testing can indeed predict *in vivo* responses. The established tissue slices culture system can be extended for testing novel compounds relevant to PCa treatment. Maintenance of primary PCa tumors has been challenging probably due to the slow growing characteristics and fast proliferation of basal cells. Also, obtaining aggressive metastatic PCa material is met with limitations as metastatic disease is predominantly found in bone restricting easy access. Nowadays, prostate-specific membrane antigen (PSMA) guided biopsy and salvage lymphadenectomy is reported, which may offer new opportunities for acquiring aggressive PCa material for *ex vivo* drug response tests. Our tissue slice culture platform for PCa defined in this thesis may be helpful to standardize *ex vivo* culturing of patient material and shows the promising future of personalized medicine in PCa treatment.

Besides analyzing treatment effects by directly assessing tumor slices themselves, we investigated the extracellular vesicles (EVs) secreted from tissue slices in culture medium, and characterized their abundance and RNA content compared to the original tissue slices (chapter 4). As a promising field in liquid biopsy, EVs has drawn particular interest in recent years as they are able to capture tumor heterogeneity and they can be reassessed periodically. We identified abundant presence of EVs in the tissue slice culture media, from which RNAs could be obtained. Importantly, we detected that gene expression alterations after anti-androgen treatment were highly similar between tumor

slices and EVs. This implies that EVs may reflect the biological effects on the original cells in the tumor slice and that this may yield reliable markers for monitoring treatment response over time in the same tumor slice. Evaluating these EVs in tissue models allows the determination of tissue origin of these factors, which is difficult to accomplish *in vivo*. Most *in vivo* studies on EVs obtained from blood, urine and malignant ascites are difficult to interpret because of multiple potential cellular sources of these EVs. In addition, several challenges present when isolating EVs from body fluid, such as limited availability of biospecimens and the presence of high-abundance proteins and lipoprotein particles. Increasing evidence showed that EVs play a crucial role in cell-to-cell communication, however, isolated tumor cells do not adequately recapitulate important aspects of tissue function related to cell-to-cell communications *in vivo*. In such case, 3D models have major value in investigating the role of EVs in cancer development and testing anti-cancer compounds under controlled laboratory conditions. Different types of vesicles, such as exosomes, microvesicles and apoptotic bodies, were defined by biogenesis and roughly correlated with their size. However, the classification of individual EVs is difficult and the origin of the individual EVs in cell culture medium and body fluids cannot yet be determined. Whether there are functional differences between EV subtypes is not known yet, and it is unclear how this might affect current knowledge of EVs. Thus, it is imperative to overcome the technical challenges and standardize the procedures that associated with homogenous EV purification and accurate quantification.

In addition to organotypic tissue slices culture, the second method first dissociates the tumors enzymatically and mechanically, followed by embedding dissociated cells into a 3D matrix. In such case, tumor cells will grow as tumor organoids. PCa organoids have been proven difficult to establish and very little data are available comparing PCa organoids to the *in vivo* tumors and thus it is unclear how well these PCa organoids recapitulate structural and functional aspect of their original tumors. In chapter 5, we investigated the irradiation effects on PCa organoids and compared them to their matched tissue slices. Tumor morphology and prostatic characteristics are well preserved in organoids, with AR expression and prostate-specific antigen (PSA) secretion. A comparable response to irradiation between organoids and tissue slices was observed in terms of tumor cell proliferation, apoptosis and DDR kinetics, suggesting that PCa organoids may be used for testing irradiation-drug combinations in a medium throughput screening. This result warrants further validation with more tumor models and the *in vitro* response should be compared to the *in vivo* effect in order to get a more complete view. As generally acknowledged, PCa research has been hampered by the lack of suitable *in vitro* model systems. Although powerful *in vivo* models are available, these are often expensive and time-consuming. In this thesis, we have described two types of novel *in vitro* models. Compared to the tissue slice model, the organoid model is not restricted to short-term culture and limited proliferation capacity and therefore allows for larger-scale screening once organoid lines have been established. Nevertheless, organoids also have their limitations, as they still lack stroma and immune cells, while this may partly be preserved in tissue slices. Compared to organoids, assays based on tissue slices can be done within a few days to weeks after obtaining material, which is compatible with regular clinical decision making and could be incorporated into the diagnostic routine before start of treatment. Thus, models should be chosen based on the specific situation and research question.

Radiation therapy, the first-line treatment for localized PCa, is commonly combined with adjuvant androgen deprivation therapy (ADT) for high-risk PCa patients, as the combination regimen significantly improves overall PCa-related survival. Previous preclinical studies have investigated the molecular mechanism of radiosensitization by ADT and suggested a connection between AR-signaling and the DDR machinery. However, opposing conclusions were drawn from these studies about the DNA repair pathways that cause the radiosensitization. In chapter 6, we tested the radiosensitizing effect of next generation anti-androgen apalutamide and ADT in a preclinical PCa progression cell model and an androgen-dependent tissue slices model. We demonstrate that these treatments can act as a radiosensitizer in both AR-expressing preclinical PCa models. The mechanism of action causing this radiosensitization involves regulation of the non-homologous end-joining (NHEJ) DNA repair pathway by AR-signaling. We resolved the controversy by providing solid evidence that the homologous recombination (HR) repair is not directly regulated by AR signaling. HR reduction upon anti-androgen treatment on a cell population level was caused by a change of the cell cycle profile, but the few cells in S phase were still HR proficient. Our data also suggest that PCa patients harboring HR mutations could possibly benefit to a greater degree from combination of apalutamide and irradiation compared to HR wild type patient, as intrinsic HR repair defects in these patients plus compromised NHEJ repair by apalutamide will render the tumor cells exquisitely vulnerable to irradiation. It is to be expected that due to increased use of next generation sequencing approaches, it is likely that more PCa patients with HR defects will be detected. In early stage, for PCa patients harboring HR defects, such as *BRCA1* or *2* mutations, a greater benefit can be expected from such combination treatment. If the disease progresses, these patients can then be offered with PARP inhibitors treatment. However, the implementation and standardization of genomic testing still remains a major challenge. Besides blood based germline mutation and biopsy based somatic mutation testing, new studies are looking into circulating tumor cells or cell-free DNA based detection of a panel of clinically actionable genes to select eligible patients.

Overall, this thesis first describes the development and application of 3D *in vitro* PCa models: tissue slices culture and organoids culture. These 3D platform for PCa defined in this thesis may be helpful to standardize *ex vivo* culturing of patient material and shows the promising future of personalized medicine in PCa treatment. Next, the abundance and RNA content of EVs secreted from tissue slices in culture medium were analyzed, showing that EVs may reflect the biological effects on the original cells in the tumor slice and that this may yield reliable markers for monitoring treatment response over time in the same tumor slice. Lastly, using PCa progression cell model and tissue slices model, we demonstrate that AR suppression treatments can act as a radiosensitizer in both AR-expressing preclinical PCa models and the mechanism of action causing this radiosensitization involves regulation of the NHEJ DNA repair. The studies in this thesis provide new strategies for generation of novel 3D *in vitro* PCa model and broaden our understanding of DDR defects and AR-DDR interplay in PCa, this knowledge can be used to improve diagnostic, prognostic and therapeutic approaches for PCa management.

Nederlandse samenvatting

Prostaatkanker is de meest voorkomende vorm van kanker na huidkanker en staat in de top 5 van het hoogste aantal kanker-gerelateerde sterfgevallen in mannen. Prostaatkanker legt dan ook een zware druk op de gezondheidszorg. Prostaatkanker is nog steeds ongeneeslijk bij uitgezaaide ziekte, ondanks beter begrip van de fundamentele processen van prostaatkanker biologie en de ontwikkeling van nieuwe medicijnen en therapeutische strategieën. Dit komt mede doordat patiënten resistentie ontwikkelen tegen de behandelingen. Er is in de afgelopen jaren uitgebreid onderzoek gedaan om prostaatkanker beter te begrijpen en te behandelen, door het ontwikkelen van ontwikkeling van betrouwbare preklinische modellen, verhoging van therapeutische effectiviteit, persoonsgerichte therapie en het voorspellen van therapie effectiviteit. Met name de rol van de DNA schade response (DDR) heeft veel aandacht getrokken in de afgelopen jaren, omdat er DDR-defecten gevonden worden in prostaatkanker patiënten. Dit kan impact hebben op de behandelkeuze, aangezien DDR-gerichte medicijnen veel potentie hebben voor persoonsgerichte behandeling. Tevens zorgt de recent ontdekte interactie tussen de DDR en androgenen receptor (AR) signalering voor een groot aantal nieuwe mogelijke strategieën voor therapieverbetering.

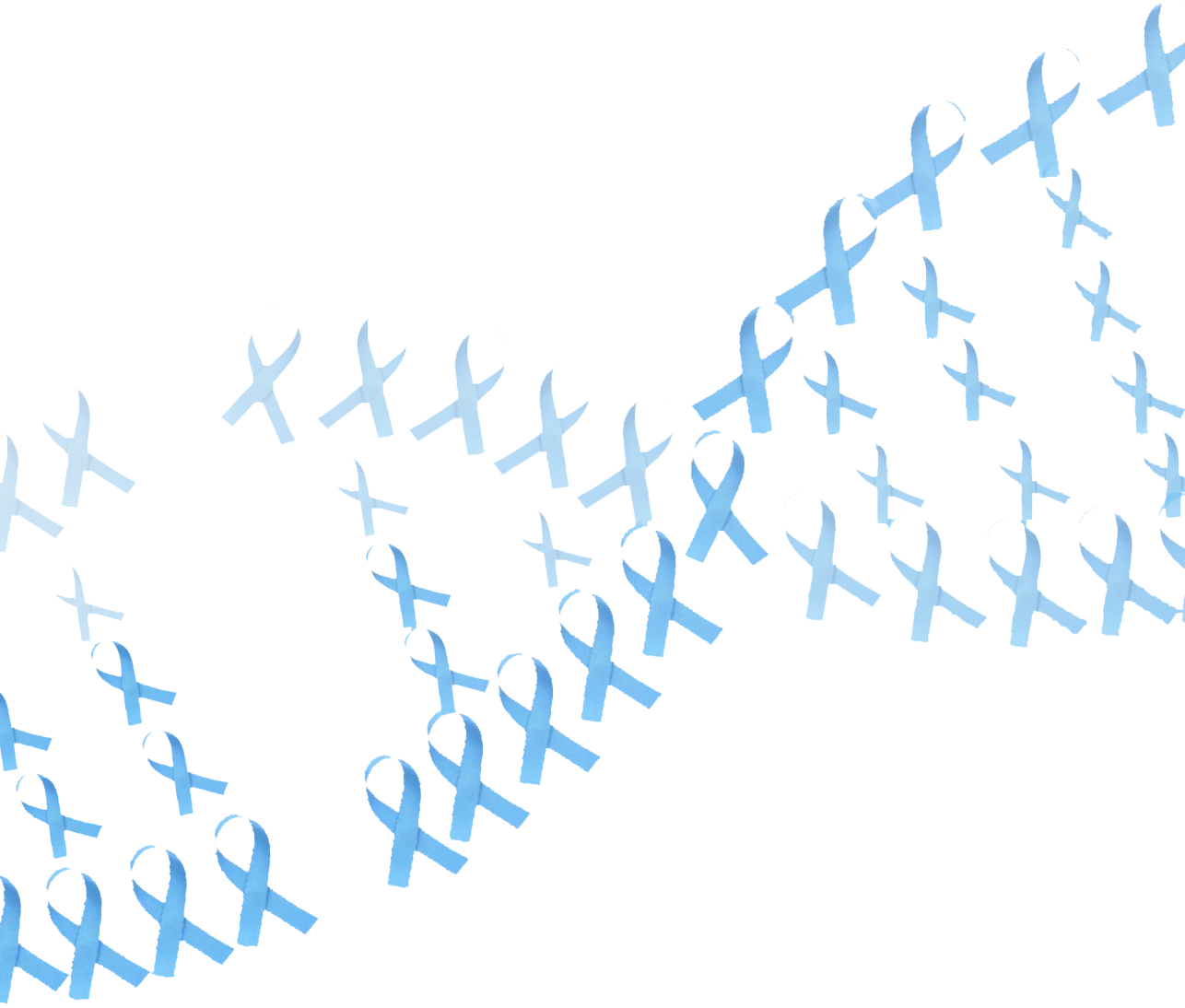
Dit proefschrift beschrijft de ontwikkeling van nieuwe 3D *in vitro* prostaatkanker modellen, analyse van DNA dubbelstrengs breuk (DSB) reparatie mechanismen en de gevolg van de DDR op prostaatkanker behandeling. Preklinisch onderzoek naar prostaatkanker wordt voornamelijk uitgevoerd met behulp van een beperkt aantal traditionele 2D tumorcellijnen. De homogeniteit en gebruiksgemak maakt deze cellijnen erg waardevolle modellen voor high-throughput experimenten. Ze hebben echter geen complexe samenstelling en cel-tot-cel interacties zodat dit niet altijd goede representatieve modellen zijn wat ertoe kan leiden dat ontwikkelingen (bv nieuw ontwikkelde medicijnen) niet altijd makkelijk van het lab naar de kliniek vertaald kunnen worden. Om dit probleem op te lossen, worden er in dit proefschrift twee verschillende 3D *in vitro* modellen besproken. **Hoofdstuk 3** bespreekt de ontwikkeling en analyse van organotypische prostaatkanker tumorplakjes. Deze weefselplakjes behouden de morfologie en functie van de originele tumor. De kweekcondities zijn geoptimaliseerd zodat de weefselplakjes in leven blijven, hun prolifererende capaciteit behouden en verdere prostaatkanker karakteristieken behouden voor minimaal 6 dagen. Verscheidene specifieke analyse methoden voor de detectie van proliferatie en celdood werden gebruikt om de respons op *ex vivo* anti-androgenen therapie en poly-(ADP-ribose)-polymerase (PARP) remmers. Deze *ex vivo* responsen waren vergelijkbaar met *in vivo* responsen; weefselplakjes kunnen een goed model systeem zijn om de effectiviteit van therapieën te meten. Tevens opent dit deuren voor het gebruik van primaire humane tumorplakjes voor persoonsgerichte therapie selectie.

Verder hebben we ook extracellulaire vesicles (EVs), die uitgescheiden worden door de weefselplakjes in het kweekmedium, geanalyseerd. Van deze EVs hebben we de RNA inhoud vergeleken met de originele weefselplakjes (**hoofdstuk 4**). De afgelopen jaren is er in het veld van 'vloeibare biopten' veel aandacht voor EVs omdat ze overeenkomen met de tumor heterogeniteit en ze zijn periodiek opnieuw te beoordelen. Wij hebben een grote hoeveelheid EVs gemeten in het kweekmedium en daaruit RNA geïsoleerd. Veranderingen in genexpressie na antiandrogeen therapie waren hetzelfde in de EVs en de weefselplakjes. Dit impliceert dat effecten van de tumor ook gemeten kunnen worden in EVs en dat EVs dus een betrouwbare marker kunnen zijn in de weefselplakjes therapieresponsen in de tijd te meten.

Naast weefselplakjes zijn er andere *in vitro* 3D modellen beschikbaar voor

prostaatkanker onderzoek, waaronder tumor organoïden. Hiervoor worden tumoren enzymatisch en mechanisch gedissocieerd en ingebed in een 3D matrix zodat ze als sferoïde kunnen groeien. Prostaatkanker organoïden zijn een nieuw modelsysteem en het is dus nog volledig onbekend hoe goed deze organoïden de structuur en functie van de oorspronkelijke tumor weergeven. In **hoofdstuk 5** onderzoeken we de effecten van ioniserende straling in prostaatkanker organoïden en vergelijken deze met de effecten in bijbehorende weefselplakjes. Weefsel morfologie en prostaatkanker karakteristieken worden goed behouden in organoïden, zoals AR expressie en prostaat-specifiek antigeen (PSA) uitscheiding. Organoïden en weefselplakjes reageren vergelijkbaar op ioniserende straling (proliferatie, apoptose, DDR kinetiek), wat zou kunnen betekenen dat dat prostaatkanker organoïden mogelijk gebruikt kunnen worden voor het testen van stralings-gerelateerde behandelingen.

Radiotherapie is de eerstelijns therapie voor gelocaliseerd prostaatkanker en deze therapie wordt vaak gecombineerd met adjuvante hormoonbehandelingen omdat deze combinatie de overleving significant verbetert. Verscheidene preklinische studies hebben het mechanisme van radiosensitisatie van hormoonbehandelingen onderzocht en in deze studies werd een link gevonden tussen de AR-signalering en de DDR. Er werden echter tegenstrijdige conclusies getrokken over welke DNA reparatie route hiervoor verantwoordelijk is. In **hoofdstuk 6** hebben we de effecten van de antiandrogeen apalutamide en andere hormoonbehandelingen getest in combinatie met radiotherapie in verscheidene prostaatkanker modellen. We laten zien dat deze behandelingen inderdaad de ioniserende stralingseffecten kunnen versterken in AR-positieve preklinische modellen. Verder laten we zien dat dit effect veroorzaakt wordt door de niet-homologe end-joining (NHEJ) DNA reparatie route. Hiermee hebben we een controversie opgelost omdat we laten zien dat de homologe recombinatie (HR) DNA reparatie route niet direct gereguleerd wordt door de AR-signalering. Antiandrogeen behandeling onderdrukte HR in de gehele celpopulatie, maar dit werd veroorzaakt door een verandering in in het aantal cellen in celdeling, met minder S fase cellen. Prostaatkanker patiënten met een HR defect kunnen mogelijk beter reageren op een combinatie van apalutamide en radiotherapie in vergelijking met HR proficiënte patiënten, omdat intrinsieke HR reparatiedefecten in deze patiënten in combinatie met een aangetast NHEJ reparatie systeem (door apalutamide) de tumorcellen extra gevoelig zullen maken voor ioniserende straling.



APPENDIX

Acknowledgements

PhD Portfolio

Curriculum Vitae

List of Publication

Acknowledgements

Something, such as pursuing a PhD, it is only when you have got through, you can know the real flavor of it. As the four years' PhD Life is approaching to the end, numerous past memories (both happy ones and also suffering ones) are showed up again in my mind. All those small pieces of cliché made my PhD so unique and I can honestly say that the journey of doing a PhD is much more challenging and difficult than I originally thought, with scientific troubles and non-scientific troubles are around, but it is deserved to be memorized forever for me. Especially, my dear supervisors, colleagues, friends and family, your invaluable kindness and supports, make me where I am now. Here, I want to express my most sincere gratitude to all of you.

Sincerely, I would like to thank my promotor. Dear Roland, first of all, I really appreciated your support for these four years. I had some struggles in the middle of my PhD. I am so lost at that time and you tried to encourage me and push me to the right direction. You taught me to focus on the current topic and keep the peace with peer PhD students. Your strictness and directness push me to make progression. Your tips about how to use fragmentated time really helps a lot in my last year. Without your help, I cannot make my project into papers and eventually into the whole thesis of my PhD. Moreover, I sincerely thank you for all of your effort on revising my manuscripts and the whole thesis and adapting those ones into simple but precise academic paper work.

Dear Julie, I cannot thank you enough for all the helps you give me along the journey. And I cannot image how far I can go in this campaign without you. Scientifically, you taught me many different experimental skills, taught me how to present data and how to write a story. In addition, beyond research, you are such a kind person that you are always the source of help whenever I have a problem. The first half of my PhD is full of bumps, I was so frustrated and discouraged. It is you that put more effect and prioritize my stuff and gave me strength and helped me to figure out a solution to achieve our final goal. I also admire your execution, braveness, and ability to organize and manage, which all makes you a good PI. I sincerely appreciate and cherish everything you did for me. I feel so lucky to have you as my supervisor. Hartelijk bedankt!

Dear Dik, sincerely, I would like to thank you for accepting me as a PhD student in the department together with Prof. Hoeijmakers. Though, the planned PhD has been far off track. I still remember you encouraged me every time when I rushed to your office and reported some negative data. With your calm tongue and patient explanation, you made me feel much better when facing all the negative data and give me the courage to continue. I admire your knowledge not only on your expertise, also in history, geography, politics and etc. After work talk with you is always interesting and intriguing.

Dear Wytse, it is my great honor to have you as one of my co-promotors. It took me one year to pronounce your name right. Sorry for so many “whisky” that I called you. Your input in the aspect of prostate cancer is crucial to my PhD. Thanks for offering precious PDX tumors and introducing the apalutamide projects to me, which made my PhD possible. I appreciate that you always provide me opportunities to join conferences, though due to my personal issue, I could not make them.

I would like to thank Chinese Scholarship Council (CSC) for granting my staying in Netherlands for four years. Hope this ambitious project of my motherland, will definitely bring the scientific prosperity and strength to China in the near future.

Dear Luca, what a coincidence to meet you here! I read so many your papers during my master internship and even applied a PhD position in your group. But at that time, I didn't realize that you are in the Netherlands. Thanks for bringing the apalutamide project, this collaboration made my PhD possible. You always give me a lot of precious suggestion from the clinical view. As time goes on, when I start to conceive a new project, I also start with: what is the clinical meaning? what is my final target?

I would like to extend my great gratitude to my lovely lab mates. Nicole, Anja and Hanny, my practical experiment tutors, a big "thank you" goes to you all. Even though I didn't have the chance to work together with you on some projects, but whenever I encountered technical problems, you were always there to help me patiently. You also gave me a lot of useful tips for better adaptation to Dutch life. Furthermore, thanks for organizing various group activities: it was full of laugh and fun, and I will cherish them forever. Titia, we started PhD at the same time, thanks for being roommates for 4 years and all the laugh and fun in the office. You are so brave in expressing your points of view, I really need to learn it from you. I wish you all the best with finishing your PhD and a bright career as pathologist after that. Sanjiban, thanks for sharing your experience with me and help for the extracellular vesicle project. Our before-going-home chats helped me to forget my stress at work and refill me energy for the next day. It is a pity that I do not have a chance to say goodbye in person when you left The Netherlands last year, but we will keep in touch. I wish you and your family all the best in India. Stefan, you are such a smart and nice man and stays positive all the time! I could feel the passion and energy from you for the scientific research. Wish all the best to your bright future. Danny, you have so much passion and enthusiasms on science and music. Your great sense of humor made the office hours full of joy. It was really enjoyable to discuss with you about the projects, ideas and detail techniques. I wish you all the good luck with your PhD! Marjolijn, thanks for being my paranymph, you are an easy-going person that are always open for help and bring a lot of hilarious moments in the tough PhD life. Good luck with your thesis! I wish you all the best in your career and loads of happiness with your Mr. Right.

I would like to extend my great gratitude to all my colleagues in department of molecular genetics. Nathalie, our PhD overlapped for two years. I wish I could know you earlier. I really enjoy our talk about work and life. I still remember the days that we biked home together. Jeroen, really appreciate for your help and all the valuable suggestions for my projects. Di and Calvin, I cannot remember how many times I came to your office when I felt boring or tired of my experiment. You always patiently listen to me and give me suggestions, thanks very much for your company and listening in my dark time and wish you two a sweet life and success in your scientific career! Chirantani and Marilena, thanks a lot for sharing with me your experience on PFGE. You were very patient and explained the procedures step by step. I avoided detours on this research based on your protocol and guidance. I wish you success in your career! Cecile, Charlie, Gosia, Alex, Marta, Nicole, Sari, Petra, Jiang, Joyce, Natasha, Giorgia, Marvin, Masaki, Karen, Arshdeep, Maarten, Dejan, Nathalie, Yongxin, Yannika, Yingying, Yifan, Yanto, Eline, Janette, Ziqing, Thom, Maayke, Wei, Christina, Aida,

Lennart, Arjan, Yasmin, Barbara, Serena, Hester, Cristina, Ingrid, Martine, Vivek and all the others I have not mentioned. Everybody is always willing to share knowledge and equipment and to help with different techniques and analyzing methods, which stimulated my research tremendously. I also really enjoyed the chats that I had with many of you in the hallway, cell culture, on PhD retreats and during the activities outside the lab.

I would like to express my heartfelt appreciation for the members from experimental urology lab. Dear Guido, it is my great honor to have you as the inner committee member. You are such a talented and knowledgeable person who always bring up sparking and inspiring ideas. Thanks for all the talks after work, these talks with your wisdom taught me a lot and inspired me so much. It is really enjoyable time to discuss scientific questions with you. Lianne, thanks for standing next to me for the defense. We shared a lot from life to work. I still remember the dim time when we both had our papers rejected and we encouraged each other, and thanks for your generosity and kindness. Just keep a bit longer you will have your great PhD done! Annelies, it was very nice to meet you at the end of my PhD, and collaborate on the organoids project. We both became parents in PhD, it makes PhD life a bit harder, but I believe it is worthy and you can manage your PhD very well. Sigrun and Wilma, Thanks for providing me a lot help in the urology lab. It's quite challenging to handle all the fastidious prostate cancer cell lines, you gave me a lot of detailed technical tips for better maintaining them and designing my experiments. Martin and Natasja, thanks for helping me with the EVQuant. Hajar, it was so nice to have you in apalutamide project. We have so much fun together and you helped me to know the Dutch culture and taught me so many Dutch words. Wish you a successful career as a urologist! Anita, thank you for all the hard work and enthusiasm in apalutamide project. You have all the potentials to be a great scientist, I wish you a successful and enjoyable PhD life in Leiden!

时光荏苒 白驹过隙，在荷兰四年的时光转瞬而过。很感谢在这段青春的岁月里遇见了你们，我的小伙伴们。高雅夫妇、吴斌夫妇、潇磊夫妇、张凯夫妇、杨珺文夫妇、赵满芝夫妇、孙伟夫妇、白冠男夫妇、黄玲夫妇、荆若愚夫妇、窦颖莹夫妇、温蓓夫妇、周国影夫妇、张超平夫妇、高文、平臻、朱长斌、常江、曹婉璐、刘嘉焯、屈长波、李杉、栗梦、梁秋实、丁世豪、刘俊、鲁涛、李博、陈帅、杨蕾、陈章玲、葛周虹、徐笑非、孙媛媛、杨琴、王璐、王晓路、刘卉、张爽、陈金栾、成婧。一次次的聚餐聊天，饮酒谈心以及狼人大战让荷兰的生活变得有了家味，多姿多彩。

感谢我的岳父岳母，谢谢你们把优秀的女儿托付给我！亲爱的岳母，感谢你不远万里来到荷兰，对我，瑶瑶，尤其是自远的悉心的照顾。你们是我们坚强的后盾。

老爸老妈，谢谢你们这么多年一直坚定地支持着我追逐我的梦想！医路十一载，我们聚少离多，此时此刻，我只希望学成回国可以陪伴在你们身边。远在荷兰，相隔万里，我无时无刻不在感受到你们浓浓的关切和爱意。每当受苦、受累、受委屈的时候都会立刻想到你们，家，永远是心底最温馨的港湾。谨以此书，包裹

我所有的爱，献给你们。

My adorable son Ethan, you bring me so many joyful moments which I never had before. My heart is melted by your smiles. Life is so beautiful to have you!

最后一份特别的感谢给我的老婆瑶瑶。你的出现，让我相信了什么叫一见钟情，什么叫上天的安排，我是如此幸运娶你为妻，谢谢你一直陪着我，给予我坚持下去的动力。在我博士生涯最黑暗的时候，鼓励我，帮助我走出阴霾。现在我们面临着人生重要的选择，我相信只要我们双手紧握，再难的路都可以一起走完！

PhD Portfolio

Name PhD student Wenhao Zhang
Department Molecular Genetics
Research school MGC
PhD period 1st September 2015- 1st September 2019
Promotor Prof. dr. Roland Kanaar
Copromotor: Dr. J. Nonnekens, Dr. D.C. van Gent,
 Dr. Ir. W.M. van Weerden

PhD training

Course	Year	ECTs
Irradiation protection 5B	2015	1
Technology Facilities	2016	1.2
Confocal microscope	2016	1
Genetics PhD course	2016	3
Genome Maintenance and Cancer	2016	1
Patient Oriented Research	2016	0.3
Basic and Translational Oncology	2016	1.8
CRISPR/Cas9	2017	3
Safely working in the Laboratory	2017	0.3
Functional Imaging and Super resolution	2017	1.8
Biomedical English Writing and Communication	2018	3
Biostatistical Methods I: Basic Principles	2018	2
Scientific Integrity	2018	0.3

Workshops and seminars	Year	ECTs
23 rd MGC workshop	2016	1.5
24 th MGC workshop	2017	1.5
Immuno-Imaging and Molecular Therapy	2017	2
Journal club	2015-2018	1

Molecular Genetics work discussion	2015-2019	3
MGC DNA repair meeting	2015-2019	1

Symposium	Year	ECTs
Daniel den hoed day	2016	0.5
MGC symposium	2015-2018	2
Radiotherapy research day	2017, 2018	1
Proton therapy day	2019	0.5

Conference	Year	ECTs
10 th Quinquennial conference on response to DNA damage (Egmond aan zee)	2016	2
EACR25 Biennial congress of EACR (Amsterdam, poster presentation)	2018	2
Androgen Meeting (Edinburgh, poster presentation) *	2018	0.5
ESUR19 (Porto, poster presentation 2×) *	2019	0.5

*Due to personal issue, not able to attend.

Lecturing and supervising students	Year	ECTs
Genetics courses for BSc nanobiology	2016,2017,2018	1
Supervising 2 exchange students (6 months)	2016	1
Hajar chatatou (master internship, 6 months)	2018	1
Anita Chen-yi Liao (master internship, 6 months)	2018-2019	1
Total ECTS		43

Curriculum Vitae

Wenhao Zhang was born in Qinghai, China, on September 7th, 1989. He was raised by his beloved parents Xiaowei Yuan and Shifeng Zhang in his hometown. In 2008 he graduated from high school and started to study medicine (seven-year Sino-French program) in Wuhan University, Hubei Province. During his medical training, he conducted clinical rotations in Zhongnan Hospital, and performed his master research internship under supervision of Prof. Dr. Xinhua Zhang at the Department of Urology in the same hospital. He investigated the expression of phosphodiesterase Type 5 (PDE5) in human and rat benign prostatic hyperplasia and revealed the underlying mechanism of PDE5 inhibitors in treating low urinary tract symptoms (LUTS). In 2012, he obtained scholarship from French Ministry of Education for a half-year internship in Brabois Hospital, Lorraine University, France. After obtaining his medical degree and passing the National Medical Licensing Examination in China in 2015, he started the 4-years PhD program supported by the China Scholarship Council (CSC) at the Erasmus Medical Center, Rotterdam, the Netherlands. The Ph.D. project was based on a collaboration between the Departments of Molecular Genetics (Dr. Julie Nonnekens, Dr. Dik C. van Gent) and Experimental Urology (Dr. Wytske M. van Weerden). His PhD focus on development of novel 3D prostate cancer models and understanding the cross-talk between DNA damage response and androgen receptor signaling. After his PhD, he will start residency training in the department of gynecological oncology, West China 2nd Hospital, Sichuan University, Chengdu, China.

List of publication

1. **Zhang W**, Liao C, Chatatou H, van Weerden WM, Incrocci L, van Gent DC, Nonnekens J. Apalutamide sensitizes prostate cancer to ionizing radiation via inhibition of non-homologous end-joining DNA repair. *Cancers* 2019, 11, 1593.
2. **Zhang W**, van Weerden, Incrocci L, van Gent DC, Nonnekens J. Role of the DNA damage response in prostate cancer formation, progression and treatment. *Prostate cancer and prostatic disease* 2019, in press.
3. **Zhang W**, van Weerden WM, de Ridder CMA, Erkens-Schulze S, Schonfeld E, Meijer TG, et al. Ex vivo treatment of prostate tumor tissue recapitulates in vivo therapy response. *Prostate*. 2019;79(4):390-402.
4. **Zhang W**, Zhang XH: Clinical and preclinical treatment of urologic diseases with phosphodiesterase isoenzymes 5 inhibitors: an update. *Asian journal of andrology* 2016, 18:723 31.
5. **Zhang W**, Zang N, Jiang Y, Chen P, Wang X, Zhang X: Upregulation of Phosphodiesterase type 5 in the Hyperplastic Prostate. *Sci Rep* 2015, 5:17888.
6. **Zhang W**, Chen P, Wang X, Zhao K, Negi DS, Zhuo L, Qi M, Wang X, Zhang X: Lycopene and Risk of Prostate Cancer: A Systematic Review and Meta-Analysis. *Medicine (Baltimore)* 2015, 94 (3 3): e1260.

Propositions

1. PARP inhibitors will become part of the standard care for metastatic castration resistant prostate cancer patients who harbor homologous recombination deficiency. (this thesis)
2. *Ex vivo* tumor slice culture is an ideal system for drug efficacy assessment. (this thesis)
3. Extracellular vesicles may reflect the biological effects on the original tissue and thus could be used as a biomarker for monitoring treatment response. (this thesis)
4. Biomarkers for intrinsic radiosensitivity are essential for prediction of the benefits of radiotherapy. (this thesis)
5. Androgen receptor suppression treatments induced radiosensitization in prostate cancer is caused by inhibition of non-homologous end-joining repair, not homologous recombination repair. (this thesis)
6. Future cancer treatments may be more realistically aiming for control of cancer making it a chronic disease rather than to reach cure.
7. Artificially boosting the immune response is one of the most exciting, and promising advancements in the treatment of cancer (Immunotherapy, 2018).
8. The first lesson when earning a PhD is to learn to accept disappointment. To realize this will bring your success even more rewarding.
9. We necessarily draw conclusions based on the data we have, but we must acknowledge that this does not always represent truth.
10. We really need to make good use of fragmented time, not to fragment our time.
11. À cœur vaillant rien d'impossible. (Jacques Cœur)

Wenhao Zhang, Rotterdam, 18th February, 2020

